University of Nebraska - Lincoln
DigitalCommons@University of Nebraska - Lincoln

Student Research Projects, Dissertations, and Theses - Chemistry Department

Chemistry, Department of

Winter 12-4-2014

Analysis of Drug Interactions with Lipoproteins by High Performance Affinity Chromatography

Matthew R. Sobansky
University of Nebraska-Lincoln, sobansky53@yahoo.com

Follow this and additional works at: http://digitalcommons.unl.edu/chemistrydiss

Part of the Analytical Chemistry Commons, Circulatory and Respiratory Physiology Commons, Medical Biochemistry Commons, and the Other Medicine and Health Sciences Commons

Sobansky, Matthew R., "Analysis of Drug Interactions with Lipoproteins by High Performance Affinity Chromatography" (2014). *Student Research Projects, Dissertations, and Theses - Chemistry Department*. 49.
http://digitalcommons.unl.edu/chemistrydiss/49

This Article is brought to you for free and open access by the Chemistry, Department of at DigitalCommons@University of Nebraska - Lincoln. It has been accepted for inclusion in Student Research Projects, Dissertations, and Theses - Chemistry Department by an authorized administrator of DigitalCommons@University of Nebraska - Lincoln.

ANALYSIS OF DRUG INTERACTIONS WITH LIPOPROTEINS BY HIGH PERFORMANCE AFFINITY CHROMATOGRAPHY

by

Matthew R. Sobansky

A DISSERTATION

Presented to the Faculty of
The Graduate College at the University of Nebraska
In Partial Fulfillment of Requirements
For the Degree of Doctor of Philosophy

Major: Chemistry

Under the Supervision of Professor David S. Hage

Lincoln, Nebraska

December, 2014

ANALYSIS OF DRUG INTERACTIONS WITH LIPOPROTEINS BY HIGH PERFORMANCE AFFINITY CHROMATOGRAPHY

Matthew R. Sobansky, Ph.D.

University of Nebraska, 2014

Advisor: David S. Hage

High density lipoprotein (HDL), low density lipoprotein (LDL), and very low density lipoprotein (VLDL) are lipoproteins previously shown to bind many basic and neutral hydrophobic drugs in serum. These interactions impact the distribution, delivery, metabolism, and excretion of drugs and are important in determining drug activity, pharmacokinetics, and toxicity in the human body. Information about drug-lipoprotein interactions and the strength of these interactions can be useful in determining the distribution of drugs following administration.

The research presented in this dissertation uses high performance affinity chromatography (HPAC) and packed columns to study binding of the drug propranolol to immobilized lipoproteins such as HDL, LDL, and VLDL. Through these studies, two types of interactions were identified between the lipoproteins and propranolol and verapamil. The first interaction has a relatively high affinity and likely involves binding of the drug by surface apolipoproteins. This high-affinity saturable interaction was stereoselective for LDL. HDL and VLDL did not exhibit stereoselectivity. The second

type of interaction observed in each lipoprotein had a lower affinity involved partitioning of the drug into the non-polar core of lipoproteins.

Additional work analyzing the theory and experimental conditions needed for the detection of multiple binding mechanisms in HPAC columns when using frontal analysis is also presented. This work focuses on the evaluation of binding models that incorporated both a saturable type of binding and a non-saturable interaction. These evaluations make it possible to determine the experimental conditions that would be required for detection of this type of multi-mode interaction.

These studies demonstrate that HPAC is a useful tool in characterizing mixed-mode interactions, as can occur with complex particles like lipoproteins. The affinity columns containing immobilized lipoproteins allowed these studies to be conducted using the same column for hundreds of experiments with short analysis times. The combined result of these advantages was the ability to quickly obtain precise data over a variety of drug concentrations. The results of these experiments indicate that similar columns prepared with other lipoproteins or biological membranes can be used in similar HPAC binding studies.

ANALYSIS OF DRUG INTERACTIONS WITH LIPOPROTEINS BY HIGH PERFORMANCE AFFINITY CHROMATOGRAPHY

Table of Contents

Chapter One – Introduction…………………………………………………… 1

Chapter Two - Analysis of drug interactions with high density lipoprotein by high-performance affinity chromatography…………………………………… 52

Chapter Three – Identification and analysis of stereoselective drug interactions with low density lipoprotein by high-performance affinity chromatography….. 92

Chapter Four - Analysis of drug interactions with very low density lipoprotein by high-performance affinity chromatography…………………………………. 124

Chapter Five – Evaluation of mixed mode interactions between drugs and lipoproteins by high performance affinity chromatography……………………. 154

Chapter Six – Summary and future work……………………………………..... 184

Table of Figures

Figure 1-1 - General model for drug interactions with proteins and other binding agents……………………………………………………………………… 3

Figure 1-2 - Structure of a lipoprotein…………………………………………... 9

Figure 1-3 - The process of lipoprotein transport……………………………….. 12

Figure 1-4 - Structure of propranolol……………………………………………. 15

Figure 1-5 - Structure of verapamil……………………………………………… 17

Figure 1-6 - Lipoprotein immobilization to silica by the Schiff base method…... 24

Figure 1-7 - Typical system for performing zonal elution studies………………. 27

Figure 1-8 - Typical chromatograms obtained during lipoprotein column stability studies…………………………………………………………………... 31

Figure 1-9 - Typical system for performing frontal analysis……………………. 35

Figure 1-10 - Typical breakthrough curves obtained during frontal analysis studies with columns containing immobilized lipoproteins……………………... 37

Figure 1-11 - Possible drug-lipoprotein binding mechanisms…………………... 42

Figure 2-1 - Change in the retention factor for *R*-propranolol as function of mobile phase volume……………………………………………………………….. 63

Figure 2-2 - Typical frontal analysis results obtained for the application of *R*-propranolol to an HDL column………………………………………………….. 66

Figure 2-3 - Double-reciprocal plot of frontal analysis data obtained for the binding of *R*-propranolol to an HDL column……………………………………. 68

Figure 2-4 - Examination of frontal analysis data for *R*-propranolol on an HDL column……………………………………………………………………………… 71

Figure 2-5 - Double-reciprocal plot of frontal analysis data obtained for the binding of racemic verapamil to an HDL column……………………………….. 81

Figure 2-6 - Examination of frontal analysis data for verapamil on an HDL column……………………………………………………………………………… 83

Figure 3-1 - Chromatograms depicting the change in retention for *R*-propranolol on an LDL column………………………………………………….. 102

Figure 3-2 - Typical frontal analysis chromatograms obtained when *R*-propranolol was applied to a LDL column………………………………………. 104

Figure 3-3 - Double-reciprocal plots of frontal analysis data obtained for the binding of *R*- and *S*-propranolol to a LDL column……………………………… 106

Figure 3-4 - Best fit results of plots to various binding models of frontal analysis data obtained for *R*-propranolol on an LDL column…………………… 109

Figure 4-1 - Typical frontal analysis results obtained for the application of various concentrations of *R*-propranolol solutions to a VLDL column………… 134

Figure 4-2 - Double-reciprocal plots obtained in frontal analysis studies examining the binding of *R*- and *S*-propranolol to a VLDL column…………… 137

Figure 4-3 - Fit of various binding models to frontal analysis data obtained for *R*-propranolol on a VLDL column………………………………………………. 140

Figure 5-1 - Frontal analysis data for the binding of *R*-propranolol to LDL as examined according to binding isotherms described by the non-saturable, one site saturable, and mixed mode binding models………………………………… 166

Figure 5-2 - Frontal analysis data for the binding of *R*-propranolol to LDL as examined using a double reciprocal plot……………………………………… 168

Figure 5-3 - Percent deviation from a linear response in the value of m_{Ltot}/m_{Lapp} for a double-reciprocal frontal analysis plot of a mixed mode system as a function of the ratio of the total affinity of non-saturable sites versus the affinity of saturable sites……………………………………………………………… 172

Figure 5-4 - Percent deviation from a linear response in the value of m_{Ltot}/m_{Lapp} for a double reciprocal frontal analysis plot for a mixed mode system as a function of the value of $1/K_{a1}$……………………………………………………. 174

Figure 5-5 - Surface plot showing the relative deviation from a linear response in the value of m_{Ltot}/m_{Lapp} for a double reciprocal frontal analysis plot for a mixed mode system…………………………………………………………… 177

Figure 5-6 - Contour plot showing the relative deviation from a linear response in the value of m_{Ltot}/m_{Lapp} for a double reciprocal frontal analysis plot for a mixed mode system…………………………………………………………… 179

Table of Tables

Table 1-1 - Typical Properties of Human Lipoproteins…………………………. 11

Table 1-2 - Binding models used with frontal analysis data for drugs on lipoprotein columns.……………………………………………………….. 44

Table 2-1 - Reported binding parameters for the interactions of propranolol and verapamil with HDL.……………………………………………………….. 54

Table 2-2 - Binding parameters obtained for *R*-propranolol on a HDL column at various temperatures.……………………………………………………… 73

Table 2-3 - Binding parameters obtained for *S*-propranolol on a HDL column at various temperatures.……………………………………………………… 74

Table 2-4 - Binding parameters obtained for racemic verapamil on a HDL column at 37°C………………………………………………………….. 85

Table 3-1 - Reported binding parameters for the interactions of propranolol with LDL……………………………………………………………… 94

Table 3-2 - Binding parameters obtained for *R*-propranolol on a LDL column at various temperatures……………………………………………………….. 111

Table 3-3 - Binding parameters obtained for *S*-propranolol on a LDL column at various temperatures………………………………………………………….. 112

Table 4-1 - Comparison of binding parameters for *R*- and *S*-propranolol with various lipoproteins at pH 7.4 and 37 °C.……………………............................. 127

Table 4-2 - Binding parameters obtained for *R*-propranolol on a VLDL column at various temperatures.…………………... 144

Table 4-3 - Binding parameters obtained for *S*-propranolol on a VLDL column at various temperatures………………………………………………………... 145

Table 5-1 - Double-reciprocal expressions for binding models used with frontal analysis data for drugs on lipoprotein columns.…………………………………. 160

Table 6-1 - *In vitro* conditions that have been used to synthesize glycated LDL.. 193

CHAPTER ONE

INTRODUCTION

Portions of this chapter have previously appeared in M.R. Sobansky and D.S. Hage, "Analysis of Drug Interactions with Lipoproteins by High-Performance Affinity Chromatography", In: Advances in Medicine and Biology, Vol. 53, L.V. Berhardt (ed.), Nova Science Publishers, 2012, Chapter 9.

Drug interactions with serum proteins and other binding agents within the blood play an important role in determining the apparent activities of many pharmaceutical agents that have entered the circulatory system. For example, the distribution and pharmacokinetics of numerous drugs within the body is impacted by the binding of these agents [1-3]. Direct and/or indirect competition between a drug and another agent (e.g., another drug or endogenous compound) for the same binding sites on a serum agent may also significantly impact drug-drug or drug-solute interactions [4-8]. Furthermore, the solubility of hydrophobic compounds may be enhanced by the binding of solutes in the blood [9].

The ability of a pharmaceutical agent to illicit a response is significantly impacted by these typically reversible binding mechanisms. This is due to the fact that only an unbound drug molecule contained within the blood is able to reach its receptor and target tissue, to be metabolized by the liver, or to be excreted by the kidneys from the circulatory system. A drug bound to proteins or other agents is generally not available for these processes or to illicit a response [10]. The effects of drugs binding to such agents in the circulatory system can be illustrated by the general model that is given in Figure 1-1. The interactions between drugs and serum agents are often significant, as demonstrated by the fact that 43% of the 1500 most frequently prescribed drugs have 90% or greater binding to serum proteins and other agents [11]. The frequent and extensive occurrence of drug and serum agent interactions mandates that the evaluation of this binding be an important part of the adsorption, distribution, metabolism, and excretion data that are required by the various health authorities for the approval a new pharmaceutical compound [10].

Lipoproteins such as high-density lipoprotein (HDL), low-density lipoprotein (LDL), and very low-density lipoproteins (VLDL) are a group of binding agents known to interact with several basic and neutral hydrophobic drugs and other solutes in blood [12-23]. Propranolol and verapamil are two examples of drugs that are known to engage in these types of interactions with lipoproteins [2,12-19]. The binding of such drugs with various lipoproteins was the focus of the research in this dissertation. The interactions of such drugs with LDL, VLDL, and HDL have been analyzed previously by means of equilibrium dialysis and capillary electrophoresis (CE) carried out in a frontal analysis mode [20-23].

Figure 1-1. General model for drug interactions with proteins and other binding agents in blood and the relationship of this binding to the ability of a drug to reach its target or to be acted on by the liver and kidneys. This figure is reproduced with permission from Ref. [54].

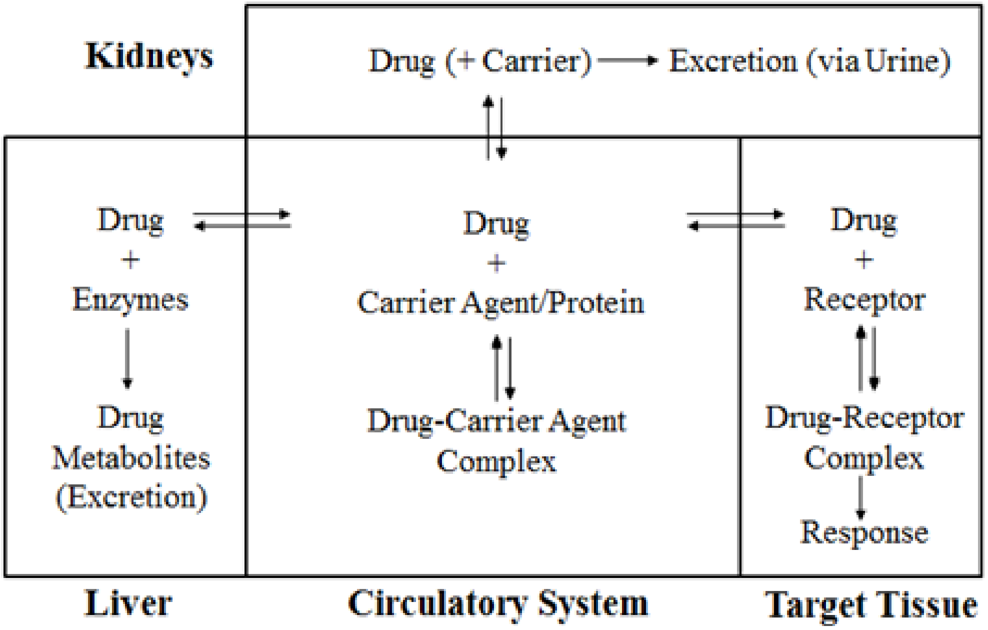
Kidneys
Drug (+ Carrier) → Excretion (via Urine)
Drug
+
Enzymes
Drug
Metabolites
(Excretion)
Drug
+
Carrier Agent/Protein
Drug-Carrier Agent
Complex
Drug
+
Receptor
Drug-Receptor
Complex
Response
Liver
Circulatory System
Target Tissue

Equilibrium dialysis is often the reference method for the evaluation of drug interactions with proteins or other macromolecules. This method is inexpensive to perform but has several drawbacks. The drawbacks of equilibrium dialysis include its requirement for a large amount of binding agent, the time consuming nature of the test, and its susceptibility to errors arising from leakage of the bound drug fraction through the membrane and/or adsorption of the drug onto the membrane [21]. CE/frontal analysis does not require the use of a membrane and overcomes many of the disadvantages associated with equilibrium dialysis. In addition, CE/frontal analysis provides a relatively quick method that requires relatively small amounts of samples and binding agents [21]. The primary handicap of CE in the evaluation drug interactions is the higher limits of detection that arise when compared to other methods that utilize bench top spectrometers or HPLC systems [24,25].

High-performance affinity chromatography (HPAC) is an alternate technique to equilibrium dialysis and CE/frontal analysis for evaluating drug - protein interactions [3,7-9]. HPAC utilizes high-performance liquid chromatography columns that contain an immobilized binding agent (e.g., HDL, LDL, or VLDL) to which a solution or sample of the drug of interest is applied [26-28]. Based upon past studies, HPAC has shown to be a valuable tool for studying drug interactions with serum proteins as information related to equilibrium constants and the stoichiometry of the interactions occurring within the column can be determined [3,7-9]. As will be demonstrated in this dissertation, the speed and ease of automation make HPAC advantageous when compared to equilibrium dialysis. HPAC provides superior precision when compared to equilibrium dialysis and CE due to the ability of HPAC to use the same preparation of binding agent for a large number of studies. This feature reduces batch-to-batch and run-to-run variations. Furthermore, HPAC can be interfaced with a variety of HPLC detectors, making it possible to use this method with a wide range of solutes while obtaining low detection limits [10].

HPAC has been employed in many previous studies that have examined drug interactions with serum proteins, such as human serum albumin (HSA) and α_1-acid glycoprotein (AGP) [10]. This technique has also been extended to work with binding agents, such as HDL, LDL, and VLDL in this research [24,25,29]. This chapter describes the basic principles of HPAC and the properties of the lipoproteins that were evaluated, as well as providing an overview of the drugs that were used as model compounds as a means to determine if HPAC was a suitable method for obtaining information regarding drug-lipoprotein interactions. Subsequent chapters within this thesis provide specific details on the experiments that were utilized to determine the nature and strength of drug-lipoprotein interactions, along with the results and significance of these experiments, and potential topics of interest for future work.

Properties of Lipoproteins

Lipoproteins such as HDL, LDL, and VLDL are soluble complexes of lipids and proteins (i.e., apolipoproteins) arranged into a macromolecular structure. The general structure of a lipoprotein is depicted in Figure 1-2.   A primary function of these complexes is to transport hydrophobic compounds such as cholesterols, triacylglycerides (triglycerides) and lipids throughout the body [12-14]. Lipoproteins are also known to interact with and transport several types of basic or neutral and hydrophobic drugs in the bloodstream [12-19,33].

As shown in Figure 1-2, triacylglycerol and cholesterol esters form the non-polar lipid core of a lipoprotein. This core is surrounded by a monolayer of phospholipids and apolipoprotein(s) covering the surface of lipoprotein. The phospholipids and apolipoprotein(s) in this layer are oriented to allow solubilization of the complex. Individual phospholipids are arranged so that the phosphate-containing head of the molecule is on the outer face of the complex while the lipid tail is positioned towards the non-polar core of the apolipoprotein [12,13].

Human lipoproteins have historically been divided into five primary classes based upon density. These five categories are, in order of increasing density, chylomicrons (CM), very low density lipoproteins (VLDL), low density lipoproteins (LDL), intermediate density lipoproteins (IDL) and high density lipoproteins (HDL) [12,14-18]. The properties that differentiate these lipoproteins are summarized in Table 1-1.

In addition to their structural differences, lipoproteins may be divided by the functional role that they serve within the body. Chylomicrons are typically formed following absorption of triacylglycerides and cholesterol within the intestinal tract. Chylomicrons are incorporated into the bloodstream, where free fatty acids are removed by lipoprotein lipase and delivered to various tissues. Chylomicron remnants are then delivered to the liver where they are repackaged as VLDL. VLDL transports endogenous triacylglycerides, phospholipids, cholesterol and cholesteryl esters throughout the body. Lipoprotein lipase removes additional triacylglycerides from VLDL, leaving IDL (i.e., VLDL remnants). IDL is then converted to LDL. LDL carries cholesterol esters formed in the liver to muscles and other extrahepatic tissues. A process known as reverse cholesterol transport utilizes HDL to remove excess cholesterol from peripheral tissues. The removed cholesterol is delivered to the liver for excretion and recycling [12,13]. The process of lipoprotein transport is depicted in Figure 1-3.

The exact lipoprotein composition and distribution in an individual is dependent on a variety of factors, including sex, age, race, metabolic condition, and disease state [12,13,16]. The typical lipoprotein levels in a healthy fasting adult male are approximately 280 mg/dL HDL, 410 mg/dL LDL, and 150 mg/dL VLDL [13]. Chylomicrons are only present immediately following a meal; therefore, typical fasting levels for this type of lipoprotein are 0 mg/dL [13]. Disruptions in the type and/or concentration of these lipoproteins may result in detrimental health effects such increased risk of cardiovascular disease [12-18].

The transport and distribution of hydrophobic or non-polar compounds of endogenous or exogenous origin is also facilitated by the presence of lipoproteins [12,14,18]. Examples of substances that are transported through interactions with lipoproteins include vitamin E and drugs such as amitriptyline, chlorpromazine, desipramine, imipramine, propranolol, verapamil, quinidine and nilvadipine [5,21,30,31,35-39].

Figure 1-2. Structure of a lipoprotein. This figure is reproduced with permission from Ref. [25].

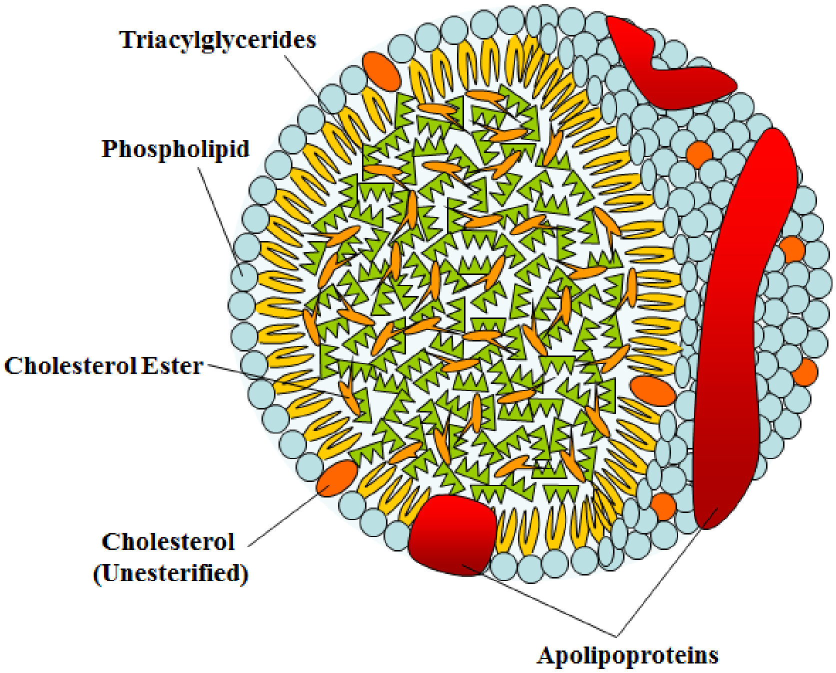
Triacylglycerides
Phospholipid
Cholesterol Ester
Cholesterol
(Unesterified)
Apolipoproteins

Table 1-1 Typical Properties of Human Lipoproteins

Lipoprotein	Density (g/mL)	Diameter (nm)	Associated Apolipoproteins	Composition (% dry weight)			
				Protein	Cholesterol	Phospholipid	Triacylglyceride
HDL	1.063-1.210	5-15	**A-I**, A-II, A-IV, C-I, C-II, C-III, D, E	55	17	24	4
LDL	1.019-1.063	18-28	**B-100**	23	45	20	10
IDL	1.006-1.019	25-50	**B-100**, C-I, C-II, C-III, E	18	29	22	31
VLDL	0.95-1.006	30-80	**B-100**, C-I, C-II, C-III, E	10	19	18	50
Chylomicron	<0.95	100-500	A-I, A-II, A-IV, **B-48**, C-I, C-II, C-III, E	2	4	9	85

Major associated apolipoproteins are shown in **bold**.

This table is adapted from Ref. [34].

Figure 1-3. The process of lipoprotein transport [34].

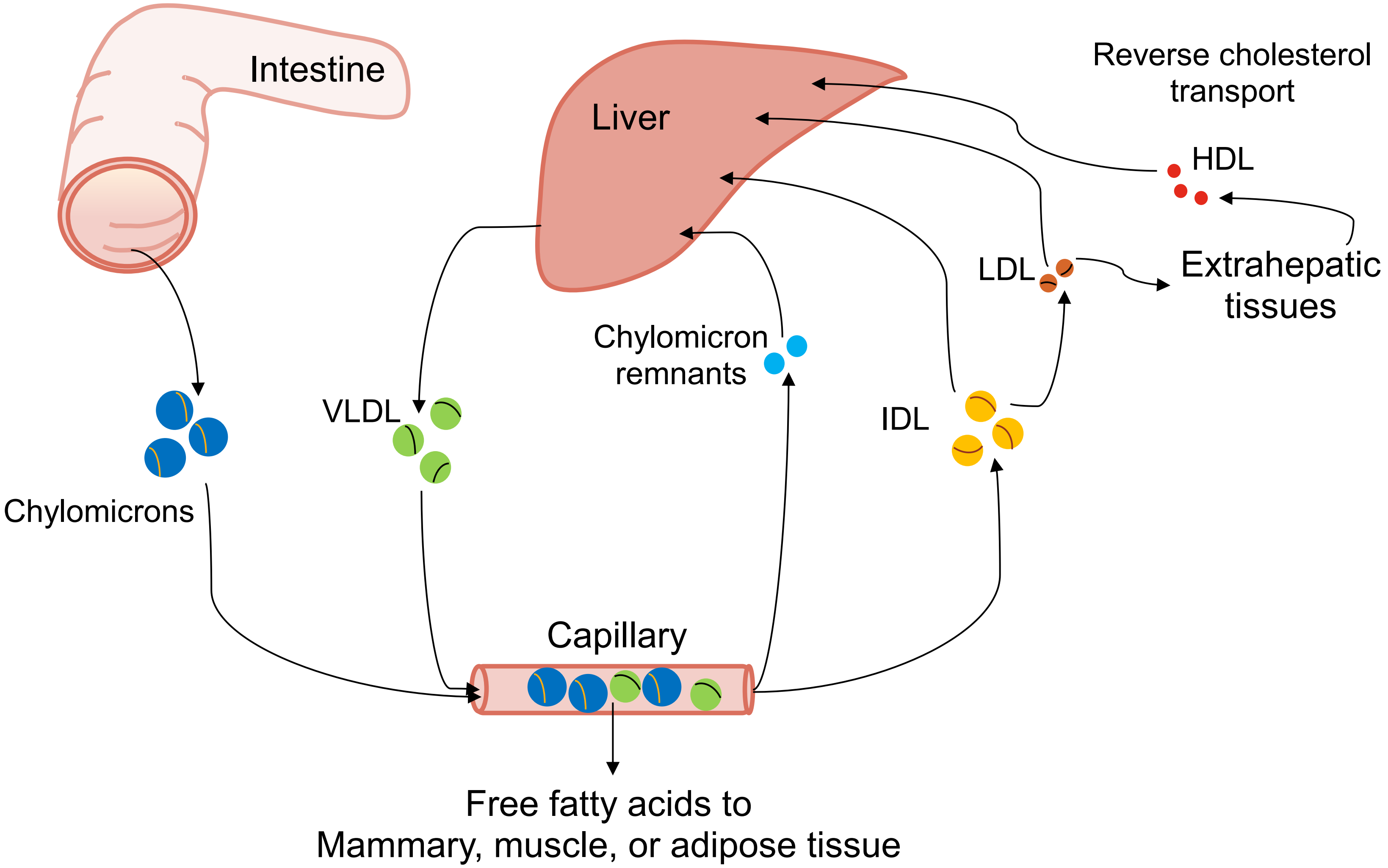
Intestine
Liver
Reverse cholesterol transport
HDL
LDL
Extrahepatic tissues
Chylomicron remnants
VLDL
IDL
Chylomicrons
Capillary
Free fatty acids to
Mammary, muscle, or adipose tissue

General properties of model drugs

Two model drugs were used in this work for the evaluation of drug-lipoprotein interactions by HPAC. The first model drug was propranolol (see Figure 1-4). This drug is a basic, chiral drug that is known to interact with several serum proteins and lipoproteins, including HSA, AGP, HDL, LDL, and VLDL [20-23]. Propranolol is a non-selective beta adrenergic blocking agent that is used in the treatment of several disorders, such as hypertension, angina, and arrhythmia [40-42]. Propranolol is basic and relatively non-polar, as indicated by its pK_a of 9.45 and its log P value of 3.00, allowing a number of interactions with lipoproteins feasible for this drug [40,43,44]. These interactions may include interactions with specific binding regions, interactions with surface phospholipids, or partition-based interactions with the non-polar core of a lipoprotein [12-19,33].

The second model drug that was evaluated was verapamil (see Figure 1-5). Verapamil is a calcium channel blocker used to treat hypertension, angina pectoris, and cardiac arrhythmia [22,45]. This drug is basic (pK_a of 8.75) and chiral, with the *S*-enantiomer showing higher pharmacological activity than the *R*-enantiomer [22,46]. Verapamil is also relatively non-polar, with a log P value of 3.79 [47]. These properties make interactions of this drug with lipoproteins possible at specific binding regions, surface phospholipids, or partition interactions with the non-polar core of the lipoprotein.

Figure 1-4. Structure of propranolol. The chiral center is indicated with an asterisk (*).

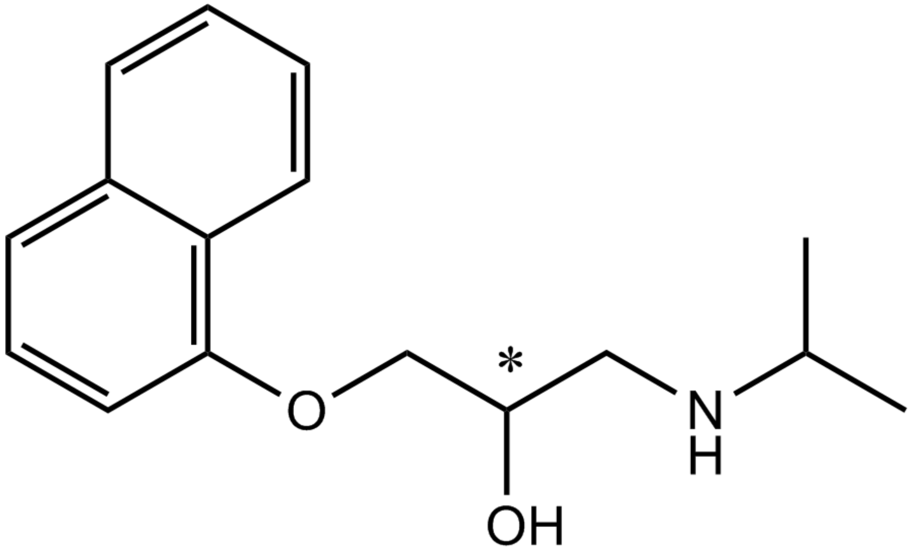
O
*
N
H
OH

Figure 1-5. Structure of verapamil. The chiral center is indicated with an asterisk (*).

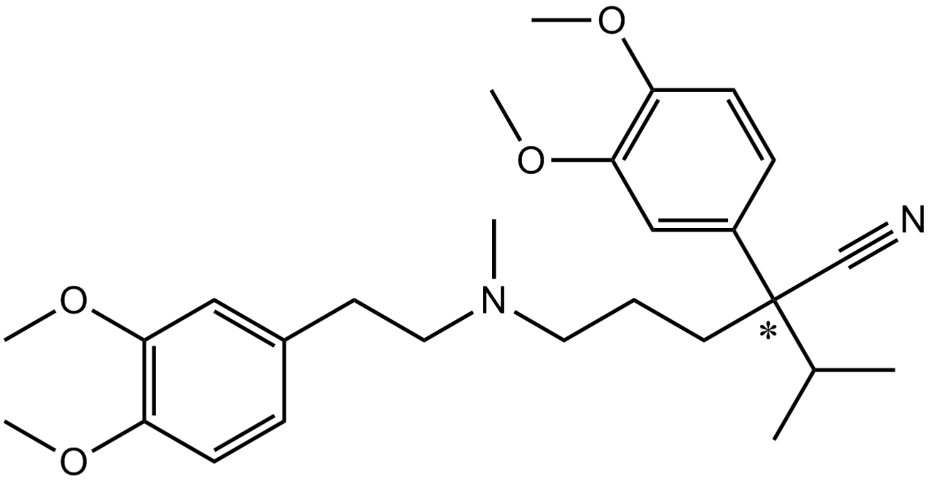

General Principles of High-Performance Affinity Chromatography

Affinity chromatography is a liquid chromatographic technique that utilizes biological agents as a stationary phase for the purification or analysis of a target compound dissolved in a sample solution [26-28]. Solute retention in affinity chromatography is based on the specific and reversible interactions that are commonly found in biological systems. These types of interactions are exploited in affinity chromatography by immobilizing one of a pair of interacting molecules on a solid support within a liquid chromatographic system. The immobilized molecule is referred to as the affinity ligand and serves as the stationary phase in the chromatographic system [10]. Examples of interactions that are commonly evaluated using affinity chromatography include the binding of a substrate by an enzyme, and the binding of an antigen by an antibody.

High performance affinity chromatography (HPAC) is a type of affinity chromatography that utilizes HPLC systems and solid supports that consist of small, rigid particles. These supports are typically comprised of materials such as silica or glass, azalactone beads, hydroxylated polystyrene media or monolith columns [10,26,27,48-51]. These materials are used due to their ability to withstand the moderate-to-high flow rates and pressures that can be present in an HPLC system. Furthermore, these supports offer the enhanced mass transfer properties needed in chromatographic separations. While HPLC instrumentation increases the cost of performing HPAC measurements compared to traditional or low pressure affinity methods, the improved speed and precision of HPAC make it preferable for analytical applications [10].

Another potential advantage of HPAC compared to other methods for determining drug interactions with serum binding agents is that the same ligand preparation can be used for multiple experiments. Thus, only a small amount of protein is required to conduct a large number of studies, which provides optimum precision by minimizing run-to-run variations [52]. Additional benefits of HPAC its ease of automation and the relatively short time periods needed for conducting binding studies. This is exemplified in the HPAC studies utilizing lipoproteins described in this research, where the typical run time was 5-10 min per analysis [24,25,29]. The analysis time is significantly less than the time needed for comparable studies using equilibrium dialysis or ultrafiltration [52]. Furthermore, the HPAC column and immobilized ligand are continuously washed with fresh mobile phase, which minimizes the effects on drug interactions by residual contaminants that may have been present in the original preparation of the binding agent [52]. Finally, the use of HPLC detectors provides low limits of detection and allows for a variety of compounds to be evaluated over a broad range of concentrations in HPAC [10,24]. These characteristics make HPAC a valuable tool for characterizing the interactions that occur between drugs and proteins, lipoproteins, or other binding agents in blood or serum. The realization of these benefits in this research is described in the subsequent chapters through the results for the HDL, LDL, and VLDL binding studies.

Experiments based on high performance affinity chromatography studies and used to examine solute-ligand interactions are typically carried out by one of two methodologies, i.e., zonal elution or frontal analysis. In each method, the immobilized ligand is the binding agent of interest and analyte application onto the column is made in the presence of only buffer or buffer containing a modifier/competing agent. At the completion of a run, the analyte’s elution time or volume are determined as a means to gain information regarding the interactions occurring between the affinity ligand and the analyte. In addition, the equilibrium constants and number of binding sites involved in the binding process can be determined. The presence of competing agents in the mobile phase allows one to obtain data regarding how these agents’ impact analyte-ligand interactions. Additionally, information on the rates of these binding processes may be acquired through examination of the analyte elution profile. These approaches have been used previously to examine the binding of numerous drugs to various proteins and transport agents in blood [9,10]. The focus of this research was the use of HPAC to study the binding mechanism, strength of binding, and stoichiometry for drug interactions with HDL, LDL, and VLDL.

The development of a stationary phase for the analysis of solute-ligand interactions using HPAC requires investigating the degree to which interactions with the immobilized agent mimic those by the same agent in its native form. Typically, this evaluation is performed by comparing the binding parameters for a model drug or solute with the immobilized agent and when using HPAC versus those obtained for the same system in its native state. Native state results are often obtained through equilibrium dialysis, ultrafiltration, or other solution-based reference methods [9,10]. Previous work with columns containing immobilized proteins such, as HSA and AGP, have routinely demonstrated that binding parameters determined using HPAC agree with values obtained using soluble HSA or AGP in drug binding studies [10]. Similar studies that have been carried out with HDL, LDL, and VLDL columns, as described in this dissertation, have led to the same conclusions [24,25,29].

Preparation of lipoprotein supports for HPAC

The effective evaluation of drug binding with a ligand by HPAC begins with the immobilization of the ligand to a support. Porous silica is one support material that is commonly used in HPAC, including the lipoprotein studies that were conducted in this dissertation. Porous silica was selected as a support material over other common supports, such as polystyrene or carbohydrate-based resins, due to silica's mechanical stability, chemical inertness, and long term stability in the presence of a physiological buffer (e.g., the pH 7.4, 0.067 M potassium phosphate buffer that was used as a mobile phase in this work) [24,25,29]. Prior to covalent immobilization of an affinity ligand to the surface of a porous silica support, surface silanol groups are modified with an organosilane containing functional groups that can later be used or modified for the immobilization process.

For these studies, the surface of the silica support was modified to a diol-bonded form prior to the immobilization of the ligands of interest (i.e., HDL, LDL, or VLDL). This modification process is shown in Step 1 of Figure 1-6. Surface modification of the silica reduces the presence of charged silanol groups, which could lead to non-specific binding of biological agents, and provides sites that can later be modified for the covalent immobilization of the desired lipoprotein [24,25,29].

Lipoproteins were immobilized on silica supports via covalent bonding to provide a stable linkage and robust affinity column [50]. The immobilization of each ligand was accomplished by using a modified form of the Schiff base method, or reductive animation, to attach lipoproteins to the diol-bonded silica [24,25,29]. This process was initiated with the periodic acid-based oxidation of the diol-bonded silica to create an aldehyde-activated support (see Step 2 in Figure 1-6) [50]. The aldehydes on the support were then reacted with primary amine groups on the apolipoproteins of HDL, LDL, or VLDL, resulting in nucleophilic addition to form an imine (Step 3). This reaction was buffered at pH 6.0 to maintain selectivity for amines with low pK_a values, such as the *N*-terminal regions of proteins [24,25,29]. Due to the reversible nature of imine formation, the resulting imines were reduced with sodium cyanoborohydride to generate a stable secondary amine (Step 4) [53]. Sodium borohydride was later added to reduce any remaining aldehydes on the support to alcohols. This helped minimize non-specific binding that may occur between sample components with these types of functional groups [53].

Zonal elution studies of drug interactions with lipoproteins

Zonal elution is the most popular method used in the analysis of solute-ligand binding in affinity chromatography. This elution method is performed using the same techniques as most typical analytical applications of liquid chromatography. For example, a narrow plug of solute is injected onto a column containing an immobilized ligand, while the elution time or volume of the solute is monitored [9-10,52]. Zonal elution has been utilized in past studies to examine the extent of drug binding by agents such as serum albumins (including HSA) and AGP [10].

Figure 1-6. Lipoprotein immobilization to silica by the Schiff base method. This Figure is reproduced with permission from Ref. [54].

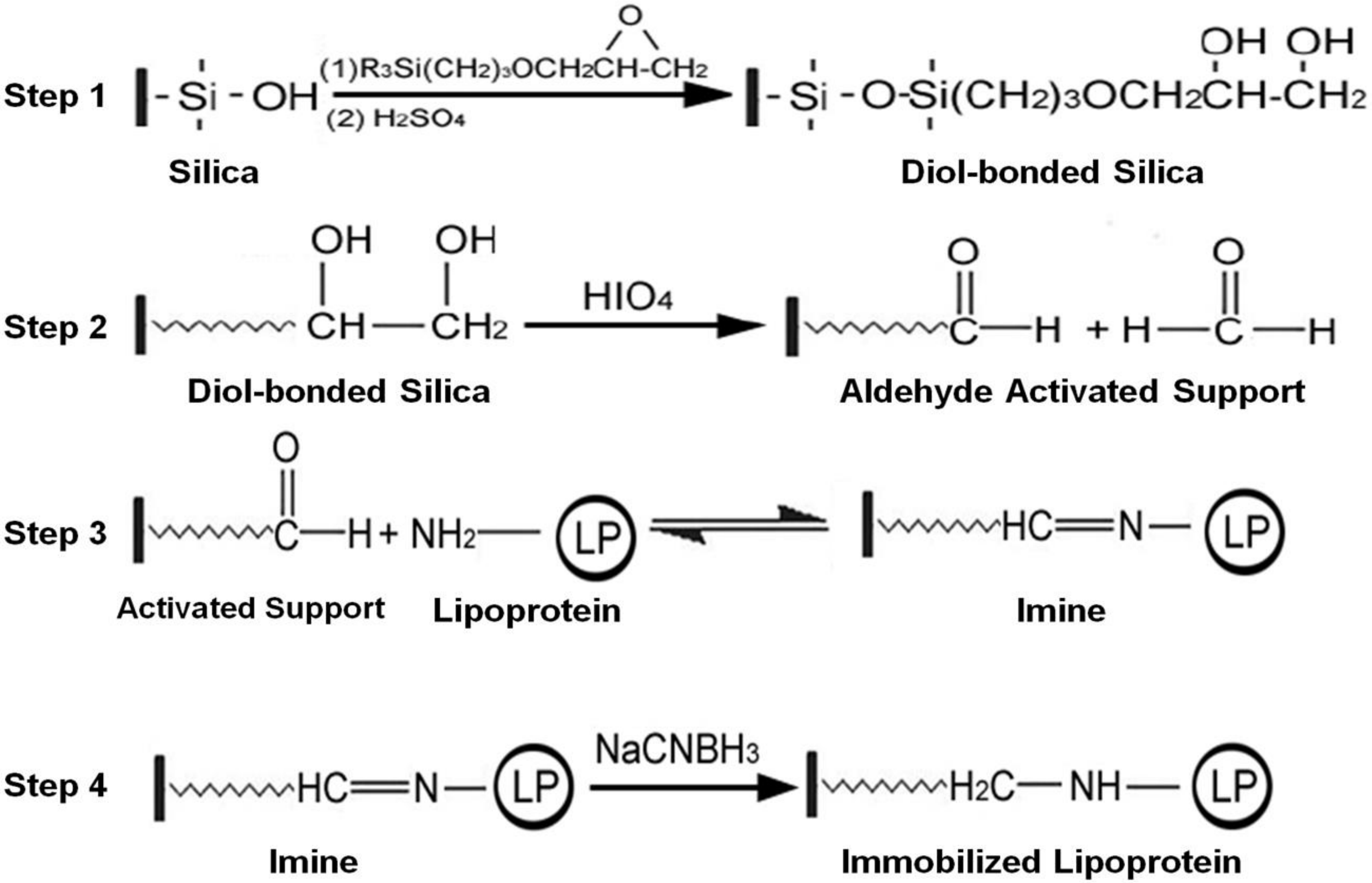
Step 1
Silica
(1)R3Si(CH2)3OCH2CH-CH2
(2) H2SO4
Diol-bonded Silica
Step 2
HIO4
Diol-bonded Silica
Aldehyde Activated Support
Step 3
Activated Support
Lipoprotein
LP
Imine
Step 4
NaCNBH3
Imine
Immobilized Lipoprotein

A typical system for performing zonal elution studies in HPAC consists of five primary components. The first component is a high pressure pump that is capable of delivering a constant flow of mobile phase through the packed column. A narrow plug of solute is injected into the mobile phase by using a closed injection loop or autoinjector. The dissolved analyte is then carried by the mobile phase to the HPAC column. The HPAC column is the source of the observed interactions between the injected analyte and the immobilized ligand. The elution profile for the analyte is monitored via an online detector as the solute emerges from the column. Finally, a computer or other recording device is used to obtain the detector's response as a function of the elution time or applied mobile phase volume, thus providing the final chromatogram that is utilized for analysis. A typical setup for a zonal elution HPAC system is shown in Figure 1-7.

Prior work has employed zonal elution and other ligands to measure the degree and affinity of solute-ligand binding, to examine changes in binding with variations in the mobile phase composition (e.g., pH, ionic strength, or polarity) or column temperature, and to see how alterations in solute or ligand structure may affect these interactions [10]. The fact that the retention of an injected analyte is a direct measure of the number of binding sites within a column and the strength with which the analyte is binding to the immobilized ligand is exploited in these studies. These relationships are described by Eqs. (1)-(2).

$$k = [(n_1 K_{a1} + \cdots + n_n K_{an}) m_L]/V_M \qquad (1)$$

$$k = [n K_a m_L]/V_M \qquad (2)$$

Figure 1-7. Typical system for performing zonal elution studies. This Figure is reproduced with permission from Ref. [54].

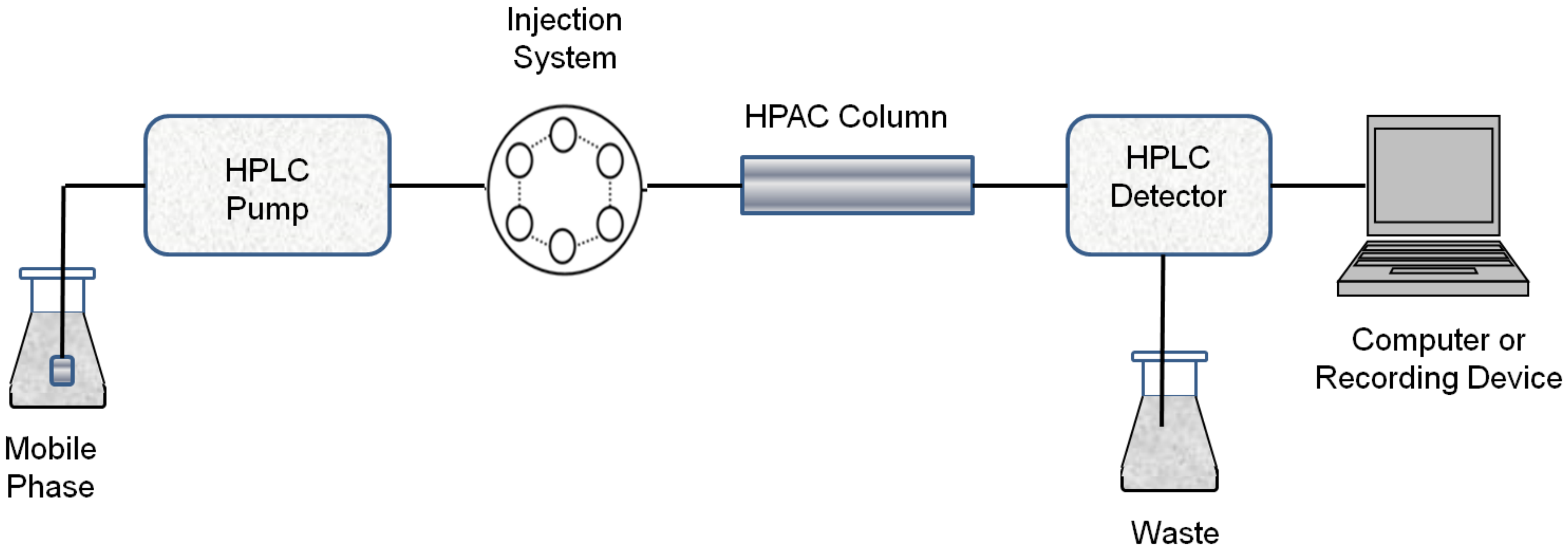
Injection
System
HPAC Column
HPLC
Pump
HPLC
Detector
Mobile
Phase
Waste
Computer or
Recording Device

These equations demonstrate that the retention factor (k) for an analyte on an affinity column is related to the number of binding sites in the column and the association equilibrium constants for the analyte at each of these sites [9,10,52]. The association equilibrium constants for the analyte at its individual binding sites on the ligand are defined as terms K_{a1} through K_{an} in Eq. (1). The stoichiometry for the analyte in each type of interaction is described in Eq. (1) by the terms n_1 through n_n. The summation of the terms n_1K_{a1} through n_nK_{an} in Eq. (1) is the global affinity or global association equilibrium constant, nK_a, as given in Eq. (2) [10]. The term V_M (Eqs. (1)-(2)) refers to the void volume of the column. Finally, m_L is the total moles of binding sites for the analyte in the column [9-10,52]. A review of these equations reveals that a change in the number of binding sites, the distribution of these sites, or the strength of binding at an individual site can result in a shift of analyte retention on an affinity column. This concept has been used in the course of experimentation associated with this dissertation in the evaluation of the stability of HPAC columns containing immobilized lipoproteins. These studies were executed by monitoring the retention of the model drug propranolol on columns containing HDL, LDL, or VLDL over time [24,25,29].

R-Propranolol and/or *S*-propranolol were used in these studies to evaluate column stability because these drugs are known to bind to HDL, LDL, and VLDL [20]. The stability of the lipoprotein columns was evaluated by measuring the retention of these analytes through a series of injections made onto new HPAC columns containing immobilized HDL, LDL, or VLDL [24,25,29]. The goal of these studies was to determine when a change in the retention of *R*- or *S*-propranolol occurred; this change indicated that a variation had occurred in the stability of the lipoprotein column. This evaluation was used to determine if retention was consistent over a long enough period of column use, thus enabling more extensive HPAC studies. After confirming that column stability was sufficient with such columns, similar columns were utilized in more extensive experiments, such as the measurement of the equilibrium binding constants and binding stoichiometry between applied drugs and immobilized lipoproteins. Typical chromatograms that were obtained during these types of evaluations are shown in Figure 1-8. The acceptable period of use for each of the lipoprotein columns was more than sufficient for the types of drug binding studies that were planned in the next phase of experiments [24,25,29].

Figure 1-8. Typical chromatograms obtained during lipoprotein column stability studies. This depicted study was carried out using *R*-propranolol and a 2.1 × 100 mm i.d. column containing immobilized LDL. The column was held at 37 °C and contained a mobile phase of pH 7.4, 0.067 M phosphate buffer flowing at 1.0 mL/min. The dashed vertical line depicts the central moment of the peak for *R*-propranolol at the beginning of this experiment. The volumes indicate the total volume buffer applied at the time the measurement was made. This figure is reproduced with permission from Ref. [25].

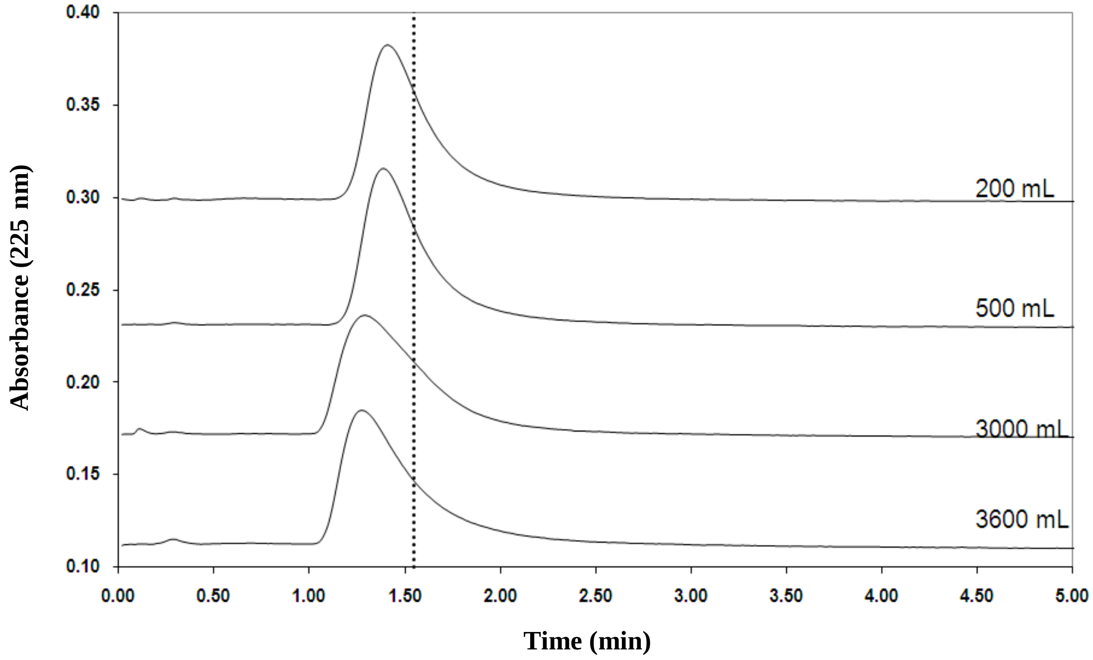
0.40
0.35
0.30
0.25
0.20
0.15
0.10
Absorbance (225 nm)
0.00
0.50
1.00
1.50
2.00
2.50
3.00
3.50
4.00
4.50
5.00
Time (min)
200 mL
500 mL
3000 mL
3600 mL

Frontal analysis studies of drug interactions with lipoproteins

A second method commonly used in the execution of HPAC binding studies is frontal analysis. Frontal analysis is performed by continuously applying a solution containing a known concentration of an analyte at a fixed flow rate to a column containing an immobilized ligand; this is analogous to a titration of the ligand binding sites that are available within the column for the analyte [9,10,52]. This technique has been used previously to quantitatively determine the amount of ligand in a column and the binding affinity of numerous solutes and serum proteins, including HSA and AGP [10]. Frontal analysis was employed throughout this dissertation to evaluate the HDL, LDL, and VLDL columns that were prepared and to determine and quantify the types of interactions these ligands had with an applied drug [24,25,29].

A typical chromatographic system used in performing HPAC in the frontal analysis mode is similar to that used for zonal elution but with one significant difference. In frontal analysis, a typical system utilizes at least two high pressure pumps or delivery lines that are capable of delivering various mobile phase solutions to the system. The application buffer is applied by one of the pumps or delivery lines, while the second pump/line delivers a solution containing a known concentration of the desired analyte dissolved in the application buffer. Typically, the application buffer is a solution designed to mimic the pH and surroundings of the ligand in its natural environment. In this dissertation, such work was conducted by using pH 7.4, 0.067 M phosphate buffer as the application solution to mimic serum conditions. Control of the solution applied to the HPAC column at any given time is maintained by using a high pressure valve. A third pump can be used to a pass an elution buffer through the column to release any analyte that has been retained; however, this was not necessary for the lipoprotein-drug interactions monitored in this dissertation. An on-line detector is used to monitor the elution profile for the analyte, and a computer or recording device is used to collect this data for analysis. The typical setup for a frontal analysis HPAC system is shown in Figure 1-9.

The binding capacity and equilibrium binding constants of an affinity column for an applied analyte are often measured by using frontal analysis studies. Over the course of a run, the analyte applied to the column by the application buffer results in the saturation of the fixed binding sites on the ligand, resulting in an increase in the amount of analyte that elutes from the column. The detector response over the course of the run generates a breakthrough curve, as illustrated in Figure 1-10. These breakthrough curves are generated at several concentrations of the analyte and at a known mobile phase composition and temperature. The volume of the analyte solution, or the moles of applied analyte, that are required to reach the mean position of this breakthrough curve is determined by integration of the curve. The mean position of the breakthrough curves can then be related to the concentration of the applied analyte, the amount of ligand in the column, and the equilibrium constants for the analyte-ligand interaction if the association and dissociation kinetics of the analyte-ligand interaction are known or assumed to be fast relative to the time scale of the experiment [8,9]. This binding information is obtained by fitting the results of the frontal analysis experiments to expressions that represent one or more binding models. The models utilized in this dissertation for the assessment of drug-lipoprotein interactions are summarized in Table 1-2; which will be discussed further in the next section.

Figure 1-9. Typical system for performing frontal analysis. This Figure is reproduced with permission from Ref. [54].

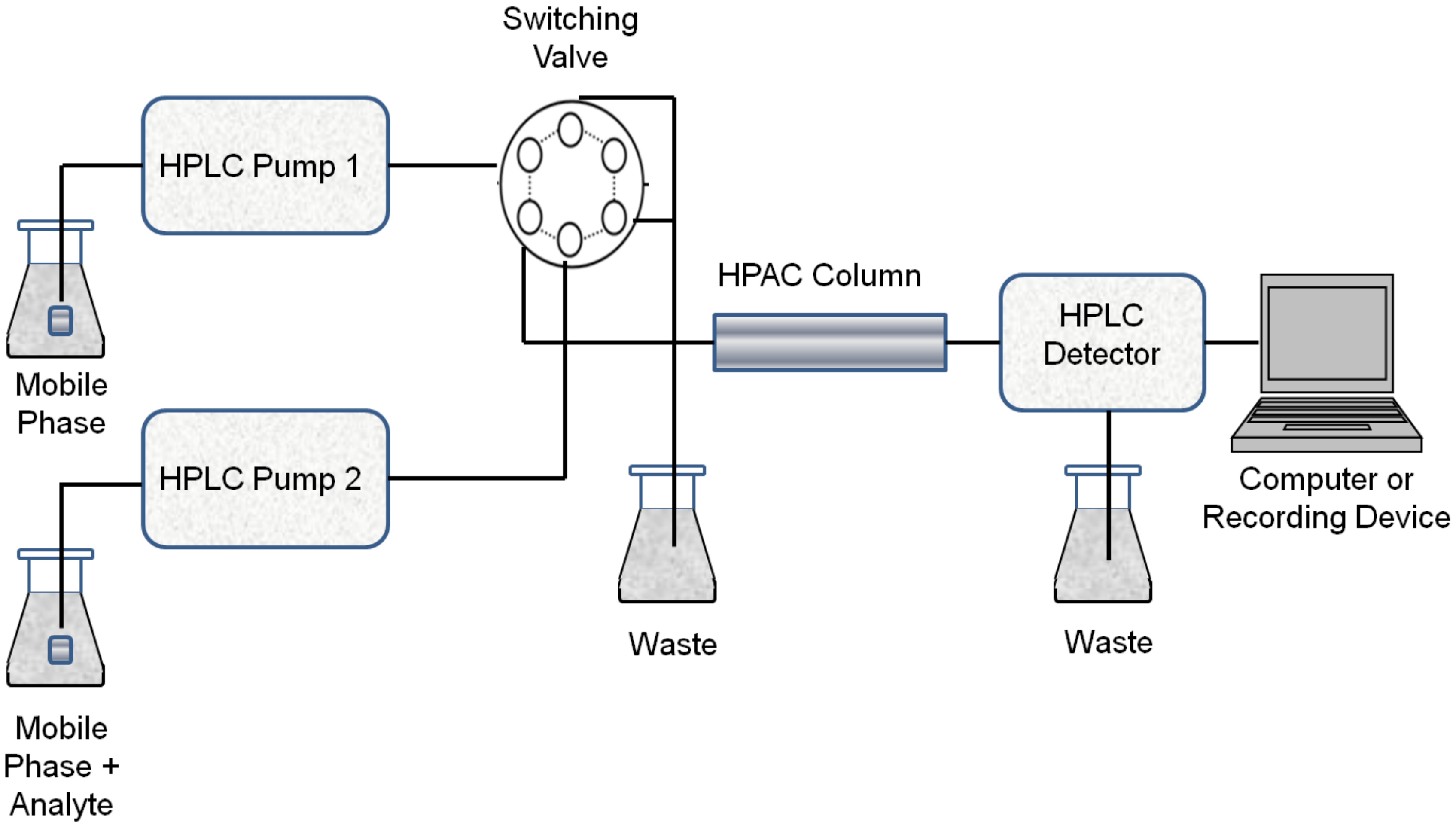
Switching Valve
HPLC Pump 1
Mobile Phase
HPLC Pump 2
Mobile Phase + Analyte
HPAC Column
HPLC Detector
Computer or Recording Device
Waste
Waste

Figure 1-10. Typical breakthrough curves obtained during frontal analysis studies with columns containing immobilized lipoproteins. This particular study was carried out using a 2.1 × 50 mm i.d. column containing immobilized HDL. The column was held at 37 °C while various concentrations of *R*-propranolol dissolved in pH 7.4, 0.067 M phosphate buffer were applied at 1.0 mL/min. These chromatograms are reproduced with permission from Ref. [24].

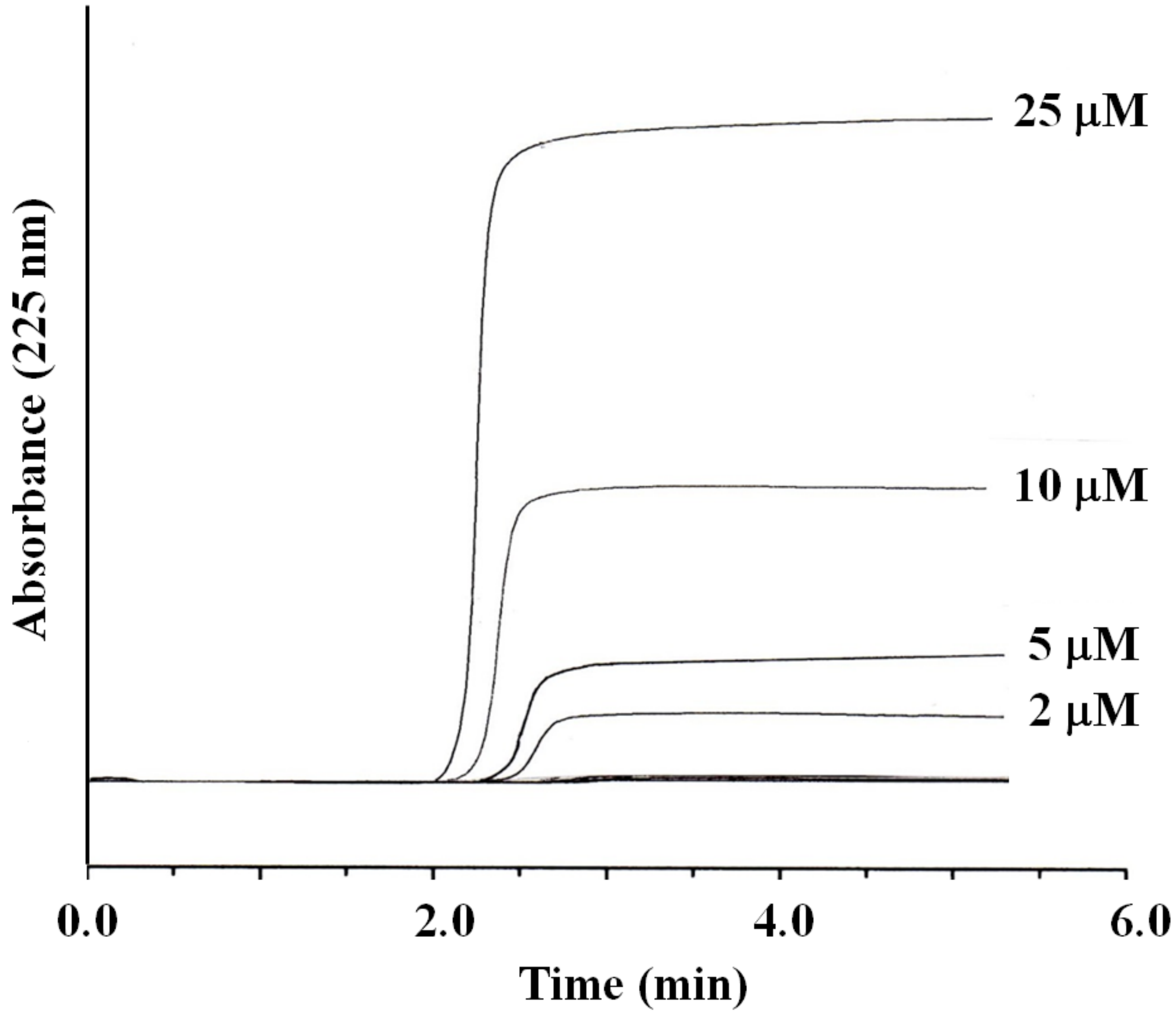
Absorbance (225 nm)
25 μM
10 μM
5 μM
2 μM
0.0
2.0
4.0
6.0
Time (min)

Various types of information about a solute-ligand interaction can be obtained from properly designed frontal analysis experiments. These experiments can provide details regarding the affinity and number of binding sites for a solute on an affinity ligand and the type of interaction(s) between the solute and ligand (e.g., single site versus multi-site binding, and saturable versus non-saturable interactions) [9,10]. Frontal analysis may also be employed to evaluate the effects of temperature, solvent composition, pH, or the impact of a competing agent on solute-ligand interactions, [9,10]. The speed and relatively large amount of information that can be obtained in a frontal analysis experiment on a HPAC system make this technique advantageous when compared to solution-based methods, such as equilibrium dialysis, for binding studies [9,10,52]. While HPAC may be operated in either frontal analysis or zonal elution modes, only frontal analysis is capable of simultaneously providing information on both the number of binding sites and equilibrium constants for a solute with an immobilized binding agent. The ability to obtain this information in a single set of experiments has made frontal analysis the preferred method in many drug-protein binding studies and for high-throughput screening of drug-protein interactions [9,10,52].

A properly designed frontal analysis experiment requires the consideration and optimization of several factors prior to execution. One such factor is the choice of the affinity column. The column should be prepared in a way that provides a ligand that is stable over the course of the study and that mimics the ligand's behavior in its native environment [9,10]. The possibility of non-specific binding by the analyte to the support or other non-ligand components of the column must be minimized as well. This non-specific binding can be reduced through the proper selection of immobilization conditions. Any remaining non-specific binding may be accounted for and corrected by carrying out equivalent frontal analysis studies on a control column with no immobilized ligand present [9,10]. Analyte concentrations utilized in frontal analysis experiments should be selected by considering the expected equilibrium constants for the interaction and specific analyte properties (i.e., detectability and solubility) [8-10]. Finally, the approach utilized in determination of the breakthrough times must be considered. The point that is halfway between the baseline and the plateau can be used to find the breakthrough time for a symmetrical curve. Determination of the breakthrough time for an asymmetrical curve can be determined by finding the centroid of the first derivative of the curve or by determination of the point at which the area below the front portion of the curve is equal to the area above the latter portion of the curve [10]. This latter method was used in these studies as a non-symmetrical curve was typically seen for lipoprotein columns.

Potential models for drug-lipoprotein interactions

The structure of lipoproteins, as described earlier, lends itself to a number of possible interactions with drugs or other solutes. For example, previous studies have suggested that such substances may interact with the hydrophobic core or with phospholipids on the surface of the lipoprotein [21-23]. In addition, it is possible that the analyte may undergo more specific binding with the specific apolipoproteins that are incorporated in the lipoprotein particle or that a combination of several types of interactions may be present [24,25,29]. A depiction of these potential binding mechanisms is shown in Figure 1-11. Each of these four binding mechanisms was considered when analyzing frontal analysis data that were obtained for various drugs with HPAC columns containing immobilized lipoproteins [24,25,29].

The most basic interaction model evaluated for the drug-lipoprotein binding studies in this dissertation was one in which the drug interacted with the hydrophobic core of the lipoprotein or with a large group of non-saturable sites [20,21,24,25]. This type of interaction is represented in Table 1-2 by the non-saturable, or partition type, model in Eq. (3). A similar model in which the drug interacts with a single group of saturable sites, as might occur on the apolipoproteins at the surface of a lipoprotein, was also considered [24,25,29]. This type of interaction is represented by Eq. (4) in Table 1-2. The model described by Eq. (5) in Table 1-2 is a mixed-mode model, in which a combination of saturable sites and a group of non-saturable interactions are present [24,25,29]. This model is described by Eq. (5) in Table 1. Finally, a model where multiple, but distinct, site-specific interactions were present was evaluated by using Eq. (6) in Table 1-2 [24,25,29].

Figure 1-11. Possible drug-lipoprotein binding mechanisms. This Figure is reproduced with permission from Ref. [54].

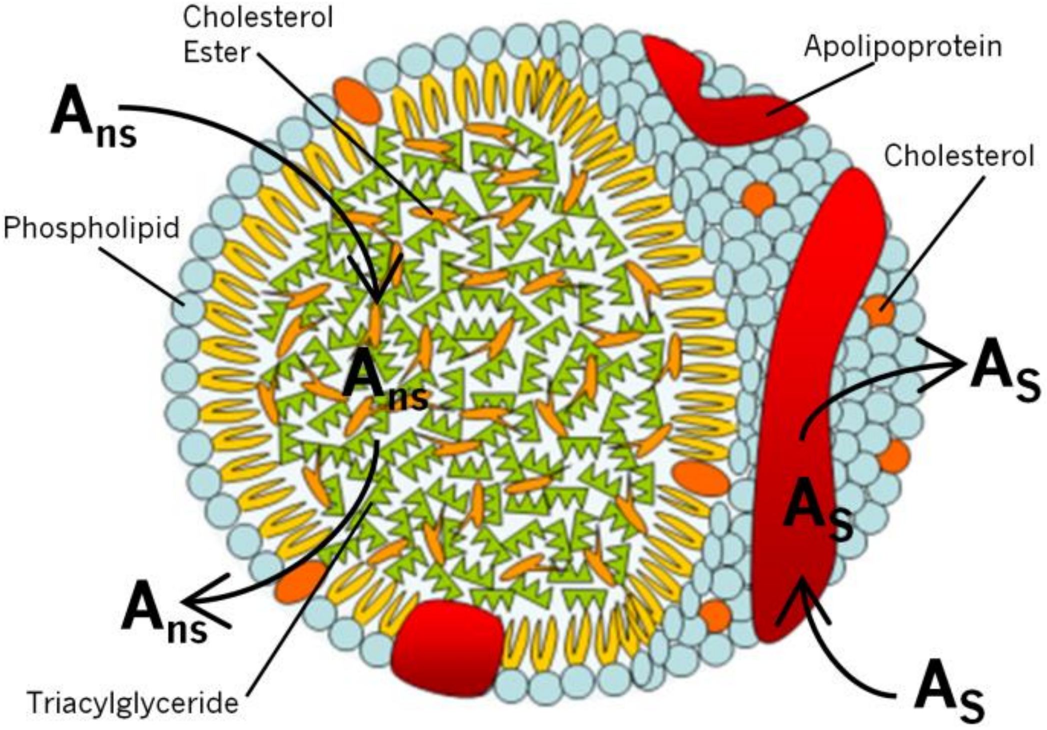
Cholesterol Ester
Apolipoprotein
A_{ns}
Cholesterol
Phospholipid
A_{ns}
A_S
A_S
A_{ns}
A_S
Triacylglyceride

Table 1-2. Binding models used with frontal analysis data for drugs on lipoprotein columns

Binding model	Predicted response[a]	
Non-saturable interaction	$m_{\mathrm{Lapp}} = m_{\mathrm{L1}}K_{\mathrm{a1}}[\mathrm{D}]$	(3)
Single group of saturable sites	$m_{\mathrm{Lapp}} = (m_{\mathrm{L1}}K_{\mathrm{a1}}[\mathrm{D}])/(1 + K_{\mathrm{a1}}[\mathrm{D}])$	(4)
Saturable sites + non-saturable interaction	$m_{\mathrm{Lapp}} = (m_{\mathrm{L1}}K_{\mathrm{a1}}[\mathrm{D}])/(1 + K_{\mathrm{a1}}[\mathrm{D}]) + m_{\mathrm{L2}}K_{\mathrm{a2}}[\mathrm{D}]$	(5)
Two groups of saturable sites	$m_{\mathrm{Lapp}} = (m_{\mathrm{L1}}K_{\mathrm{a1}}[\mathrm{D}])/(1+K_{\mathrm{a1}}[\mathrm{D}]) + (m_{\mathrm{L2}}K_{\mathrm{a2}}[\mathrm{D}])/(1+K_{\mathrm{a2}}[\mathrm{D}])$	(6)

[a] Symbols: m_{Lapp}, moles of applied analyte required to reach the mean position of the breakthrough curve; m_{L1}, total moles of active binding site 1; K_{a1}, association equilibrium constant for binding of the analyte to the ligand at site 1; [D], concentration of the applied drug; m_{L2}, total moles of active binding site 2; K_{a2}, association equilibrium constant for binding of the analyte to the ligand at site 2.

Adapted from Refs. [24,25,29].

The frontal analysis data obtained with HDL, LDL, and VLDL were evaluated using these four binding models. The first step in evaluating these binding models was to prepare a graph of the frontal analysis results that were obtained at a given temperature by plotting the apparent moles of analyte (m_{Lapp}) required to reach the mean position of the breakthrough curve versus the concentration of applied drug ([D]) used to generate this result. This plot was then fitted to each of the equations shown in Table 1-2 to determine the model that resulted in the best description of the experimental results. The quality of each fit was examined and compared by using the correlation coefficients for the fits, the overall residual values, and the distribution of the data about the best-fit line for each model (e.g., as given by the residual plots for each set of data). The results of this approach were then used to ascertain the type of binding that was occurring between the drug and lipoprotein, the number of moles of active binding sites present for the drug within the column, the association equilibrium constants for the interactions that were occurring. The results of this experimentation are described in later chapters of this dissertation.

Overall Goal and Summary of Work

The overall goal of this dissertation is to examine the use of HPAC in the evaluation of type and strength of interactions that occur between pharmaceutical drugs and lipoproteins. This work is needed to improve the speed and accuracy involved with measurement of drug-lipoprotein interactions and gain a more complete understanding of such interactions within the body. The studies provided in **Chapter 2** examine the interactions that occur between the drugs propranolol and verapamil and HDL. This work focused on previously unidentified binding between the drugs and apolipoproteins on the surface of HDL. **Chapter 3** describes the extension of the methods developed in work with HDL to LDL. The work presented in this chapter also examined the presence of stereoselective binding of propranolol by apolipoprotein B100. **Chapter 4** addresses the application of the HPAC methods to the study of interactions between propranolol and VLDL. The binding constants determined in **Chapters 2**, **3**, and **4** were evaluated against established literature values. **Chapter 5** then utilizes theoretical modeling to examine the experimental conditions necessary to determine the type of multi-site interactions that were ascertained in earlier chapters. Finally, **Chapter 6** discusses potential future studies that can utilize the methods developed in this dissertation.

References

1. Otagiri, M. *Drug Metab. Pharmacokinet.* **2005**, *20*, 309–323.
2. Bertucci, C.; Domenici, E. *Curr. Med. Chem.* **2002**, *9*, 1463.
3. Hage, D.S. *J. Chromatogr. B.* **2002**, *768,* 3-30.
4. Lindup, W.E. In *Progress in Drug Metabolism, Vol. 10*; Bridges, J.W.; Chasseaud, L.F.; Gibson G.G. Eds.; Tylor & Francis: New York, **1987**, Ch. 4.
5. Kwong, T.C. *Clin. Chim. Acta* **1985**, *151*, 193–216.
6. Svensson, C.K.; Woodruff, M.N.; Baxter, J.G.; Lalka, D. *Clin. Pharmacokinet.* **1986**, *11*, 450-469.
7. Wainer, I.W. *Trends Anal. Chem.* **1993**, *12*, 153-158.
8. Hage, D.S.; Tweed, S.A. *J. Chromatogr. B.* **1997**, *699,* 499-525.
9. Hage, D.S.; Chen, J. In *Handbook of Affinity Chromatography*; Hage, D.S. Ed.; CRC Press/Taylor & Francis: New York, **2006**, pp 595–628.
10. Hage, D.S.; Jackson, A.; Sobansky, M.; Schiel, J.E.; Yoo, M.Y.; Joseph, K.S. *J. Sep. Sci.* **2009,** *32*, 835–853.
11. Kratochwil, N.A.; Huber, W.; Muller, F.; Kansy, M.; Gerber, P.R. *Biochem. Pharmacol.* **2002**, *64*, 1355-1374.
12. Jonas, A. In *Biochemistry of Lipids, Lipoproteins, and Membranes*; Vance, D.E.; Vance, J.E. Eds.; Elsevier: Amsterdam, **2002**, pp 483–504.
13. Barklay, M. In *Blood Lipids and Lipoproteins: Quantitation, Composition, and Metabolism*; Nelson, G.J. Ed.; Wiley: New York, **1972**, pp 587–603.
14. Wasan, K.M.; Cassidy, S.M. *J. Pharm. Sci*. **1998**, *87*, 411–424.

15. Harmony, J.A.K.; Aleson, A.L.; McCarthy, B.M. In *Biochemistry and Biology of Plasma Lipoproteins*; Scanu, A.M.; Spector, A.A. Eds.; Marcel Dekker: New York, **1986**, pp 403-430.

16. Mbewu, A.D.; Durrington, P.N. *Atherosclerosis.* **1990**, *85*, 1–14.

17. Durrington, P.N.; In *Lipoproteins and Lipids*; Durrington, P.N. Ed.; Wright: London, **1989,** pp 255–277.

18. Havel, R.J.; Kane, J.P. In *The Metabolic and Molecular Basis of Inherited Disease*; Scriver, C.R.; Beaudet, A.L.; Sly, W.S.; Valle, D.; Childs, B.; Kinzler, K.W.; Vogelstein, B. Eds.; McGraw-Hill: New York, **1995**, pp 1129–1138.

19. Skipski, V.R.; In *Blood Lipids and Lipoproteins Quantitation, Composition, and Metabolism*; Nelson, G.J. Ed.; John Wiley: New York, **1972**, pp 471–583.

20. Glasson, S.; Zini, R.; D'Athis, P.; Tillement, J.P. ; Boissier, J.R. *Mol. Pharmacol.* **1980**, *17*, 187–191.

21. Ohnishi. T.; Mohamed, N.A.L.; Shibukawa, A.; Kuroda, Y.; Nakagawa, T.; El Gizawy, S.; Askal, H.F.; El Kommos, M.E. *J. Pharm. Biomed. Anal.* **2002**, *27*, 607–614.

22. Mohamed, N.A.L.; Kuroda, Y.; Shibukawa, A.; Nakagawa, T.; El Gizawy, S.; Askal, H.F.; El Kommos, M.E. *J. Chromatogr. A.* **2000**, *875*, 447–453.

23. Mohamed, N.A.L.; Kuroda, Y.; Shibukawa, A.; Nakagawa, T.; El Gizawy, S.; Askal, H.F.; El Kommos, M.E.; *J. Pharm. Biomed. Anal.* **1999**, *21*, 1037–1043.

24. Chen, S.; Sobansky, M.; Hage, D.S. *Anal. Biochem.* **2010,** *397*, 107-114.

25. Sobansky, M.R.; Hage, D.S. Anal. Bioanal. Chem. **2012**, *403*, 563-571.

26. Walters, R.R. *Anal. Chem.* **1985**, 57, 1099A-1101A.

27. Hage, D.S. In *Handbook of Affinity Chromatography*; Hage, D.S. Ed.; CRC Press/Taylor & Francis: New York, **2006.**

28. Ettre, L.S. *Pure Appl. Chem.* **1993**, *65*, 819-872.

29. Sobansky, M.R.; Hage, D.S. *Anal. Bioanal. Chem*. **2014**, *406*, 6203-6211.

30. Borga, O.; Azarnoff, D.L.; Forshell, G.P.; Sjoqvist, F. *Biochem. Pharmacol.* **1969**, *18*, 2135-2143.

31. Piafsky, K.M.; Borga, O. *Clin. Pharmacol. Ther*. **1977**, *22*, 545-549.

32. Hollósy, F.; Valkó, K.; Hersey, A.; Nunhuck, S.; Kéri, G.; Bevan, C. *J. Med. Chem.* **2006**, *49*, 6958-6971.

33. Kwong, T.C. *Clin. Chim. Acta* **1985**, *151*, 193–216.

34. Nelson, D.L.; Cox, M.M.; In *Lehninger Principles of Biochemistry*, 4th ed; W.H. Freeman: New York, **2005**.

35. Sager, G.; Nilsen, O.G.; Jacobsen, S. *Biochem. Pharmacol*. **1979**, *28*, 905-911.

36. Pike, E.; Skuterud, B.; Kierulf, P.; Lunde, P.K.M. *Clin. Pharmacol. Ther.* **1982**, *32*, 599-606.

37. Bicke, M.H. *J. Pharm. Pharmacol*. **1975**, *27*, 733-738.

38. Pike, E.; Kierulf, P.; Skuterud, B.; Bredesen, J.E.; Lunde, P.K.M. *Br. J. Clin. Pharmacol*. **1983**, *16*, 233-239.

39. Verbeeck, R.K.; Cardinal, J.A.; Allison, G.; Midha, K.K. *Biochem. Pharmacol.* **1983**, *32*, 2565-2570.

40. Hebb, A.R.; Godwin, T.F.; Gunton, R.W. *Canad. Med. Assoc. J*. **1968**, *98*, 246-251.

41. Hansson, L.; Malmerona, R.; Olander, R.; Rosenhall, L.; Westerlund, A.; Aberg, H.; Hood, B. *Klein. Wschr*. **1972**, *50*, 364-369.
42. Harrison, D.C.; Griffin, J.R.; Fiene, T.J. *N. Engl. J. Med*. **1965**, *273*, 410-415.
43. Henry, J.A.; Dunlop, A.W.; Mitchell, S.N.; Turner, P.; Adams, P. *J. Pharm. Pharmacol*. **1981**, *33*, 179-182.
44. Plumb, R.S.; Potts III, W.B.; Rainville, P.D.; Alden, P.G.; Shave, D.H.; Baynham, G.; Mazzeo, J.R. *Rapid Commun. Mass Spectrom*. 2008, 22, 2139-2152.
45. Rossi, S. In *Australia Medicines Handbook*; Rossi, S. Ed.; Australian Medicines Handbook Pty. Ltd.: Aldelaide, **2006**.
46. Hasegawa, J.; Fujita, T.; Hayashi, Y.; Iwamoto, K.; Watanabe, J. *J. Pharm. Sci.* **1984**, *73*, 442-445.
47. I. Moriguchi, S. Hirono, I. Nakagome, H. Hirano. Comparison of reliability of log P values for drugs calculated by several methods. Chem. and Pharm. Bulletin. 42 (1994), 976-978.
48. Gustavsson, P.E.; Larsson, P.O. In *Handbook of Affinity Chromatography*, 2nd ed.; Hage, D.S. Ed.; CRC Press: Boca Raton, **2006**.
49. Mallik, R.; Hage, D.S. *J. Sep. Sci.* **2006**, *29*, 1686-1704.
50. Mallik, R.; Jiang, T.; Hage, D.S. Anal. Chem. **2004**, *76*, 7013-7022.
51. Mallik, R.; Hage, D.S. *J. Pharm. Biomed. Anal.* **2008**, *46*, 820-830.
52. Hage, D.S.; Anguizola, J.; Barnaby, O.; Jackson, A.; Yoo, M.J.; Papastavros, E.; Pfaunmiller, E.; Sobansky, M.; Tong, Z. *Curr. Drug Metab*. **2011**, *12*, 313-328.
53. Kim, H.S.; Hage, D.S. In *Handbook of Affinity Chromatography*, 2nd ed.; Hage D.S. Ed.; CRC Press: Boca Raton, **2006**.

54. Sobansky, M.R.; Hage, D. S. In *Advances in Medicine and Biology*, Vol 53; Berhardt, L.V. Ed.; Nova: New York, **2012**.

CHAPTER TWO

ANALYSIS OF DRUG INTERACTIONS WITH HIGH DENSITY LIPOPROTEIN BY HIGH-PERFORMANCE AFFINITY CHROMATOGRAPHY

Portions of this chapter have previously appeared in S. Chen, M.R. Sobansky, and D.S. Hage, "Analysis of drug interactions with high-density lipoprotein by high-performance affinity chromatography", Analytical Biochemistry 2010, 397, 107-114.

INTRODUCTION

Lipoproteins, including HDL, are soluble macromolecular complexes of proteins and lipids that are present in the serum to transport hydrophobic compounds, such as cholesterols and triglycerides [1-3]. These complexes are also responsible for binding several basic and neutral hydrophobic drugs, including propranolol and verapamil [4]. The interactions that occur between drugs and biological agents, such as high density lipoprotein (HDL) and other lipoproteins, is important in determining the activity, pharmacokinetics and toxicity of drugs in the human body, as many drugs can undergo reversible interactions with serum proteins and lipoproteins [5-7]. This process impacts the distribution, delivery, metabolism, and excretion of these drugs [5-10]. As a result, the pharmaceutical industry often performs protein binding studies when designing a drug and in determining an appropriate mode of drug delivery capable of effectively treating a disease [7,8,11].

Propranolol and verapamil (refer to structures in Figure 1-4) are both known to interact with HDL. Equilibrium dialysis has been used to examine the binding of propranolol to HDL, and a method based on frontal analysis and CE has been used to study the interactions of propranolol and verapamil to HDL and other lipoproteins [12-15]. The overall affinity constants that have been measured for propranolol and verapamil with HDL in these reports are summarized in Table 2-1 [12-15].

In this chapter, HPAC was employed as a tool to study the interactions of propranolol with HDL. The stability of the HDL columns was evaluated by using zonal elution studies, as described in **Chapter 1**. An analysis of the binding mechanisms of the immobilized HDL for *R*- and *S*-propranolol and racemic verapamil was investigated by using frontal analysis. The ensuing results were compared to data obtained in previous studies utilizing soluble HDL in equilibrium dialysis or high-performance frontal analysis/CE. The overall objective of these studies were to test the feasibility of using immobilized HDL with HPAC in drug binding studies and for providing additional information on the nature of the interaction between propranolol with HDL in the circulation.

Table 2-1 Reported binding parameters for the interactions of propranolol and verapamil with HDL

Analyte	Overall affinity, nK_a (M^{-1})	Method and reference	Experimental conditions
Racemic propranolol	$1.60 (\pm 0.14) \times 10^4$	Equilibrium Dialysis [12]	pH 7.4 phosphate buffer (0.66M) 13 µM HDL, 37 °C
R-propranolol	$2.38 (\pm 0.14) \times 10^4$	High-performance frontal analysis / capillary electrophoresis [13]	pH 7.4 phosphate buffer ($I = 0.17$) 14.6 µM HDL, 37 °C
S-propranolol	$2.43 (\pm 0.15) \times 10^4$	High-performance frontal analysis / capillary electrophoresis [13]	pH 7.4 phosphate buffer ($I = 0.17$) 14.6 µM HDL, 37 °C
R-verapamil	$2.75 (\pm 0.61) \times 10^4$	High-performance frontal analysis / capillary electrophoresis [14]	pH 7.4 phosphate buffer ($I = 0.17$) 14.6 µM HDL, 37 °C
S-verapamil	$2.81 (\pm 0.33) \times 10^4$	High-performance frontal analysis / capillary electrophoresis [14]	pH 7.4 phosphate buffer ($I = 0.17$) 14.6 µM HDL, 37 °C

EXPERIMENTAL

Reagents

The human HDL (catalog number L1567, lot no. B73112), *R*-propranolol, *S*-propranolol, and racemic *R/S*-verapamil were obtained from Sigma (St. Louis, MO, USA). Macherey Nagel (Düren, Germany) was provided Nucleosil Si-300 silica (7 µm particle diameter, 300 Å pore size). All reagents for bicinchoninic acid (BCA) protein assay were purchased from Pierce (Rockford, IL, USA). A total cholesterol assay test kit was obtained from Wako (Richmond, VA, USA). All other unspecified chemicals were of the highest grades available. All solutions were prepared using water from a Nanopure purification system (Barnstead, Dubuque, IA, USA) that was filtered with Osmonics 0.22 µm nylon filters from Fisher Scientific (Pittsburgh, PA, USA).

Apparatus

The high performance liquid chromatograph consisted of two PU-980 pumps (Jasco, Tokyo, Japan), one LabPro injection valve (Rohnert Park, FL, USA), and a UV/Vis SpectroMonitor 3200 variable wavelength absorbance detector from LDC Thermoseparations (Riviera Beach, FL, USA). Chromatographic data were collected and processed using programs based on Labview 5.1 or 7.0 (National Instruments, Austin, TX, USA). Stationary phase was packed into stainless steel columns using a slurry packer from Alltech (Deerfield, IL, USA). A PolyScience circulating water bath from VWR (Buffalo Grove, IL, USA) was used to control the temperature of columns and mobile phases.

Preparation of the HDL support

The immobilization of high density lipoprotein on a silica support followed the general procedure outlined in **Chapter 1**. The first step in the process was to prepare a diol-bonded phase from Nucleosil Si-300 silica, which was accomplished according to a published procedure [16,17]. This protocol provided a surface utilized in a modified form of the Schiff base reaction to covalently attach HDL particles to the silica [18]. The immobilization was successfully completed by placing 0.2 g of the diol-bonded silica into 4 ml of 90:10 (v/v) mixture of acetic acid and water and subsequently adding 0.2 g periodic acid. The mixture was sonicated under vacuum for 15 min and shaken on a wrist action shaker for over 2 h in the dark at room temperature. The reaction yielded aldehyde-activated silica that was rinsed six times with water and four times with pH 6.0, 0.10 M potassium phosphate buffer in preparation for reaction with primary amine groups.

The immobilization of HDL was begun by suspending the aldehyde-activated silica in 1 ml of pH 6.0, 0.10 M potassium phosphate buffer and sonicating under vacuum for 5 min. A 20 mg portion of HDL and 4.3 mg of sodium cyanoborohydride ($NaCNBH_4$) were added to this slurry and the mixture was shaken in the dark at 4 ºC for 3 days. The resulting immobilized HDL support was rinsed four times with pH 7.0, 0.10 M potassium phosphate buffer. Remaining aldehyde groups on the silica were reduced by dissolving a 3.4 mg portion of sodium borohydride ($NaBH_4$) in 2 ml of pH 7.0, 0.10 M potassium phosphate buffer and adding to the HDL support. This mixture was shaken for 90 min at room temperature and subsequently rinsed six times using pH 7.0, 0.10 M potassium phosphate buffer. The final HDL immobilized support was held in pH 7.0

buffer at 4 ºC until use. A column with the same dimensions was packed with diol silica and used as a control. The HDL and control supports were downward slurry packed into 1 cm × 2.1 mm i.d. or 5 cm × 2.1 mm i.d. stainless steel columns at 3500 psi using 0.067 M potassium phosphate buffer, pH 7.4, as the packing solution. Portions of each support were retained for determining immobilization efficiency. The columns were stored in 0.067 M phosphate buffer, pH 7.4, at 4°C when not in use.

Determination of immobilization efficiency

The final HDL support was evaluated to determine the coverage of HDL on the support. These values were used to determine how much HDL was contained within the packed HPAC columns and to determine binding constants. Two different procedures were utilized to determine the HDL immobilization efficiency. The first method was to determine the protein content of the HDL support using a BCA protein assay [19,20]. To perform this evaluation, a HDL stock standard was prepared in potassium phosphate buffer (0.067 M, pH 7.4) and serial dilutions were used to generate a standard curve. A blank was prepared from diol-bonded silica. The absorbances of the blank and sample solutions were determined at 562 nm after the solutions were filtered through a 0.2 μm nylon filter. The diol-bonded silica blank response was equivalent to less than 0.1 mg of protein per gram of silica.

Total cholesterol content of the support was determined by using an enzymatic colorimetric method [20,21]. As with the BCA assay, a blank was prepared from diol-bonded silica. A series of dilutions in potassium phosphate buffer (0.067 M, pH 7.4) was performed from the standard solution included in the Wako Cholesterol E assay kit to generate a standard curve. Samples were prepared by suspending the HDL support and the diol-bonded silica control support in 0.067 M potassium phosphate buffer, pH 7.4. An aliquot of working reagent solution (prepared from color reagent and buffer solution provided with the Wako Cholesterol E assay kit) was added to all samples and standards as described by the manufacturer. Samples and standards were allowed to react as described by the manufacturer's instructions, filtered through a 0.2 μm nylon filter, and absorbance was measured at 600 nm.

Chromatographic studies

Chromatographic studies were conducted using the HPAC apparatus that was described earlier. Prior to these studies, the HDL column or control column was placed into HPLC column water jackets from Alltech and connected to a circulating water bath for equilibration at the desired temperature. All mobile phases were filtered through Osmonics 0.22 μm nylon filters and degassed under vacuum over 15 min prior to use. Elution of *R*- or *S*-propranolol was monitored at a wavelength of 225 nm, and elution of *R*- or *S*-verapamil was monitored at 229 nm. Sodium nitrate was utilized as a non-retained solute; elution of this compound was monitored at 205 nm.

Zonal elution experiments were performed as described in **Chapter 1**. These studies were used in the evaluation of HDL column stability over time. The mobile phase for the zonal elution studies was a 0.067 M potassium phosphate buffer, pH 7.4. This buffer was continuously applied to a 1 cm × 2.1 mm i.d., column containing the HDL support at a flow rate of 1.0 ml/min and a temperature of 37 ºC. The void times for the HDL and control columns were determined by injecting a 20 μL sample of 1 μM sodium nitrate. A 20 µL portion of 1 µM samples containing *R*- or *S*-propranolol was injected onto the HDL column (and also initially on the control column) every 12 h for over 300 h to evaluate changes in the retention properties of the HDL support. The central moment for each peak was determined using Seasolve Peakfit 4.12 software and reported as the retention time for each peak.

Frontal analysis studies were conducted to examine the binding of *R*- and *S*-propranolol with immobilized HDL as described in **Chapter 1**. These studies were conducted using a 5 cm × 2.1 mm i.d. column packed with the HDL support or control support. Measurements were made in the presence of 0.067 M potassium phosphate buffer pH 7.4, at a flow rate of 1.0 ml/min. The temperature for the studies was set at 4 ºC, 27 ºC or 37 ºC. Slight modifications to the flow rate (between 0.4 and 1.2 ml/min) resulted in less than a 2% change in the measured binding capacities. All determinations were achieved within the first 60 h of operation for each new HDL column. This time frame was within the usable time range determined during zonal elution studies. Solutions containing between 0.1-25 µM *R*- or *S*-propranolol or 0.25-10 µM *R*- or *S*-verapamil dissolved in the mobile phase were applied to the HDL column and control column. A total of eleven different concentrations of each propranolol enantiomer and six different concentrations of each verapamil were applied and analyzed during the frontal analysis studies. Elution of retained compounds was accomplished by passing 0.067 M potassium phosphate buffer, pH 7.4, through the column prior to the next frontal analysis experiment. The frontal analysis experiments generated breakthrough curves [7] that were integrated using Labview 5.1. Based upon the integration of this breakthrough curve, the amount of drug that required to saturate the HDL column or control column was determined.

Non-specific interactions with system components other than HDL comprised approximately 5-15% of the total retention noted for *R*- and *S*-propranolol and 15-22% of the total retention of *R*- and *S*-verapamil on the HDL column. These values are known to vary between analytes and must be evaluated on a case-by-case basis [7,22]. The values reported in this dissertation were determined by analysis of the breakthrough curves obtained on the HDL and control columns. Corrections were made for non-specific binding and the void time by subtracting the breakthrough time of the control column from that of HDL column at each concentration of drug as has been reported in past studies with the same drugs and other HPLC supports or binding agents [9,10,22,23].

RESULTS AND DISCUSSION

Composition and stability of the HDL support

The composition of the HDL support was examined by using both the BCA protein assay and the cholesterol assay, as described in the previous sections. The results of the BCA assay indicated that the support contained 68 (± 5) mg HDL per gram silica. The cholesterol assay indicated that the total cholesterol content of the support was 3.4 (± 0.4) mg cholesterol per gram silica. The protein and cholesterol content of the HDL support gradually decreased during long term storage in 0.067 M phosphate buffer, pH 7.4. The magnitude of this change was approximately the same for both the protein and cholesterol content, with the protein content decreasing by 43 (± 4)% and the cholesterol content decreasing by 56 (± 7)% over three months**.** The consistent rate of change in both the cholesterol and protein content measured before and after three months of storage indicated that these changes in the composition of the support were due to loss of intact HDL particles and not the selective loss of apolipoproteins or cholesterol.

Although the stability of columns containing immobilized lipoproteins during storage is important for HPAC methodologies, this does not prove their stability when used in a flow-based system. The fact that lipoproteins are macromolecular congregates that are held together by non-covalent interactions may make them more susceptible to degradation or collapse than traditional binding agents such as HSA or AGP [1,2]. The fact that approximately half of the original HDL particles were still immobilized to the silica support following three months of storage in buffer initially demonstrated that the HDL support might be suitable for use over shorter periods of time in a flow-based system employed in HPAC studies.

The stability of the HDL support in a flow-based chromatographic system was evaluated using zonal elution experiments in which injections of *R*- or *S*-propranolol were made onto this column over time. The retention of *R*-propranolol on the immobilized HDL support over time is shown in Figure 2-1. Similar results were obtained for *S*-propranolol. In this study, the first injection of *R*-propranolol occurred after 10 ml of mobile phase had passed through the new HDL column. Reproducible retention was obtained over the first five days (120 h) of use. During this time period, the HDL column retained *R*-propranolol for approximately 39 to 41 s, corresponding to a retention factor (*k* or k') of 2.6 to 2.7. The amount of mobile phase that was passed through this column during the first five days of use was 7.2 L, which was equivalent to 3.6×10^4 column volumes. These data confirmed that the HDL column was sufficiently stable for drug binding studies under such conditions.

Following the first five days of use, a gradual decrease in the retention of *R*- and *S*-propranolol on the HDL column occurred. This can be exemplified by evaluating the retention of *R*-propranolol after 12 days of continuous operation; after this time period, the retention factor for *R*-propranolol diminished from its original value of 2.6-2.7 to just over 1.0. This change corresponded to a decrease of roughly 9% per day after the first five days of use. Enantiomeric selectivity for *R*- or *S*-propranolol was not observed with the HDL column at any time during this study; which supports previously reported results obtained using CE-frontal analysis [13].

Figure 2-1. Change in the retention factor for *R*-propranolol as function of mobile phase volume. The mobile phase was 0.067 M phosphate buffer, pH 7.4, which was passed through a 1 cm × 2.1 mm i.d. HDL column at 1 ml/min and 37^{o}C for up to 300 h. This Figure is reproduced with permission from Ref. [24].

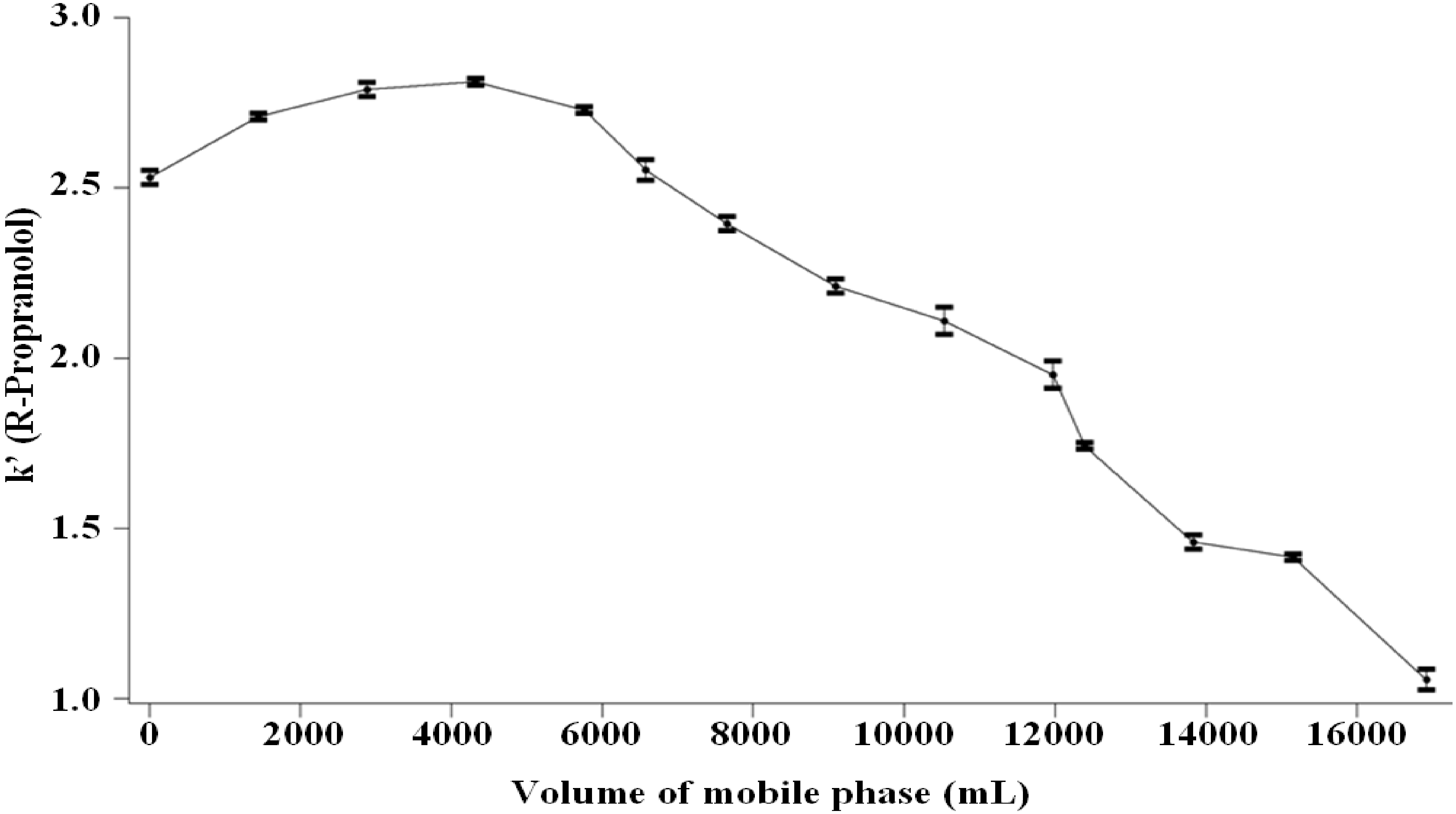
3.0
2.5
2.0
1.5
1.0
k' (R-Propranolol)
0
2000
4000
6000
8000
10000
12000
14000
16000
Volume of mobile phase (mL)

Frontal analysis studies of propranolol binding to HDL.

Frontal analysis studies were initiated to determine the binding capacity and equilibrium binding constants for interactions that may occur between *R/S*-propranolol and HDL. The data were collected within the first 120 h of column preparation, as this was the period of time in which HDL columns were previously determined to be stable. Typical frontal analysis breakthrough curves are shown in Figure 2-2. These curves were obtained while analyzing *R*-propranolol on the HDL columns. The mean position of each breakthrough curve (m_{Lapp}) was determined via integration and used in conjunction with the known concentration of applied drug ([A]) to generate double-reciprocal plots of $1/m_{Lapp}$ versus 1/[A]. When a single type of binding is present, this type of plot should result in a linear relationship. In the event of multiple types of binding are present, the double-reciprocal plot will show negative deviations from linear at high analyte concentrations or low values of 1/[A] [7]. The double-reciprocal plots for *R*- and *S*-propranolol interactions with HDL at each temperature examined in this study resulted in a negative deviation at low values of 1/[A]. This deviation was indicative of multiple interactions between *R*- and *S*-propranolol and HDL. A representative double-reciprocal plot is shown in Figure 2-3.

Figure 2-2. Typical frontal analysis results obtained for the application of *R*-propranolol to a 2.1 × 50 mm HDL column at analyte concentrations of 0.1, 0.2, 0.3, 0.4, 0.5, 1, 2, 5, 10 or 25 µM. These results were obtained at 1.0 ml/min and 37ºC in the presence of 0.067 M phosphate buffer, pH 7.4. This Figure is reproduced with permission from Ref. [24].

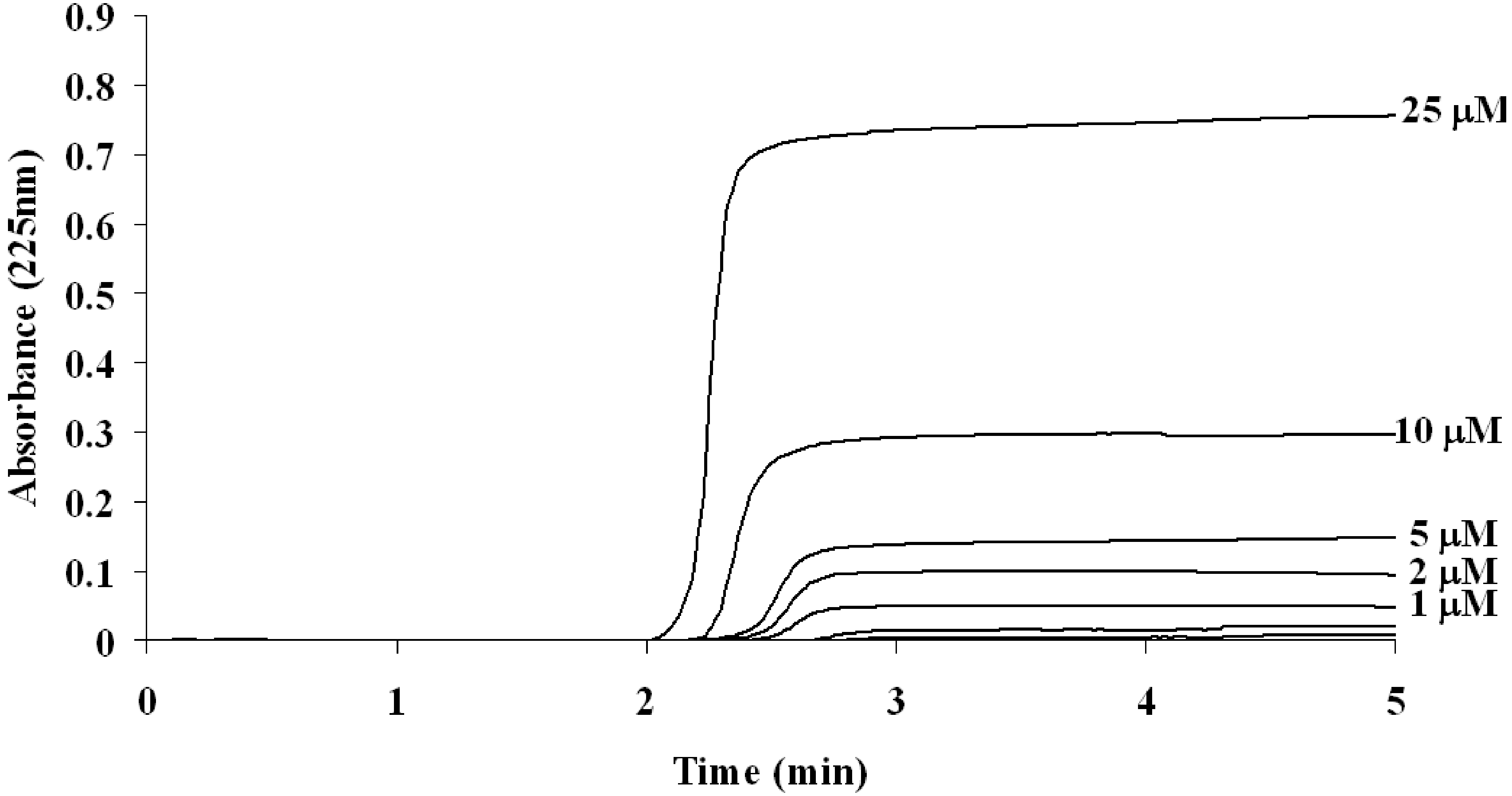

0.9
0.8
0.7
0.6
0.5
0.4
0.3
0.2
0.1
0
Absorbance (225nm)
0
1
2
3
4
5
Time (min)
25 μM
10 μM
5 μM
2 μM
1 μM

Figure 2-3. Double-reciprocal plot of frontal analysis data obtained for the binding of *R*-propranolol to a 2.1 × 50 mm HDL column at 37°C and in the presence 0.067 M phosphate buffer, pH 7.4, at a flow rate of 1.0 ml/min. The best fit line was obtained using data points in the upper region of this plot, which are designated by the closed squares (■) and cover *R*-propranolol concentrations that ranged from 0.1 μM to 2.5 μM. Data points in the lower region of this plot (i.e., at higher concentrations of *R*-propranolol) showed negative deviations from the linear fit to the upper data points and are represented by open squares (□). The equation for the best fit line to the data represented by the closed squares was $y = 5.45\ (\pm\ 0.07) \times 10^2 + 2.7\ (\pm\ 0.6) \times 10^8$; the correlation coefficient of this best fit line was 0.99985 ($n = 12$). This Figure is reproduced with permission from Ref. [24].

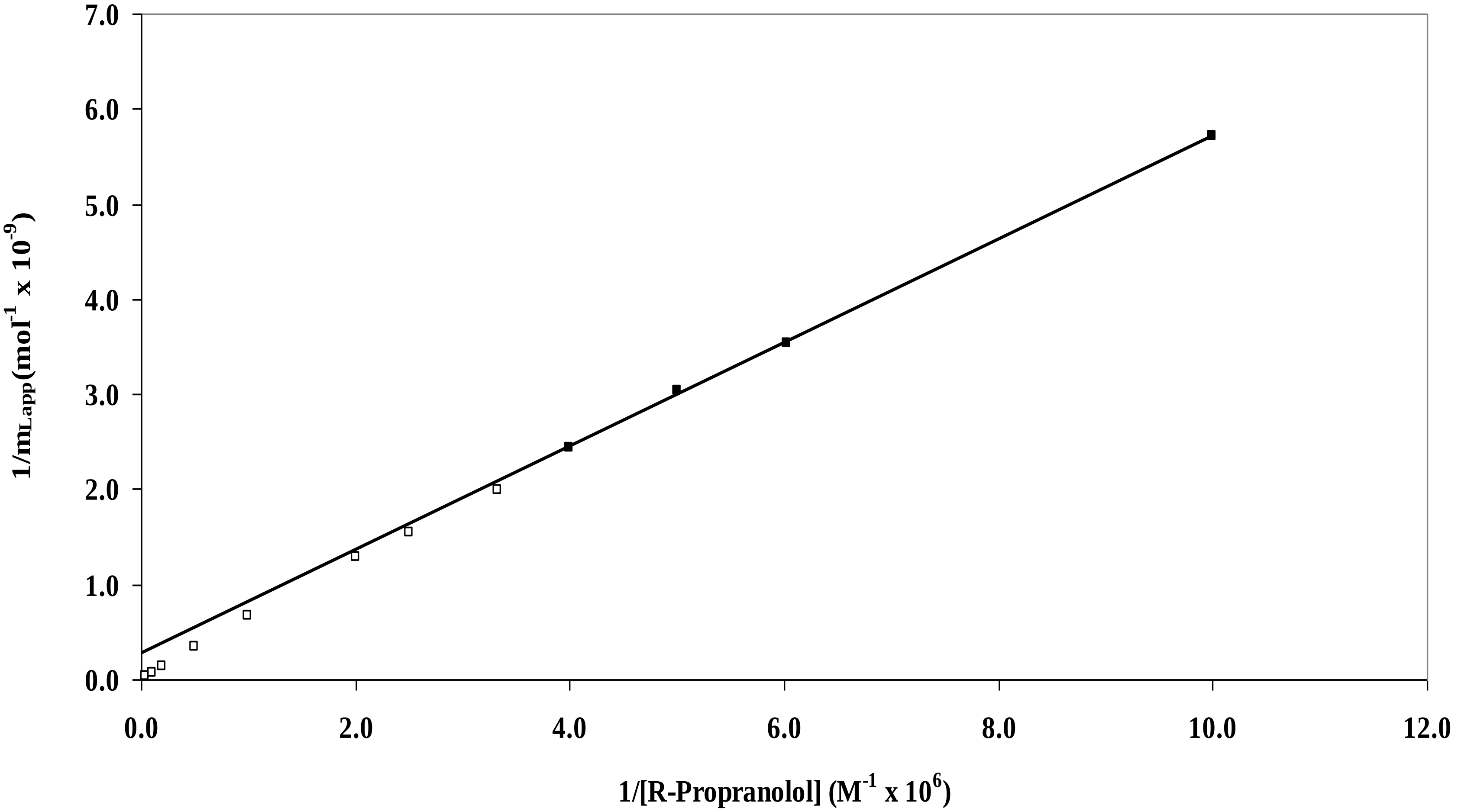
7.0
6.0
5.0
4.0
3.0
2.0
1.0
0.0
$1/m_{Lapp}(mol^{-1} \times 10^{-9})$
0.0
2.0
4.0
6.0
8.0
10.0
12.0
$1/[\text{R-Propranolol}]\ (M^{-1} \times 10^{6})$

Examination of the double-reciprocal plots revealed that multiple types of interactions were present and indicated that further analysis was necessary to determine the nature of the interactions that were occurring between *R/S*-propranolol and HDL. Therefore, the frontal analysis data was next evaluated by using plots of m_{Lapp} versus [A] for *R*- and *S*-propranolol. Examination of these plots revealed the presence of a non-linear relationship; examples are given in Figure 2-4. These data were subsequently fit to equations representing four distinct binding models (refer to summary in Table 1-2) that described the potential interactions of the applied drugs with HDL.

One type of binding that may occur between an analyte and HDL is saturable, site specific binding to apolipoproteins present on the surface of HDL [12-14]. This type of interaction is represented by the “single group of saturable sites” binding model. The “two groups of saturable sites” model depicts saturable site-specific binding to multiple locations and would be expected if the apolipoprotein contained two binding regions. The second possible type of binding is non-specific binding of the drug with the phospholipid layer and/or interior hydrophobic core, as represented by the “non-saturable interaction” binding model [12-14]. The presence of both saturable and non-saturable binding in combination can also be considered through the fourth binding model. Table 2-2 and Table 2-3 contain the association equilibrium constants, binding capacities, or global affinity constants that were obtained when fitting the frontal analysis results for each propranolol enantiomer to the four binding models.

Figure 2-4. Examination of frontal analysis data for *R*-propranolol on an HDL column at 37^{o}C when fit according to various binding models. These models were as follows: (a) one group of non-saturable interactions, (b) one group of saturable sites, (c) two separate groups of saturable sites, and (d) a group of non-saturable interactions plus a group of saturable sites. The insets show the residual plots for the fit of each model to the experimental data. These results were obtained in the presence of 0.067 M phosphate buffer, pH 7.4.. The correlation coefficients were as follows: (a) 0.99937, n = 12; (b) 0.99989, n = 12; (c) 0.99996, n = 12; and (d) 0.99996, n = 12. This figure is reproduced with permission from Ref. [24].

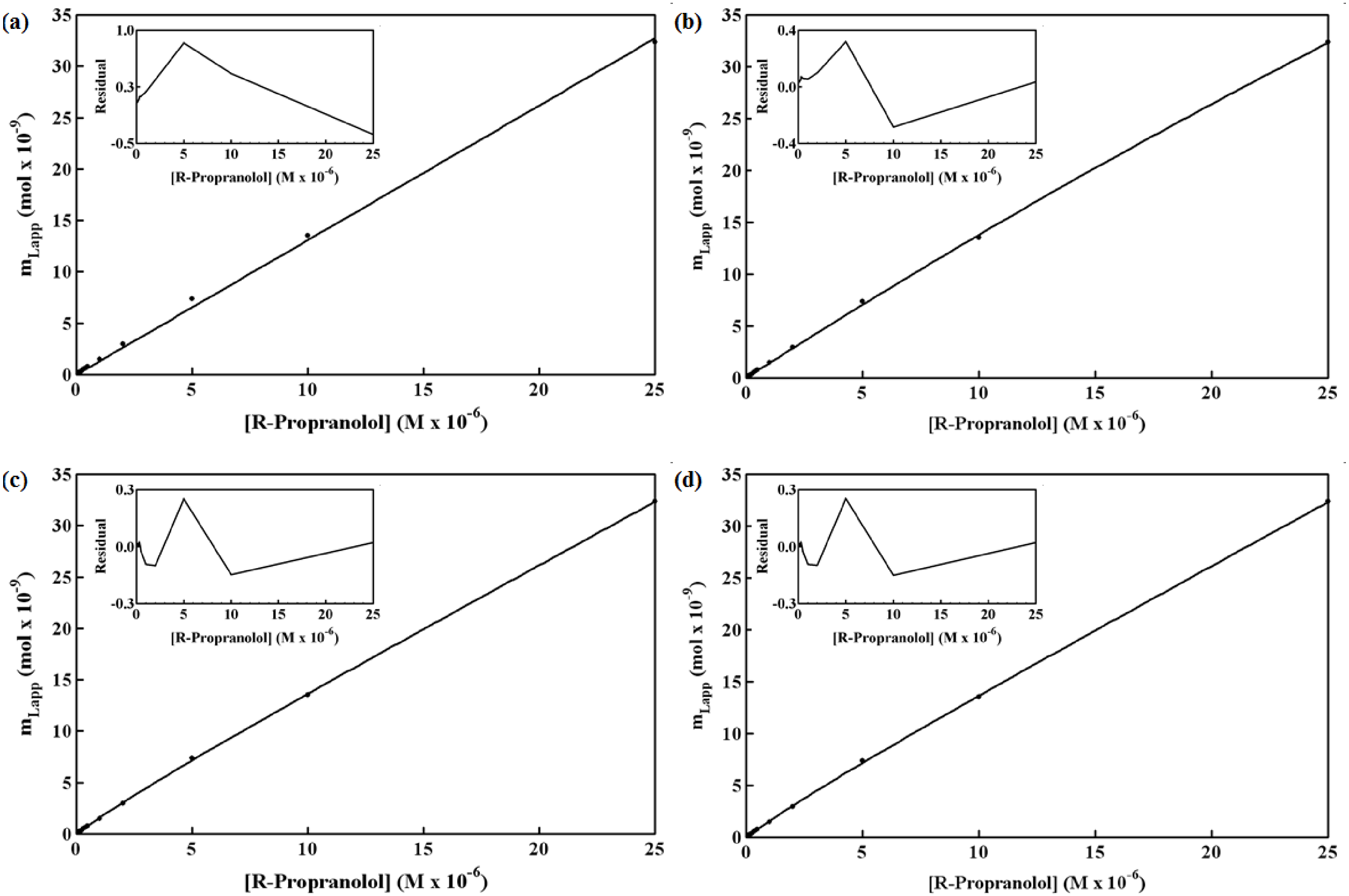
(a)
(b)
(c)
(d)
m_{Lapp} (mol x 10^{-9})
[R-Propranolol] (M x 10^{-6})
0
5
10
15
20
25
30
35
Residual
1.0
0.3
-0.5
0.4
0.0
-0.4
0.3
0.0
-0.3

Table 2-2 Binding parameters obtained for *R*-propranolol on a HDL column at various temperatures[a]

Enantiomer	Binding Model	Temperature	m_{L1} (mol)	K_{a1} (M^{-1})	m_{L2} (mol)	K_{a2} (M^{-1})	nK_a[b] (M^{-1})
R-Propranolol	Non-saturable Interaction	4 °C	-	-	-	-	4.4 (± 0.1) x 10^{4}
	Single group of saturable sites	4 °C	1.4 (± 0.1) x 10^{-7}	1.2 (± 0.1) x 10^{4}	-	-	-
	Two groups of saturable sites	4 °C	3.8 (± 3.0) x 10^{-9}	2.0 (± 1.3) x 10^{5}	4.5 (± 5.3) x 10^{-7}	2.8 (± 3.7) x 10^{3}	-
	Two interactions: saturable + non-saturable	**4 °C**	**6.4 (± 0.8) x 10^{-9}**	**1.4 (± 0.2) x 10^{5}**	**-**	**-**	**3.7 (± 0.3) x 10^{4}**
R-Propranolol	Non-saturable Interaction	27 °C	-	-	-	-	4.8 (± 0.1) x 10^{4}
	Single group of saturable sites	27 °C	1.7 (± 0.1) x 10^{-7}	9.7 (± 0.9) x 10^{3}	-	-	-
	Two groups of saturable sites	27 °C	4.1 (± 0.2) x 10^{-7}	2.6 (± 0.1) x 10^{3}	1.6 (± 0.6) x 10^{-8}	3.8 (± 0.6) x 10^{4}	-
	Two interactions: saturable + non-saturable	**27 °C**	**5.4 (± 0.6) x 10^{-9}**	**1.4 (± 0.2) x 10^{5}**	**-**	**-**	**3.9 (± 0.3) x 10^{4}**
R-Propranolol	Non-saturable Interaction	37 °C	-	-	-	-	4.4 (± 0.1) x 10^{4}
	Single group of saturable sites	37 °C	3.0 (± 0.4) x 10^{-7}	4.7 (± 0.7) x 10^{3}	-	-	-
	Two groups of saturable sites	37 °C	2.1 (± 6.7) x 10^{-7}	2.4 (± 13000) x 10^{3}	1.5 (± 13000) x 10^{-7}	6.1 (±13000) x 10^{3}	-
	Two interactions: saturable + non-saturable	**37 °C**	**2.2 (± 0.7) x 10^{-9}**	**1.9 (± 0.8) x 10^{5}**	**-**	**-**	**4.1 (± 0.3) x 10^{4}**

[a] The numbers in parentheses represent a range of ± 1 S.D. All of these results were measured in pH 7.4, 0.067 M potassium phosphate buffer.

[b] The value for nK_a for a non-saturable interaction was obtained by dividing the best-fit result for $m_L K_a$ by the estimated moles of HDL in the column. This latter value was obtained by using the protein content of the HDL support, which was determined using an average molar mass for HDL of 1.8 × 10^{5} g/mol.

The best fit model is represented in **bold**.

Table 2-3 Binding parameters obtained for *S*-propranolol on a HDL column at various temperatures[a]

Enantiomer	Binding Model	Temperature	m_{L1} (mol)	K_{a1} (M^{-1})	m_{L1} (mol)	K_{a1} (M^{-1})	nK_a[b] (M^{-1})
S-Propranolol	Non-saturable Interaction	4 °C	-	-	-	-	4.8 (± 0.1) x 10^4
	Single group of saturable sites	4 °C	1.4 (± 0.1) x 10^{-7}	1.3 (± 0.1) x 10^4	-	-	-
	Two groups of saturable sites	4 °C	2.9 (± 1.7) x 10^{-7}	5.2 (± 3.8) x 10^3	2.2 (± 1.9) x 10^{-9}	4.4 (± 4.1) x 10^5	-
	Two interactions: saturable + non-saturable	**4 °C**	**7.8 (± 2.5) x 10^{-9}**	**1.3 (± 0.5) x 10^5**	**-**	**-**	**3.9 (± 0.3) x 10^4**
S-Propranolol	Non-saturable Interaction	27 °C	-	-	-	-	4.4 (± 0.1) x 10^4
	Single group of saturable sites	27 °C	2.1 (± 0.2) x 10^{-7}	7.5 (± 0.7) x 10^3	-	-	-
	Two groups of saturable sites	27 °C	5.3 (± 1.3) x 10^{-7}	2.5 (± 0.7) x 10^3	1.8 (± 0.4) x 10^{-9}	3.0 (± 0.7) x 10^5	-
	Two interactions: saturable + non-saturable	**27 °C**	**3.9 (± 0.2) x 10^{-9}**	**1.6 (± 0.1) x 10^5**	**-**	**-**	**4.0 (± 0.3) x 10^4**
S-Propranolol	Non-saturable Interaction	37 °C	-	-	-	-	4.4 (± 0.2) x 10^4
	Single group of saturable sites	37 °C	2.2 (± 0.1) x 10^{-7}	6.8 (± 0.5) x 10^3	-	-	-
	Two groups of saturable sites	37 °C	5.3 (± 1.6) x 10^{-7}	2.4 (± 0.8) x 10^3	1.9 (± 0.7) x 10^{-9}	2.0 (± 0.6) x 10^5	-
	Two interactions: saturable + non-saturable	**37 °C**	**4.5 (± 0.2) x 10^{-9}**	**1.1 (± 0.1) x 10^5**	**-**	**-**	**3.7 (± 0.2) x 10^4**

[a] The numbers in parentheses represent a range of ± 1 S.D. All of these results were measured in pH 7.4, 0.067 M potassium phosphate buffer.

[b] The value for nK_a for a non-saturable interaction was obtained by dividing the best-fit result for $m_L K_a$ by the estimated moles of HDL in the column. This latter value was obtained by using the protein content of the HDL support, which was determined using an average molar mass for HDL of 1.8 × 10^5 g/mol.

The best fit model is represented in **bold**.

Double-reciprocal plots for the frontal analysis data indicated that multiple types of interactions between *R*- and *S*-propranolol and immobilized HDL were present, which was confirmed by the non-reciprocal plots shown in Figure 2-4, These plots provided a better fit with models involving more than one type of interaction. The models describing situations that contained single interactions did give acceptable correlation coefficients; however, the residual plots for these both these fits (see Figure 2-4 insets) resulted in a non-random pattern of data points about the best-fit line. Meanwhile, the two site binding models resulting in higher correlation coefficients (0.9998 or higher), lower residuals and a random distribution of the data about the best-fit line.

Further analysis of the two models involving multiple interactions generated additional information about the binding occurring in the drug-HDL systems. As depicted in Figure 2-4, the model based on two groups of saturable/non-saturable interactions (Figure 2-4c) resulted in essentially the same correlation coefficient (e.g., values for r greater than 0.9999) and residual plot as the two-site saturable model (Figure 2-4d). Despite the similarity between the two plots, the saturable/non-saturable model generated precise best-fit equilibrium constants (i.e., refer to the standard deviations listed for the K_{a1}, m_{L1} and $n\ K_a$ values for this model versus those listed for K_{a1}, m_{L1}, K_{a2} and m_{L1} in the model based on two groups of saturable sites). The differences in precision of the equilibrium constants can be explained by the fact that as K_{a2} [D] in the denominator of the model representing two groups of saturable sites approaches zero, the equation for this model approaches that of a model based on the presence of one saturable and one non-saturable interaction (refer to expressions in Table 1-2). This situation occurred in the fit of the two groups of saturable sites model to the frontal analysis data obtained for *R*- and *S*-propranolol interactions with HDL. The fact that under these conditions both fits are describing the same overall model in which a high affinity saturable site and a lower affinity, essentially non-saturable site is present explains the large uncertainly that resulted for the two groups of saturable sites fit and explains why the residual plots in Figures 2-4c and Figure 2-4d are so similar. The binding model where there was one high affinity saturable binding site and one lower affinity non-saturable interaction gave the best fit to the frontal analysis data.

The binding model based on two types of interactions, one saturable and one non-saturable, yielded the best fit equilibrium binding constants for *R*- and *S*-propranolol with HDL that are shown in bold in Tables 2-2 and 2-3 . The association equilibrium constant (K_{a1}) for the saturable interaction of HDL with *R*-propranolol had a value of 1.9 (± 0.8) × 10^5 at 37ºC, and *S*-propranolol had a K_{a1} of 1.1 (± 0.1) × 10^5 at 37ºC. These values represent relatively high affinity and specific binding that is likely occurring between propranolol and apolipoproteins on the surface of HDL [6-10]. This is supported by a closer examination of the m_{L1} values that were obtained with the moles of apolipoproteins that were estimated to be present in the HDL column (see following discussion). The second interaction that was identified represented low affinity and non-specific binding. This interaction had an overall affinity of 4.1 (± 0.3) × 10^4 M^{-1} at 37ºC for *R*-propranolol with HDL and 3.7 (± 0.2) × 10^4 M^{-1} at 37ºC for *S*-propranolol. This non-specific interaction is believed to occur between *R*- or *S*-propranolol and phospholipids or the non-polar core of HDL, as has been suggested in previous studies [12,13].

The impact temperature has on the interactions between *R*- and *S*-propranolol and HDL was also evaluated. The equilibrium binding constants determined for *R*- and *S*-propranolol with HDL are provided in Tables 2-2 and 2-3. Examination of the binding constants revealed that no appreciable effect on the magnitude of each association equilibrium constant with a change in temperature between 4^{o}C and 37^{o}C. The K_{a1} values obtained for both *R*- and *S*-propranolol were all in the range of 1.3 to 1.9 $\times 10^5$ M^{-1}, and the nK_{a2} values fell in the range of 3.7 to 4.1 $\times 10^4$ M^{-1}. In each case, the correlation coefficients for frontal analysis plots, analyzed according to a saturable/non-saturable model, were greater than 0.9999. The K_{a1} and nK_{a2} values that were obtained utilizing this model for the *R*- and *S*-enantiomers of propranolol overlapped within a range of ± 1 S.D. and were statistically equivalent at each temperature. This statistical equivalence between both types of interactions in this two site model indicated that interactions between *R/S*-propranolol and HDL were not stereoselective. This is the same conclusion suggested by the binding data reported in Ref. [13] (see Table 2-1). Furthermore, the binding constants measured for the low affinity interactions in this study was in agreement with the values reported in Ref. [13] at 37 °C when using a model based on a single type of non-saturable interaction.

Further examination of the high affinity binding sites was performed by comparing the measured binding capacity of this site with the known composition of the HDL support. The total moles (m_{L1}) of these high affinity binding sites, as determined through frontal analysis, were in the range of 2.2 to 7.8 nmol for both *R*- and *S*-propranolol between 4 and 37°C (averages, 4.7 nmol and 5.4 nmol, respectively). As was previously shown, the BCA assay conducted during the evaluation of the support indicated that 30 (± 2) nmol of HDL particles were present in the column. The relatively strong binding constants determined for the high affinity sites and the fact that their binding capacity was less than the total moles of HDL in the column strongly supported the conclusion that the apolipoproteins were culpable for these interactions. The fact that the binding capacities determined for the high affinity regions were less than the total number of HDL particles is likely related, in part, to immobilization effects. Previous studies have shown that immobilization effects are typically responsible for roughly a 50% loss in protein activity when using the Schiff base coupling method employed in this report (refer to Ref. [7] and references cited therein). In addition, an HDL particle contains multiple types of apolipoproteins per particle (i.e., up to 5-6 maximum) [1]. In a situation where only certain types of apolipoproteins are involved in this interaction, it is expected that the binding capacity is less than the total moles of HDL particles. Typical HDL apolipoprotein levels are ApoA1 (70%), ApoA2 (20%), and minor apolipoproteins (Apo E and Apo Cs, with 10% total) [1]. Further research is required to determine if there are indeed only particular apolipoproteins in this group that bind to *R*- and *S*-propranolol.

The typical concentrations *R*- and *S*-propranolol in clinical samples was used to evaluate the relative impact of the selective versus non-selective interactions of agents with HDL. The typical physiological concentration of HDL in serum is 13-14.6 μM [12,13], and the therapeutic range of propranolol in serum is 0.19-0.39 μM [25]. According to the data presented in Tables 2-2 and 2-3 for the saturable and non-saturable binding model, the high affinity sites on HDL are responsible for 25-40% of the binding that is occurring between *R*- and *S*-propranolol and this lipoprotein under such conditions. These high affinity sites are estimated to have been 85-97% saturated by *R*- or *S*-propranolol during the CE binding studies in Ref. [13]. Furthermore, the high affinity binding sites would have accounted for only 1-10% of the overall drug binding measured at the concentrations that were used in Ref. [13]. This explains why these interactions were not directly observed in this later study. A wider range of *R*- and *S*-propranolol concentrations was used with the measurements made using equilibrium dialysis [12]. However, the typical concentrations used in these studies were also sufficiently large to have made detection of the high affinity interactions possible.   In addition, it is important to remember that even in this study a relatively good fit occurred for the data with a single site, non-saturable model (see Figure 2-4) and the detection of two types of interactions between *R*- and *S*-propranolol and HDL was only possible through a close evaluation of this data and comparison of the frontal analysis data with several interaction models.

Frontal analysis studies of verapamil binding to HDL

As discussed in **Chapter 1**, the second drug that was used to evaluate binding by the HDL columns was verapamil. Studies were performed using racemic verapamil because HDL has been previously reported to have no stereoselective interactions with *R*- and *S*-verapamil [14]. Furthermore, evaluation of *R*- and *S*-propranolol binding in this study also indicated free of stereoselective binding to HDL.

Figure 2-5 shows a double-reciprocal plot of frontal analysis data that was obtained for verapamil on an HDL column. As was reported with propranolol, these results yield deviations from a linear response at high concentrations of verapamil.

Furthermore, analysis of non-reciprocal plots using the same data showed that the response deviated from the linear behavior predicted for only a non-saturable binding model (see equation in Table 1-2), with a correlation coefficient of r = 0.9952 (*n* = 6) obtained for the fit. While this correlation coefficient was reasonable, the model also gave a non-random distribution of data about the best fit line. A higher correlation coefficient (*r* = 0.9999) was obtained when using a model based on a single group of saturable sites, but this model was eliminated based upon the non-linearity observed in the double-reciprocal plot.

As with *R*- and *S*-propranolol, the binding model that yielded the best fit for the frontal analysis data for verapamil was based on a group of saturable sites and a set of non-saturable interactions (refer to summary in Table 2-4). The correlation coefficient for this binding model was *r* = 0.9999, and a random distribution of data about the best fit line was seen in the residual plot. In this fit, the sites responsible for saturable binding had an association equilibrium constant for verapamil of 6.0 (± 2.1) × 10^4 M^{-1} at 37 ^{o}C. The non-saturable interaction of verapamil with HDL had an estimated overall affinity of 2.5 (± 1.5) × 10^4 M^{-1}. These values supported the overall affinities of 2.7-2.8 × 10^4 M^{-1} that were previously reported for the binding of *R*- and *S*-verapamil with soluble HDL [14]. Plots of each fit are shown in Figure 2-6.

Figure 2-5. Double-reciprocal plot of frontal analysis data obtained for the binding of racemic verapamil to a 2.1 × 50 mm HDL column at 37°C in the presence of 0.067 M phosphate buffer, pH 7.4, at a flow rate of 1.0 ml/min. The best fit line was obtained using data points in the upper region of this plot, which are designated by the closed squares (■) and include verapamil concentrations that range from 0.25 μM to 0.5 μM. Data points in the lower region of this plot (i.e., at concentrations of verapamil from 1 μM to 10 μM) that showed negative deviations from the linear fit to the upper data points are represented by open squares (□). The equation for the best fit line to data represented by the closed squares is $y = 2.38\ (\pm\ 0.01) \times 10^2 + 5.78\ (\pm\ 0.3) \times 10^7$; the correlation coefficient of this best fit line was 0.9999 ($n = 6$).

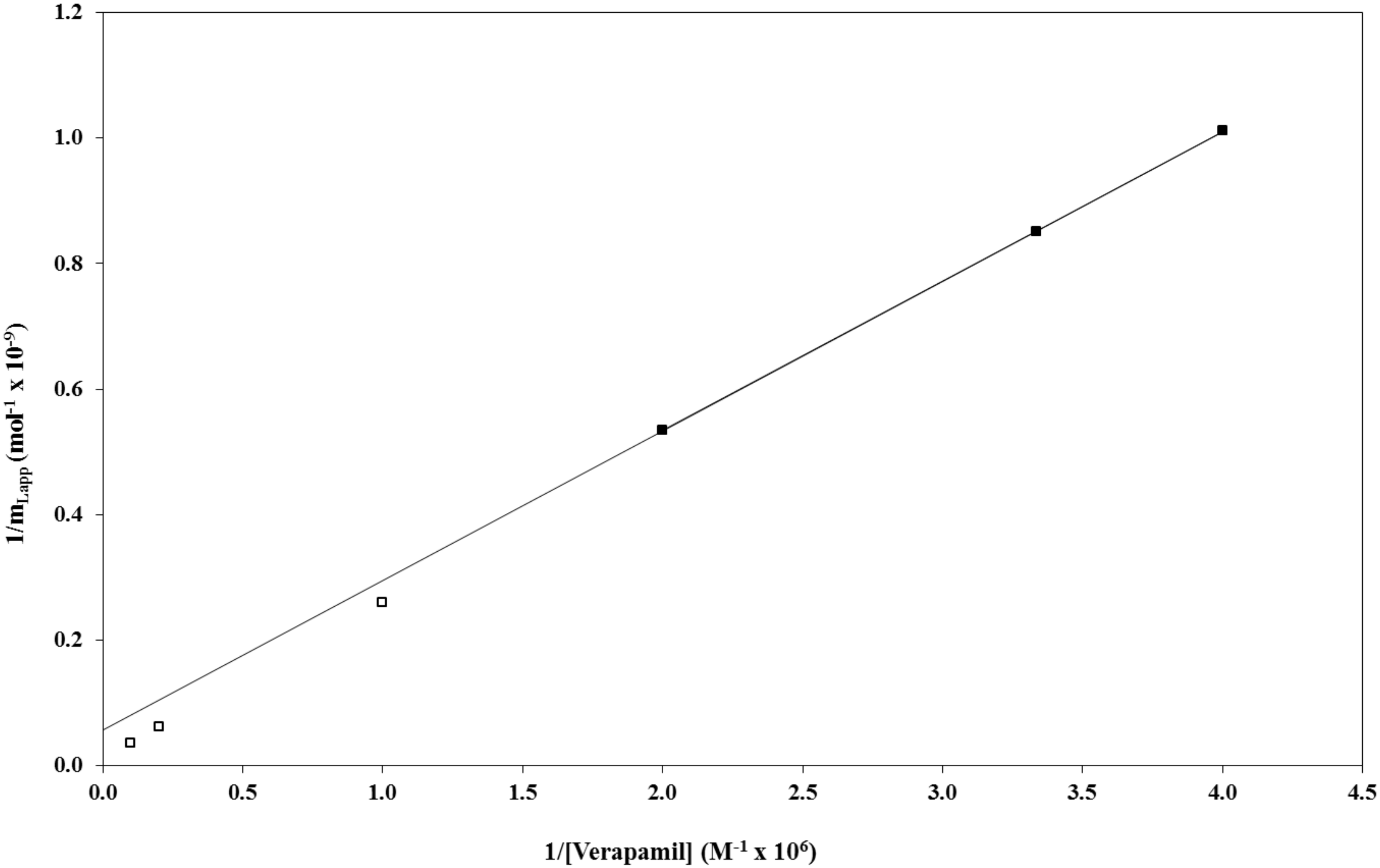
1.2
1.0
0.8
0.6
0.4
0.2
0.0
$1/m_{Lapp}$ (mol^{-1} x 10^{-9})
0.0
0.5
1.0
1.5
2.0
2.5
3.0
3.5
4.0
4.5
1/[Verapamil] (M^{-1} x 10^{6})

Figure 2-6. Examination of frontal analysis data for verapamil on an HDL column at 37°C according to various binding models. These models were as follows: (a) one group of non-saturable interactions, (b) one group of saturable sites, (c) two separate groups of saturable sites, and (d) a group of non-saturable interactions plus a group of saturable sites. The insets show the residual plots for the fit of each model to the experimental data. These results were obtained in the presence of pH 7.4, 0.067 M phosphate buffer. The correlation coefficients were as follows: (a) 0.9952, *n* = 6; (b) 0.9999, *n* = 6; (c) 0.9999, *n* = 6; and (d) 0.9999, *n* = 6.

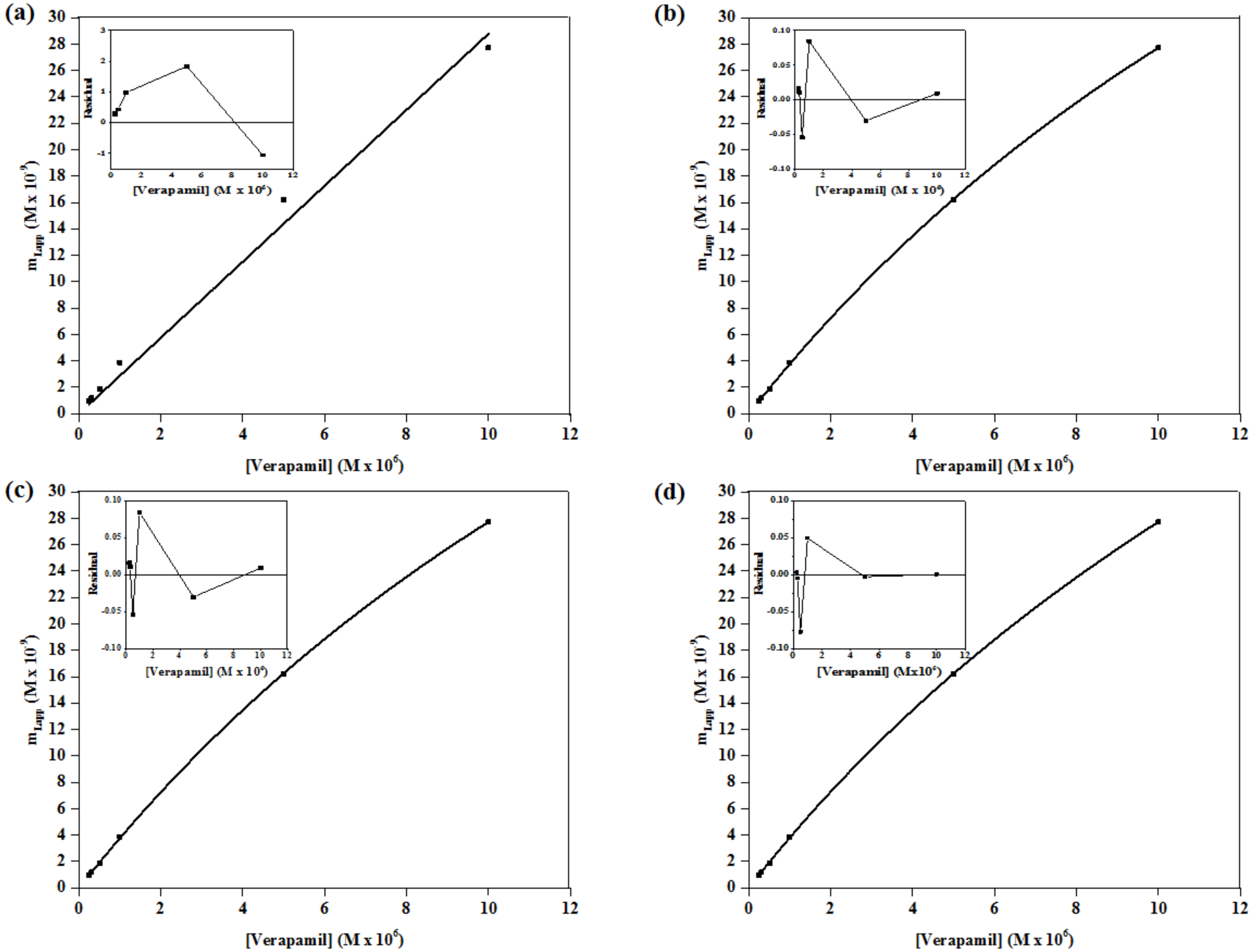
(a)
(b)
(c)
(d)
m_{Lapp} (M x 10^{-9})
[Verapamil] (M x 10^6)
Residual
[Verapamil] (M x 10^6)
[Verapamil] (Mx10^6)
0
2
4
6
8
10
12
14
16
18
20
22
24
26
28
30
-1
1
2
3
0.10
0.05
0.00
-0.05
-0.10

Table 2-4 Binding parameters obtained for racemic verapamil on a HDL column at 37°C[a]

Compound	Binding Model	Temperature	m_{L1} (mol)	K_{a1} (M^{-1})	m_{L2} (mol)	K_{a2} (M^{-1})	nK_a[b] (M^{-1})
Verapamil	Non-saturable interaction	37 °C	-	-	-	-	9.9 (± 0.3) x 10^{4}
	Single group of saturable sites	37 °C	9.4 (± 0.2) x 10^{-8}	4.2 (± 0.1) x 10^{4}	-	-	-
	Two groups of saturable sites	37 °C	4.3 (± 410) x 10^{-8}	6.3 (± 200) x 10^{4}	8.6 (± 260) x 10^{-8}	1.5 (± 240) x 10^{4}	-
	Two interactions: saturable + non-saturable	**37 °C**	**5.4 (± 1.6) x 10^{-8}**	**6.0 (± 2.1) x 10^{4}**	-	-	**2.5 (± 1.5) x 10^{4}**

[a] The numbers in parentheses represent a range of ± 1 S.D. All of these results were measured in pH 7.4, 0.067 M potassium phosphate buffer.

[b] The value for nK_a for a non-saturable interaction was obtained by dividing the best-fit result for $m_L K_a$ by the estimated moles of HDL in the column. This latter value was obtained by using the protein content of the VLDL support, which was determined by using an average molar mass for HDL of 1.8×10^{5} g/mol.

The best fit model is represented in **bold**.

A model based on two groups of saturable sites resulted in a good fit to the data (refer to Figure 2-6), as evidenced by a correlation coefficient of r = 0.9999. The equilibrium binding constants predicted by this model both had moderate or lower affinities for verapamil. This model gave an association equilibrium constant of 6.3 (± 2.0) × 10^4 M^{-1} for the first group of saturable binding sites for verapamil on HDL. This value is similar to that generated for the saturable binding site in the saturable/non-saturable model. The second group of saturable sites had an estimated association equilibrium constant of 1.5 × 10^4 M^{-1}; however, this value had a large uncertainty of ± 2.4 × 10^6 M^{-1}. Similar to the propranolol studies, this uncertainty was due to the fact that the two-site saturable model is approaching the saturable/non-saturable model and describing same type of behavior. Therefore, it was determined that the saturable/non-saturable model provided a more appropriate description of the verapamil-HDL interaction. This conclusion is consistent with the outcome of the experiments conducted with *R*- and *S*-propranolol on the HDL columns.

The overall affinities obtained for the non-saturable interactions of verapamil and propranolol with HDL were similar. This binding is most likely the result of interactions between the drugs and phospholipids or the non-polar core of HDL, which has been previously suggested for both propranolol and verapamil in work with soluble HDL [12-14]. The estimated binding affinity of verapamil at its saturable sites on HDL was significantly smaller than that obtained for propranolol at its saturable regions (i.e., roughly one third). However, the two drugs had a much larger difference in the number of saturable sites that were available for binding. The number of saturable sites available for verapamil binding was 54 (± 16 nmol) in an HDL column, which was approximately

10 times greater than the 4.7-5.4 nmol estimated for the saturable sites of *R*- or *S*-propranolol. The binding capacity for the saturable binding of verapamil was comparable to the total moles of immobilized HDL in the column (30 nmol) and the expected moles of apolipoproteins that were present [1]. These results demonstrated that apolipoproteins were probably responsible for the saturable binding of verapamil with HDL, as was suggested earlier for propranolol. The large difference in binding capacities for verapamil and propranolol at their saturable sites suggest that different apolipoproteins or different regions on the same apolipoproteins may be interacting with these two drugs.

The *R*- and *S*-enantiomers of verapamil have a typical therapeutic concentration of 0.1 – 0.2 µM in serum [26]. The relative importance of saturable versus non-saturable interactions in the binding of verapamil with HDL was evaluated using this information along with the binding parameters in Table 2-4 and the known serum concentration for HDL (13.0 – 14.6 µM). Under these conditions, the saturable interactions would account for approximately 70-80% of the overall binding between *R*- or *S*-verapamil and HDL under normal therapeutic conditions. The saturable sites would have accounted for roughly 40 – 60% of the overall measured binding under the experimental conditions used in Ref. [14]; however, the similarity in the affinities for the saturable and non-saturable sites of verapamil and the fact that only a non-saturable model was considered in Ref. [14] explains why these saturable interactions were not noted in this previous solution phase study.

CONCLUSIONS

HDL was used for drug binding studies in HPAC following the immobilization of HDL in chromatographic columns. Zonal elution experiments demonstrated that the immobilized HDL column could be used over the course of approximately 5 days of consistent use without any significant loss of retention for drugs such as *R*- and *S*-propranolol. Frontal analysis studies with this type of column revealed that propranolol and verapamil had two distinct types of interactions with the immobilized HDL. The first binding mechanism had a high affinity and is likely due to the apolipoproteins on HDL. The other interaction between the drugs and HDL had a lower affinity and was believed to be due to non-saturable interactions with the phospholipids or non-polar core of HDL. The high affinity sites had association constants of 1.1-1.9 × 10^5 M^{-1} for *R*- or *S*-propranolol and 6.0 × 10^4 M^{-1} for *R/S*-verapamil at 37°C. The overall affinity (nK_a) for the weaker interactions at 37°C was estimated to be 3.7-4.1 × 10^4 M^{-1} for *R*- or *S*-propranolol and 2.5 × 10^4 M^{-1} for *R/S*-verapamil at 37°C. The non-saturable interaction values obtained for each drug were in good agreement with the results of previous solution phase studies [12-14]. There was no evidence of stereoselective interactions between HDL and the drugs that were analyzed at temperatures ranging from 4 to 37°C.

The results obtained in this work demonstrate the suitability of using immobilized HDL in high-performance affinity chromatography to study the interactions that occur between this lipoprotein and drugs or other analytes. When compared with equilibrium dialysis (i.e., the method used in Ref. [12] and a common reference method for drug binding studies), primary advantages of this technique are its ability to obtain analysis times of only a few minutes per run and to reuse the same lipoprotein ligand for many experiments. The use of CE with lipoproteins in drug binding studies requires less protein than the technique described in this study for a single analysis. However, the ability to reuse HPAC columns that contain immobilized lipoproteins results in a method that needs a similar amount of ligand when dealing with a large number of samples or studies. For example, the CE studies in Ref. [13] were conducted using 1.5 pmol HDL per injection. In this current study, the same HDL column (containing approximately 30 nmol of HDL) was used for over 300 studies, or an average of 10 pmol HDL per analysis. Furthermore, the ability to use the same HDL preparation for multiple studies decreased the effects of batch-to-batch variations in the ligand. The ability to utilize HPLC detectors with such columns allowed for examining a relatively wide range of low and high drug concentrations and enabled the identification of a high affinity interaction between HDL and propranolol and verapamil. These interactions were not observed in previous studies using CE or equilibrium dialysis [12-14]. The sum of these features demonstrates that columns containing immobilized HDL are powerful tools when used in the study of drug-lipoprotein interactions by HPAC.

ACKNOWLEDGEMENTS

This work was supported by the National Institute of Health under grant R01 GM 044931 and was performed in facilities renovated with support under grant RR015468-01.

REFERENCES

1. Jonas, A. In *Biochemistry of Lipids, Lipoproteins, and Membranes*; Vance, D.E.; Vance, J.E. Eds.; Elsevier: Amsterdam, **2002**, pp 483–504.
2. Barklay, M. In *Blood Lipids and Lipoproteins: Quantitation, Composition, and Metabolism*; Nelson, G.J. Ed.; Wiley: New York, **1972**, pp 587–603.
3. Wasan, K.M.; Cassidy, S.M. *J. Pharm. Sci*. **1998**, *87*, 411–424.
4. Kwong, T.C. *Clin. Chim. Acta* **1985**, *151*, 193–216.
5. Otagiri, M. *Drug Metab. Pharmacokinet.* **2005**, *20*, 309–323.
6. Bertucci, C.; Domenici, E. *Curr. Med. Chem.* **2002**, *9*, 1463.
7. Hage, D.S. *J. Chromatogr. B.* **2002**, *768*, 3-30.
8. Hage, D.S.; Jackson, A.; Sobansky, M.; Schiel, J.E.; Yoo, M.Y.; Joseph, K.S. *J. Sep. Sci.* **2009,** *32*, 835–853.
9. Xuan, H.; Hage, D.S. *Anal. Biochem.* **2005**, *346*, 300–310.
10. Mallik, R.; Xuan, H.; Guiochon, G.; Hage, D.S. *Anal. Biochem.* **2008** *376*, 154–156.
11. Mbewu, A.D.; Durrington, P.N. *Atherosclerosis.* **1990**, *85*, 1–14.
12. Glasson, S.; Zini, R.; D’Athis, P.; Tillement, J.P. ; Boissier, J.R. *Mol. Pharmacol.* **1980**, *17*, 187–191.
13. Ohnishi. T.; Mohamed, N.A.L.; Shibukawa, A.; Kuroda, Y.; Nakagawa, T.; El Gizawy, S.; Askal, H.F.; El Kommos, M.E. *J. Pharm. Biomed. Anal.* **2002**, *27*, 607–614.
14. Mohamed, N.A.L.; Kuroda, Y.; Shibukawa, A.; Nakagawa, T.; El Gizawy, S.; Askal, H.F.; El Kommos, M.E. *J. Chromatogr. A.* **2000**, *875*, 447–453.

15. Mohamed, N.A.L.; Kuroda, Y.; Shibukawa, A.; Nakagawa, T.; El Gizawy, S.; Askal, H.F.; El Kommos, M.E.; *J. Pharm. Biomed. Anal.* **1999**, *21*, 1037–1043.

16. Hage, D.S.; Chen, J. In *Handbook of Affinity Chromatography*; Hage, D.S. Ed.; CRC Press/Taylor & Francis: New York, **2006**, pp 595–628.

17. Tweed, S.; Loun, B.; Hage, D.S. *Anal. Chem.* **1997**, *69*, 4790- 4798.

18. Loun, B.; Hage, D.S. *Anal. Chem*. **1994**, *66*, 3814-3822.

19. Smith, P.K.; Krohn, R.I.; Hermanson, G.T.; Mallia, A.K.; Gartner, F.H.; Provenzano, M.D.; Fujimoto, E.K.; Goeke, N.M.; Olson, B.J.; Klenk, D.C. *Anal. Biochem*. **1985**, *150*, 76–85.

20. Wiechelman, K.J.; Braun, R.D.; Fitzpatrick, J.D. *Anal. Biochem.* **1988**, *175*, 231-237.

21. Allain, C.C.; Poon, L.S.; Chan, C.S.G.; Richmond, W.; Fu, P.C. *Clin. Chem.* **1974**, *20*, 470–475.

22. Kim, H.S.; Mallik, R.; Hage, D.S. *J. Chromatogr. B*. **2006**, *837*, 138-146.

23. Mallik, R.; Xuan, H.; Hage, D.S. *J. Chromatogr. A.* **2007**, *1149*, 294–304.

24. Chen, S.; Sobansky, M.; Hage, D.S. *Anal. Biochem.* **2010,** *397*, 107-114.

25. Tietz N.W. In *Textbook of Clinical Chemistry*; Tietz N.W. Ed.; WB Saunders: Philadelphia, **1986**.

26. Mallik, R.; Yoo, M.J.; Chen, S.; Hage, D.S. *J. Chromatogr. B*. **2006**, *837*, 138-146.

CHAPTER THREE

IDENTIFICATION AND ANALYSIS OF STEREOSELECTIVE DRUG INTERACTIONS WITH LOW DENSITY LIPOPROTEIN BY HIGH-PERFORMANCE AFFINITY CHROMATOGRAPHY

Portions of this chapter have previously appeared in M.R. Sobansky, and D.S. Hage, "Identification and analysis of stereoselective drug interactions with low density lipoprotein by high-performance affinity chromatography", Analytical and Bioanalytical Chemistry, 2012, 403, 563-571.

INTRODUCTION

The information presented in **Chapter 1** demonstrated how the interaction of drugs with serum proteins and other binding agents in blood is important in determining the apparent activity, distribution and pharmacokinetics of many pharmaceutical compounds in the body [1-7]. Lipoproteins, such as low density lipoprotein (LDL), are one group of serum binding agents that are known to be involved in the interactions with various drugs and other compounds present in the serum [7-15]. Propranolol (refer to Figure 1-4) is one drug that has binds with LDL and other lipoproteins. This binding has been examined with methods based on equilibrium dialysis and CE carried out in a frontal analysis mode [16-19]. An alternative approach is HPAC, which will be examined in this report. The HPAC was shown to be suitable for the analysis of drug-lipoprotein studies with HDL in **Chapter 2**.

In this study, the interactions between propranolol and LDL were evaluated by using HPAC. This work will build upon the methods that were previously developed for the examination drug interactions with immobilized HDL [20], as presented in the previous chapter, and HSA or AGP [3-6,21-26]. The first step in these studies was to develop a support that contains LDL immobilized on HPLC grade silica. This material was packed into columns and used in zonal elution and frontal analysis studies, as described in **Chapter 1**. The stability of the LDL columns was assessed with zonal elution studies. Frontal analysis experiments were executed to examine the binding mechanisms for LDL with *R*- and *S*-propranolol at various temperatures, and the results were compared to measurements obtained with soluble LDL in previous work (refer to Table 3-1). Additional information regarding the nature of the interactions between *R*- and *S*-propranolol with LDL within the body circulation was obtained from these studies. The advantages and limitations of using immobilized LDL columns with HPAC for drug binding studies, including those that involve chiral pharmaceutical agents, are also reported.

Table 3-1 Reported binding parameters for the interactions of propranolol with LDL

Analyte	Overall affinity, nK_a (M^{-1})	Method and reference	Experimental conditions
Racemic propranolol	1.76 (± 0.01) x 10^5	Equilibrium Dialysis [16]	pH 7.4 phosphate buffer (0.66M) 1 µM LDL, 37 °C
R-propranolol	4.01 (± 0.24) x 10^5	High-performance frontal analysis / capillary electrophoresis [17]	pH 7.4 phosphate buffer (I = 0.17) 1.9 µM LDL, 37 °C
S-propranolol	4.02 (± 0.34) x 10^5	High-performance frontal analysis / capillary electrophoresis [17]	pH 7.4 phosphate buffer (I = 0.17) 1.4 µM LDL, 37 °C

EXPERIMENTAL

Reagents

Human LDL (catalog number L7914, lot no. 036K1143), bovine serum albumin (BSA), and the individual enantiomers of *R*- and *S*-propranolol were purchased from Sigma (St. Louis, MO, USA). Nucleosil Si-500 silica (7 µm particle diameter, 500 Å pore size) was acquired from Macherey Nagel (Düren, Germany). Materials for the bicinchoninic acid (BCA) protein assay were from Pierce (Rockford, IL, USA). The kit for performing the total cholesterol assay was purchased from Wako (Richmond, VA, USA). All other chemicals and reagents were of the highest grades available. Solutions were prepared using water from a nanopure purification system (Barnstead, Dubuque, IA, USA) and filtered using Osmonics 0.22 µm nylon filters from Fisher Scientific (Pittsburgh, PA, USA).

Apparatus

Zonal elution studies utilized a chromatographic system consisting of a PU-980 pump (Jasco, Tokyo, Japan), one LabPro injection valve (Rohnert Park, FL, USA), and a LDC Thermoseparations (Riviera Beach, FL, USA) UV/Vis SpectroMonitor 3200 variable wavelength absorbance detector. The high performance liquid chromatograph used in the frontal analysis studies consisted of two 510 HPLC pumps (Waters, Milford, MA, USA), an F60-AL injection valve (Vici, Houston, TX, USA), a CH-500 column heater (Eppendorf, Hauppauge, NY, USA) and a Waters 2487 UV/Vis variable wavelength absorbance detector. Waters Empower software was used to collect the chromatograms. Chromatographic data were processed using programs based on

Labview 5.1 or 7.0 (National Instruments, Austin, TX, USA). Supports were placed into HPLC columns by using a slurry packer from Alltech (Deerfield, IL, USA).

Preparation of LDL support

The LDL support was prepared in an approach similar to the one developed in Ref. [20] for the immobilization of HDL. This approach utilized a modified version of the Schiff base reaction to covalently attach LDL to silica. The first step in this process was to prepare a surface containing a diol-bonded phase from Nucleosil Si-500 silica, as described previously [26]. Next, a 0.3 g portion of the diol-bonded silica was added to 6 mL of a 90:10 (v/v) mixture of acetic acid and water followed by the addition of 0.3 g periodic acid. The resulting mixture was sonicated under vacuum for 20 min and mixed for over 2 h at room temperature while protecting from light to generate aldehyde-activated silica. The silica was subsequently washed four times with water and four times with pH 6.0, 0.10 M potassium phosphate buffer prior to being placed in 1 mL of pH 6.0, 0.10 M potassium phosphate buffer and sonicated for 5 min under vacuum. The addition of 5 mg LDL was preceded by the addition of 20 mg aliquot of sodium cyanoborohydride. This mixture was mixed at 4 ^{o}C for 7 days while protected from light exposure. The resulting support containing immobilized LDL was washed four times with 0.10 M potassium phosphate buffer, pH 7.0. Any remaining aldehyde groups on the silica were reduced by the slow addition of a 5.2 mg portion of sodium borohydride dissolved in 2 mL of 0.10 M potassium phosphate buffer, pH 7.0. The resulting slurry was shaken at room temperature for 90 minutes. The finished LDL stationary phase was washed six times with pH 7.0, 0.10 M potassium phosphate buffer and stored in the same pH 7.0 buffer at 4 °C until use. Diol-bonded silica was utilized as a control support. The LDL and control supports were downward slurry packed into 100 mm × 2.1 mm i.d. stainless steel columns at 3000 psi using pH 7.4, 0.067 M potassium phosphate buffer as the packing solution.

Determination of immobilization efficiency

A BCA protein assay was used to evaluate the protein content of the LDL support [28]. The assay was executed in triplicate using BSA solutions prepared 0.067 M potassium phosphate buffer, pH 7.4, as the standards and diol silica samples as the blanks. Each sample and standard solution was filtered through a 0.2 μm nylon filter prior to measuring absorbance. Cholesterol content of the immobilized LDL support was determined using a Wako Cholesterol E assay kit [29]. The sample and standard solutions were reacted in accordance with the manufacturer's instructions and filtered through a 0.2 μm nylon filter prior to absorbance measurements. As before, diol-bonded silica served as the blank. All measurements were made in triplicate. The immobilization scheme utilized in this report is known to yield good batch-to-batch reproducibility; a typical batch-to-batch variability in protein content is 5-10% for silica supports similar to those utilized in this study [4,25,26].

Chromatographic studies

Chromatographic studies were conducted using the HPAC systems described previously. Different column preparations were utilized for the zonal elution and frontal analysis studies; however, the columns were prepared from the same batch of the LDL support. The LDL and control columns were stored in 0.067 M phosphate buffer, pH 7.4, at 4°C when not in use. Prior to chromatographic experiments, the columns were equilibrated at the specified temperature. Mobile phase solutions were filtered through Osmonics 0.22 µm nylon filters and degassed under vacuum prior to use. A wavelength of 225 nm was utilized to monitor the elution of *R*- or *S*-propranolol. Sodium nitrate was used as a non-retained solute and was monitored at 205 nm.

The zonal elution experiments were carried out as described in **Chapter 1**. The stability of the LDL columns was determined using these experiments. Zonal elution studies were executed using a pH 7.4, 0.067 M potassium phosphate buffer as mobile phase. This buffer was applied to a 100 mm × 2.1 mm i.d. column containing the LDL support for 60 h at 37 ºC. The void time of the column was determined by injecting a 20 µL sample of 50 µM sodium nitrate onto the LDL column and control column. The retention of an injected analyte was monitored by performing 20 µL injections of 50 µM *R*-propranolol onto LDL and control columns at 1.0 mL/min. The retention time for each peak was determined by utilizing Peakfit 4.12 software (Systat Software, San Jose, CA) to find the central moment of the peak.

Frontal analysis experiments were performed in triplicate using 100 mm × 2.1 mm i.d. columns packed with the LDL support or control support. These studies were conducted using a mobile phase of 0.067 M potassium phosphate buffer, pH 7.4, applied at 1.0 mL/min. Measurements were made at 20 ºC, 27 ºC, and 37 ºC. Additional details regarding execution of frontal analysis tests are described in **Chapter 1**. A total of nine solutions containing *R*- or *S*-propranolol with concentrations ranging from 0.2-25 µM of 0.067 M potassium phosphate buffer, pH 7.4, were applied to the LDL and control columns. The least concentrated solution in this range was selected as it was near the lowest concentration at which the breakthrough times for *R*- and *S*-propranolol could be reliably determined on this chromatographic system. The upper end of this concentration range was selected because it provided a signal within the range of linear response for the detector and overlapped with drug concentrations that have been used in CE/frontal analysis studies [17]. The retained drug was eluted following frontal analysis measurements by passing only 0.067 M potassium phosphate buffer, pH 7.4, through the column prior to the next experiment.

Following the execution of frontal analysis studies, the moles of applied drug required to saturate the LDL column or control column was determined by integration of the resulting breakthrough curve [3] by using a program based on Labview 5.1 software**.** The impact of the void volume and non-specific binding on the apparent moles of propranolol required to saturate the support was determined by examining the breakthrough curve of *R*- or *S*-propranolol solutions on the control column. Corrections were made for these factors by subtracting the breakthrough time of the control column from that of LDL column at each concentration of drug, as described in **Chapter 2**. The non-specific interactions between *R*- or *S*-propranolol to the support accounted for approximately 12% of the total binding noted on the LDL column at an applied analyte concentration of 25 μM. The typical precision of the frontal analysis measurements was ± 4-5%. The precision varied between ± 0.1% and ± 14% at all of the conditions that were examined; the precision at even the lowest tested concentrations was ± 1-7%.

RESULTS AND DISCUSSION

Composition and stability of the LDL support

The composition of the LDL support was examined by using two methods. The BCA protein and cholesterol assays were performed in a fashion similar to that described in **Chapter 2**. According to the results of the BCA protein assay, the support was contained 6.9 (± 0.4) mg protein per gram silica. Using an average molar mass of 2.3×10^6 g/mol for LDL and a typical apolipoprotein content of 25% for LDL particles, this protein content converted to 27.7 (± 1.6) mg or 12 (± 1) nmol of LDL per gram silica [17]. The cholesterol assay results indicated the support contained 7.2 (± 1.1) mg cholesterol per gram silica; based on a typical cholesterol content of 45% for LDL particles, which corresponded to 16 (± 2.4) mg of LDL per gram silica [7,8,10,14,17]. The differences in the estimated lipoprotein levels using the two assay methods are similar to those observed during the HDL studies described in **Chapter 2**. The nK_a calculated and reported later in this report were determined using the amount of immobilized LDL based on the protein assay. Calculation of nK_a values based on the cholesterol assay would result in values that are approximately 40% lower.

The chromatographic stability of the LDL support was evaluated using zonal elution experiments. These experiments were executed by making periodic injections of *R*-propranolol onto an LDL column under controlled temperature and flow rate conditions. The retention for 20 µL injections of 50 µM *R*-propranolol as a function of time is shown in Figure 3-1. These chromatograms were obtained when the LDL column was used at 1 mL/min and 37 ºC for over 60 h. The first injection on the freshly prepared LDL column occurred after 10 mL of mobile phase (i.e., a time of 10 min at 1.0 mL/min) had been applied to the column. The retention of *R*-propranolol was reproducible over the next 60 h of continuous use, exhibiting only ± 2% variability. The average retention time under these conditions was 90.5 (± 1.8) s. This corresponded to a retention factor of 2.90 (± 0.06) and is comparable to the retention noted for the HDL columns in **Chapter 2**. Over the course of zonal elution experiments, 3.6 L (1.6×10^4 column volumes) of mobile phase was passed through the LDL column. This result indicated that, as with the immobilized HDL columns examined in **Chapter 2**, the LDL columns were suitable for drug binding studies carried out under such conditions.

Frontal analysis studies of propranolol binding to LDL

Frontal analysis studies were conducted to evaluate the interactions that occur between *R*- or *S*-propranolol and the LDL support. These experiments were conducted on a new LDL column within the period of time during which zonal elution studies indicated the LDL support was stable (i.e., when less than 3600 mL of mobile phase had passed through the column). Typical breakthrough curves obtained during frontal analysis experiments with the LDL support are shown in Figure 3-2. The moles of applied analyte (m_{Lapp}) that were required to reach the mean position of each breakthrough curve were determined via integration of the frontal analysis chromatograms. This information was used with the known concentration of the applied drug ([D]) to generate binding isotherms and to fit the data to the binding models described in Table 1-2 to determine the binding mechanisms that were occurring between LDL and *R*- or *S*-propranolol.

Figure 3-1. Chromatograms depicting the change in retention for *R*-propranolol on an LDL column as a function of mobile phase volume. The mobile phase (pH 7.4, 0.067 M phosphate buffer) was passed through a 100 mm × 2.1 mm i.d. LDL column at 37 °C and 1 mL/min. The dashed vertical line shows the central moment of the peak at the beginning of the experiment and demonstrates that no significant change occurred in the position of this central moment during the course of the study. The Figure is reproduced with permission from Ref. [30].

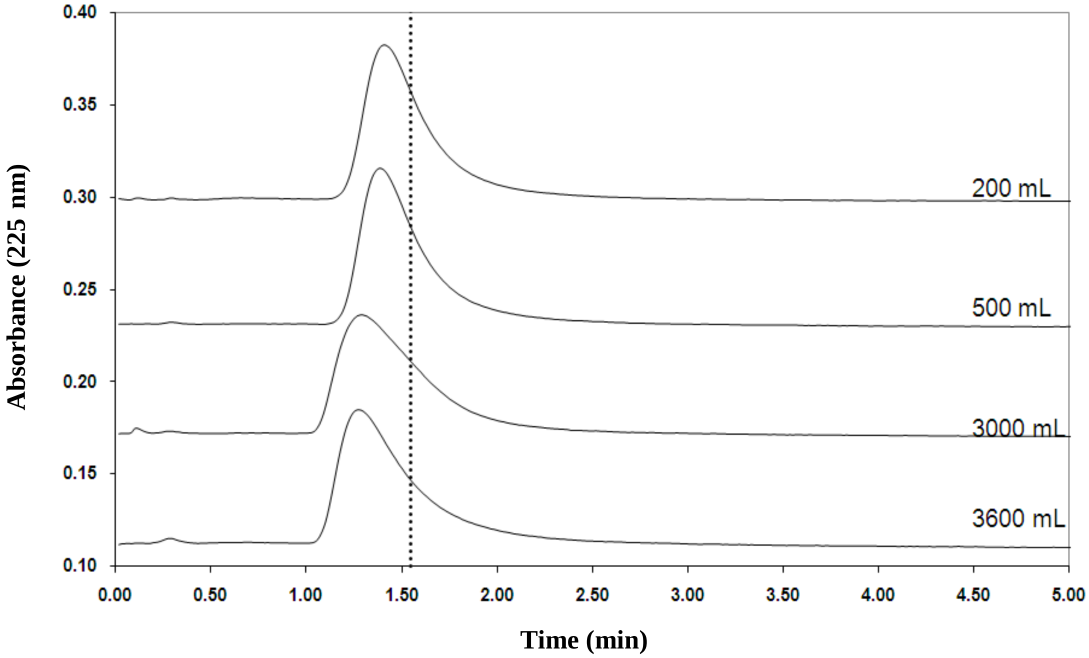
Absorbance (225 nm)
0.40
0.35
0.30
0.25
0.20
0.15
0.10
200 mL
500 mL
3000 mL
3600 mL
0.00
0.50
1.00
1.50
2.00
2.50
3.00
3.50
4.00
4.50
5.00
Time (min)

Figure 3-2. Typical frontal analysis chromatograms obtained when *R*-propranolol was applied to a 100 mm × 2.1 mm i.d. LDL column at concentrations of 0.5, 1, 5, 8, 10, 18, or 25 µM. The chromatograms were obtained at a flow rate of 1.0 mL/min and 27 ºC in the presence of 0.067 M phosphate buffer, pH 7.4. This Figure is reproduced with permission from Ref. [35].

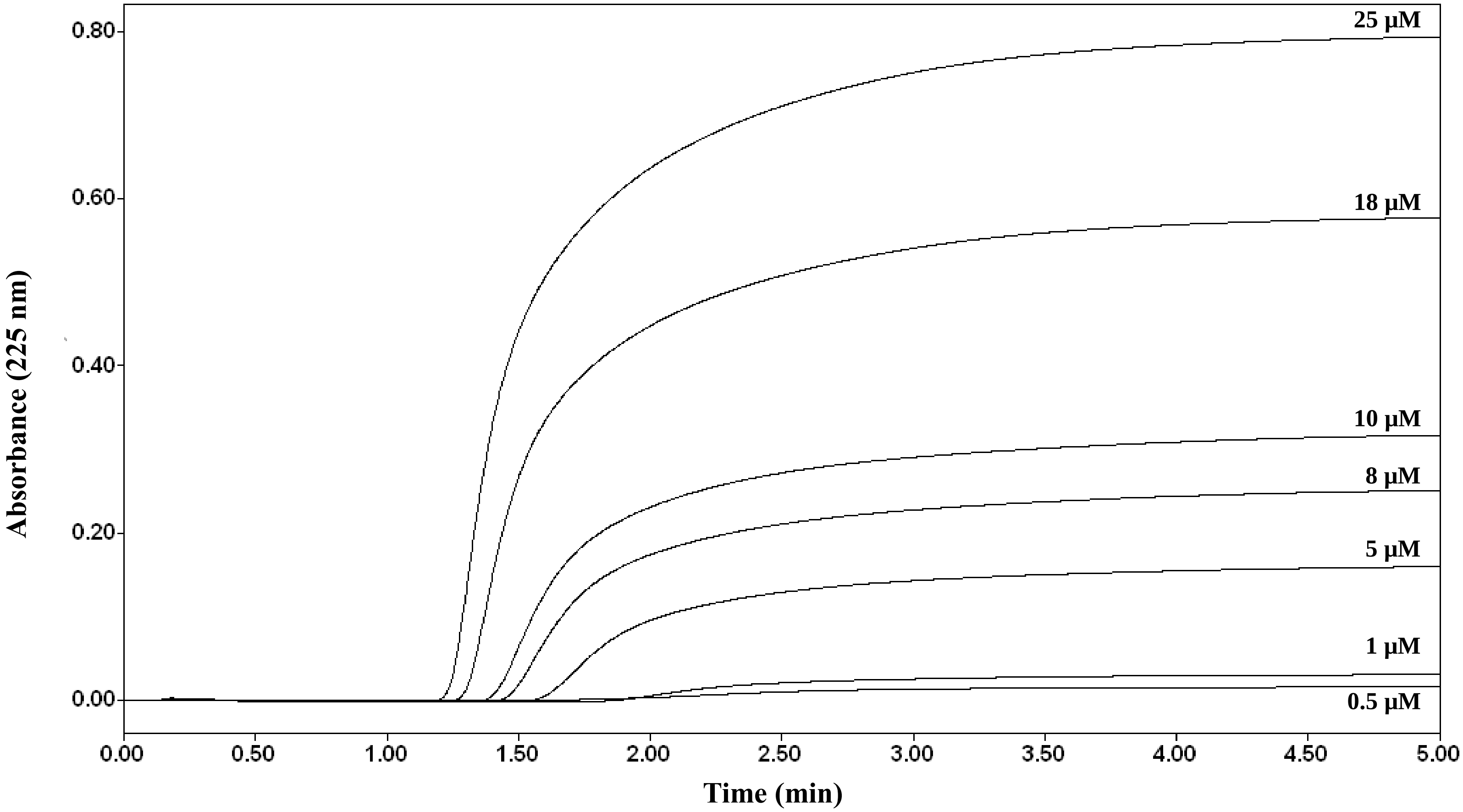
25 µM
18 µM
10 µM
8 µM
5 µM
1 µM
0.5 µM
0.80
0.60
0.40
0.20
0.00
Absorbance (225 nm)
0.00
0.50
1.00
1.50
2.00
2.50
3.00
3.50
4.00
4.50
5.00
Time (min)

Figure 3-3. Double-reciprocal plots of frontal analysis data obtained for the binding of *R*- and *S*-propranolol to a 100 mm × 2.1 mm i.d. LDL column. Chromatographic conditions included a flow rate of 1.0 mL/min, a temperature of 37ºC, and a mobile phase of 0.067 M phosphate buffer, pH 7.4. The best fit line was obtained using data points in the upper region of this plot, which are designated by the closed squares (■). Data points in the lower region of this plot (i.e., at higher concentrations propranolol) showed negative deviations from the linear fit to for *R*-propranolol but not *S*-propranolol and are represented by open squares (□).

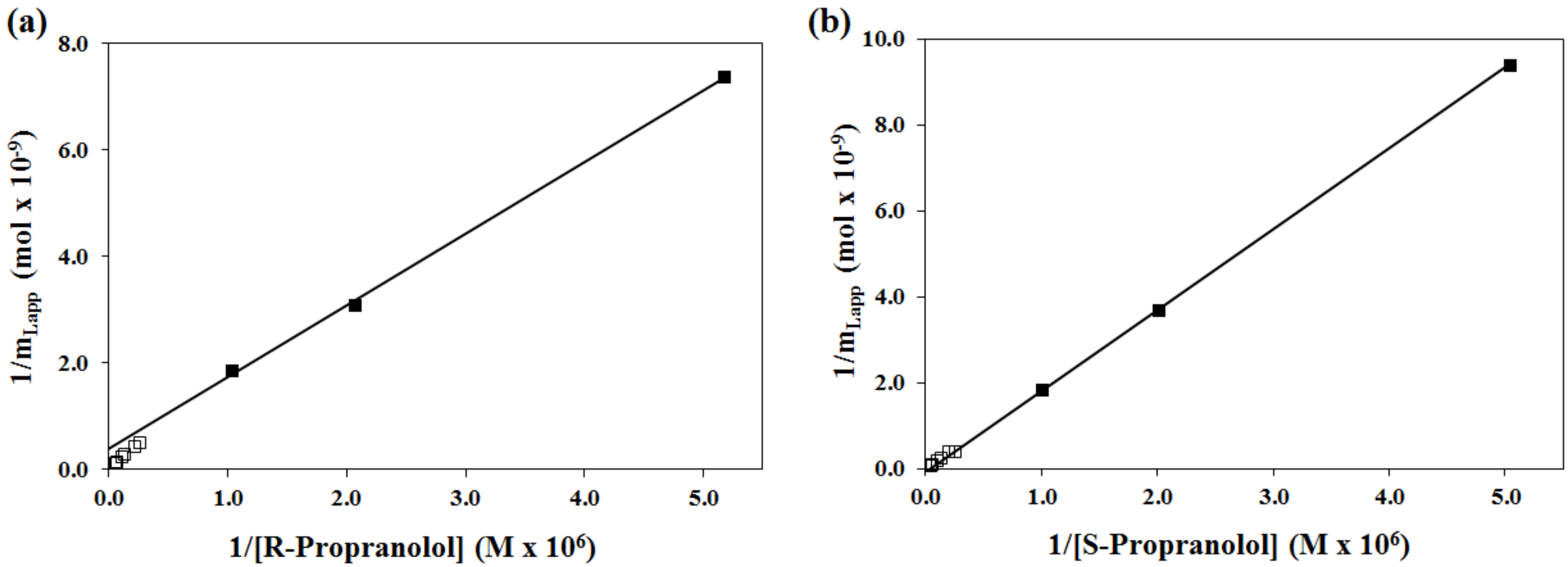
(a)
1/m$_{Lapp}$ (mol x 10^{-9})
8.0
6.0
4.0
2.0
0.0
0.0
1.0
2.0
3.0
4.0
5.0
1/[R-Propranolol] (M x 10^6)
(b)
1/m$_{Lapp}$ (mol x 10^{-9})
10.0
8.0
6.0
4.0
2.0
0.0
0.0
1.0
2.0
3.0
4.0
5.0
1/[S-Propranolol] (M x 10^6)

The values of m_{Lapp} and the known [D] were further used to prepare non-reciprocal plots to study the *R*- and *S*-propranolol interactions with LDL; examples of such graphs are given in Figure 3-4. These plots were fit to equations representing four different binding models. The binding models that were used to fit the data are summarized in Table 1-2 and Eqs. 3-6. One type of interaction that a drug may have with a lipoprotein is described by site specific binding to apolipoproteins on the surface of LDL, This type of binding is described by the model involving saturable binding at a single type of site (Eq. 3) [16-18,20]. A similar model in which the drug undergoes saturable binding at to multiple locations, as might occur if apolipoproteins contained two distinct binding regions for the applied drug, was considered in Eq. 6. The possibility of drug interaction with the hydrophobic core of LDL was also considered. This type of binding is expected to be non-saturable in nature and is described by Eq. 2 [16-18,20]. A combination of saturable sites and a group of non-saturable interactions was also considered in a mixed-mode model (Eq. 5), this type of binding was noted earlier for various drugs with HDL [17]. Fit quality was examined and compared by using the correlation coefficients for the fits, the overall residual values, and the distribution of the data about the best-fit line for each model. The binding parameters determined for each model is provided in Tables 3-2 and 3-3.

Figure 3-4. Best fit results of plots to various binding models of frontal analysis data obtained for *R*-propranolol on an LDL column at 37 ^{o}C. The models used in this analysis were as follows: (a) non-saturable interactions, (b) a single group of saturable sites, (c) two groups of saturable sites, and (d) a group of non-saturable interactions plus a group of saturable sites. The insets show the residual plots for the fit of each model to the experimental data. These results were obtained in the presence of 0.067 M phosphate buffer, pH 7.4. The correlation coefficients were as follows: (a) 0.9959, *n* = 9; (b) 0.9992, *n* = 9; (c) 0.9998, *n* = 9; and (d) 0.9998, *n* = 9. This figure is adapted with permission from Ref. [30].

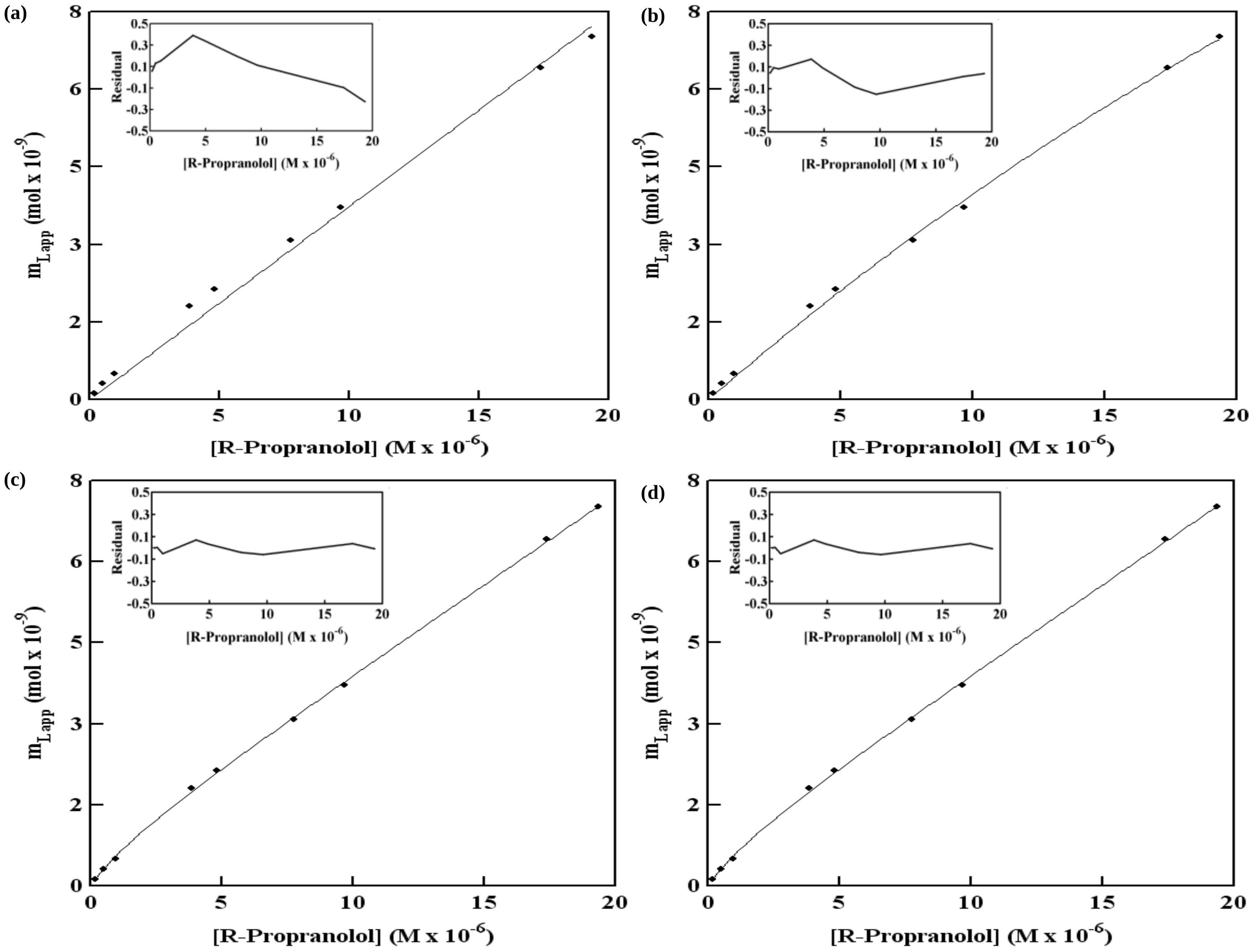
(a)
(b)
(c)
(d)
m_{Lapp} (mol x 10^{-9})
[R-Propranolol] (M x 10^{-6})
0
2
3
5
6
8
0
5
10
15
20
Residual
0.5
0.3
0.1
-0.1
-0.3
-0.5
[R-Propranolol] (M x 10^{-6})

Table 3-2 **Binding parameters obtained for *R*-propranolol on a LDL column at various temperatures**[a]

Enantiomer	Binding Model	Temperature	m_{L1} (mol)	K_{a1} (M^{-1})	m_{L1} (mol)	K_{a1} (M^{-1})	$nK_a{}^b$ (M^{-1})
R-Propranolol	Non-saturable interaction	20 °C	-	-	-	-	3.5 (± 0.1) x 10^{5}
	Single group of saturable sites	20 °C	1.4 (± 0.4) x 10^{-7}	5.3 (± 1.5) x 10^{3}	-	-	-
	Two groups of saturable sites	20 °C	9.0 (± 9.7) x 10^{-10}	4.3 (± 6.2) x 10^{5}	1.3 (± 9490) x 10^{-3}	0.5 (± 3491)	-
	Two interactions: saturable + non-saturable	**20 °C**	**9.0 (± 3.2) x 10^{-10}**	**4.3 (± 3.4) x 10^{5}**	**-**	**-**	**3.2 (± 0.1) x 10^{5}**
R-Propranolol	Non-saturable interaction	27 °C	-	-	-	-	4.3 (± 0.2) x 10^{5}
	Single group of saturable sites	27 °C	6.6 (± 0.1) x 10^{-8}	1.6 (± 0.5) x 10^{4}	-	-	-
	Two groups of saturable sites	27 °C	3.0 (± 2.8) x 10^{-9}	4.4 (± 5.2) x 10^{5}	7.9 (± 87342) x 10^{-4}	0.8 (± 9313)	-
	Two interactions: saturable + non-saturable	**27 °C**	**3.0 (± 0.9) x 10^{-9}**	**4.4 (± 2.7) x 10^{5}**	**-**	**-**	**3.5 (± 0.2) x 10^{5}**
R-Propranolol	Non-saturable interaction	37 °C	-	-	-	-	2.1 (± 0.1) x 10^{5}
	Single group of saturable sites	37 °C	3.8 (± 0.7) x 10^{-9}	1.2 (± 0.3) x 10^{4}	-	-	-
	Two groups of saturable sites	37 °C	7.5 (± 5.7) x 10^{-10}	5.2 (± 4.8) x 10^{5}	7.0 (± 81917) x 10^{-4}	0.5 (± 5831)	-
	Two interactions: saturable + non-saturable	**37 °C**	**7.5 (± 1.5) x 10^{-10}**	**5.2 (± 2.3) x 10^{5}**	**-**	**-**	**1.9 (± 0.1) x 10^{5}**

[a] The numbers in parentheses represent a range of ± 1 S.D. All of these results were measured in pH 7.4, 0.067 M potassium phosphate buffer.

[b] The value for nK_a for a non-saturable interaction was obtained by dividing the best-fit result for m_LK_a by the estimated moles of LDL in the column. This latter value was obtained by using the protein content of the LDL support, using a typical protein content for LDL of 25% (*w/w*), and an average molar mass for LDL of 2.3 × 10^{6} g/mol.
The best fit model is represented in **bold**.
This table is adapted with permission from Ref. [30].

Table 3-3 Binding parameters obtained for *S*-propranolol on a LDL column at various temperatures[a]

Enantiomer	Binding Model	Temperature	m_{L1} (mol)	K_{a1} (M^{-1})	m_{L1} (mol)	K_{a1} (M^{-1})	nK_a[b] (M^{-1})
S-Propranolol	**Non-saturable interaction**	**20 °C**	**-**	**-**	**-**	**-**	**3.2 (± 0.1) x 10^5**
	Single group of saturable sites	20 °C	2.0 (± 1.8) x 10^{-7}	3.2 (± 3.1) x 10^3	-	-	-
	Two groups of saturable sites	20 °C	0.1 (± 6.3) x 10^{-5}	0.1 (± 4.5) x 10^5	2.0 (± 96665940) x 10^{-4}	0.2 (± 6848026)	-
	Two interactions: saturable + non-saturable	20 °C	0.1 (± 1.3) x 10^{-5}	0.1 (± 2.0) x 10^5	-	-	5.4 (± 1294) x 10^4
S-Propranolol	**Non-saturable interaction**	**27 °C**	**-**	**-**	**-**	**-**	**2.8 (± 0.1) x 10^5**
	Single group of saturable sites	27 °C	4.6 (± 4.5) x 10^{-7}	1.2 (± 1.2) x 10^3	-	-	-
	Two groups of saturable sites	27 °C	4.9 (± 2636) x 10^{-9}	0.1 (± 3.3) x 10^6	8.2 (± 3776061) x 10^{-4}	0.6 (± 268838)	-
	Two interactions: saturable + non-saturable	27 °C	0.7 (± 6.0) x 10^{-7}	0.6 (± 4.6) x 10^5	-	-	2.7 (± 0.5) x 10^5
S-Propranolol	**Non-saturable interaction**	**37 °C**	**-**	**-**	**-**	**-**	**2.7 (± 0.2) x 10^5**
	Single group of saturable sites	37 °C	2.6 (± 2.4) x 10^{-7}	2.0 (± 1.9) x 10^3	-	-	-
	Two groups of saturable sites	37 °C	6.7 (± 2398) x 10^{-9}	0.1 (± 2.4) x 10^6	7.6 (± 4477418) x 10^{-4}	0.6 (± 318741)	-
	Two interactions: saturable + non-saturable	37 °C	0.1 (± 1.6) x 10^{-7}	0.2 (± 2.3) x 10^5	-	-	2.2 (± 5.4) x 10^4

[a] The numbers in parentheses represent a range of ± 1 S.D. All of these results were measured in pH 7.4, 0.067 M potassium phosphate buffer.

[b] The value for nK_a for a non-saturable interaction was obtained by dividing the best-fit result for $m_L K_a$ by the estimated moles of LDL in the column. This latter value was obtained by using the protein content of the LDL support, using a typical protein content for LDL of 25% (*w/w*), and an average molar mass for LDL of 2.3 × 10^6 g/mol.

The best fit model is represented in **bold**.

This table is adapted with permission from Ref. [30].

The overall binding between *R*-Propranolol and the immobilized LDL was the result of multiple types of interactions. This was confirmed through a comparison of the various binding models in Figure 3-4(a-d). The mixed-mode binding model involving both saturable sites and non-saturable binding generated the best fit for the interactions of LDL with *R*-Propranolol. It should be noted that the mixed-mode model for a combination of saturable and non-saturable interactions (see Figure 3-4(d)) resulted in the same correlation coefficient and residual plot as the two-site saturable model (see Figure 5(c)). However, the precisions obtained for the best-fit equilibrium constants obtained for saturable/non-saturable were much tighter than those obtained for the two-site saturable model (refer to the standard deviations listed in Table 3-2 for K_{a1}, m_{L1} and nK_a in this model versus those values listed for the best-fit parameters in a model based on two groups of saturable sites). As with the HDL studies, the apparent similarities in these two fits is explained by the equations for the two-site saturable model approaches that of a model based on saturable/non-saturable interactions. As shown in Table 1-2, as the term K_{a2}[D] in the denominator of Eq. 6 becomes much less than one, the term for the second interaction becomes mathematically equivalent to the non-saturable term in Eq. 5. This situation occurs in the fit of the two-site saturable model to the data obtained for binding between *R*-propranolol and LDL and explains the large uncertainly values that resulted. Considering that both models are actually describing the same overall model where there was a relatively high affinity saturable site and lower affinity, essentially non-saturable binding also explains why the residual plots in Figures 3-4(c-d) are so similar.

Similar interactions were predicted between *S*-propranolol and LDL, as these evaluations indicated that binding by this enantiomer gave the best fit with a model for a single type, non-saturable interaction. The fitting of frontal analysis data for *S*-propranolol/LDL interactions using the four models presented in Table 1-2 resulted in very similar fits. Specifically, the four models yielded essentially the same correlation coefficient and residual plot (i.e., values for *r* greater than 0.9985). However, the best-fit equilibrium constants for models other than the one non-saturable interaction model had large variability in their values (refer to the standard deviations listed in Table 3-3 for estimated equilibrium constants and binding capacities of these models versus the values listed for nK_a in a model based on only non-saturable binding). This is due to the fact that Eqs. 4-6 in Table 1-2 representing one-site saturable binding, two-site saturable binding, and the mixed-mode binding all approach Eq. 3 for a system containing only non-saturable interactions. This latter situation is realized when K_{a1}[D] and/or K_{a2}[D] become much smaller than one in the denominators of Eqs. 4-6 and as the term for site-specific binding in Eq. 3 becomes much smaller than the term for non-saturable interactions. Based on the analysis of these binding models, the data revealed that at all of the temperatures examined *S*-propranolol gave the best-fit with a non-saturable model. This supports the conclusion reached during the evaluation of double-reciprocal plots of $1/m_{\mathrm{Lapp}}$ versus 1/[D] that only a single type of interaction was present between *S*-propranolol and LDL.

Equilibrium binding constants and temperature studies

The best-fit results obtained for *R*- and *S*-propranolol with LDL at all temperatures that were evaluated in this report are summarized in Tables 3-2 and 3-3.

The saturable interaction between *R*-propranolol and LDL had an association equilibrium constant (K_{a1}) of 5.2 (± 2.3) × 10^5 M^{-1} at 37 ºC, which is indicative of relatively high affinity binding. This binding was probably occurring between the drug and apolipoprotein B100 (apoB100) on LDL. This hypothesis is supported by a comparison of the measured binding capacity of LDL to the moles of apoB100 that were determined to be present in the LDL column during the BCA protein assay. The total moles of binding sites determined using the frontal analysis data was consistently in the range of 0.7 to 3.0 nmol for *R*-propranolol between 20 °C and 37 °C (average, 1.6 nmol). This value is in agreement with the amount of LDL that was estimated to be present in the column (i.e., 1.9 (± 0.1) nmol) using the BCA column, where each LDL particle typically contains one apoB100 molecule [7]. Saturable binding of propranolol with apolipoproteins of HDL was also suggested in **Chapter 2**.

The second type of interaction that occurred for *R*-propranolol with LDL was non-saturable in nature and had an overall affinity (nK_a) of 1.9 (± 0.1) × 10^5 M^{-1} at 37 ºC. This interaction likely occurs between *R*-propranolol and phospholipids or the non-polar core of LDL. The presence of non-saturable interactions has been suggested in previous work examining the binding of *R*/*S*-propranolol and other drugs with both LDL and HDL [16,17,20]. An approximately equivalent overall affinity of 2.7 (± 0.2) × 10^5 M^{-1} was obtained in this study for the non-saturable binding of *S*-propranolol with LDL at 37 ºC.

The impact that temperature had on the interactions that occur between *R*- and *S*-propranolol and LDL was also examined. The results obtained during the best fit analysis did not reveal a significant effect on the equilibrium constants, binding capacities, or binding models that were obtained for *R*- and *S*-propranolol with LDL between 20 ^{o}C and 37 ^{o}C. At the temperatures employed in this study, the binding models listed in Table 3-2 and Table 3-3 gave correlation coefficients for *R*- and *S*-propranolol that were greater than 0.998. The K_{a1} values measured for the saturable binding of *R*-propranolol with LDL varied from only 4.3-5.2 × 10^5 M^{-1} over this temperature range. The nK_a values for non-saturable binding by *R*-propranolol with LDL were in the range of 1.9-3.5 × 10^5 M^{-1}, while the nK_a values for the *S*-enantiomer were in a similar range of 2.7-3.2 × 10^5 M^{-1} under the given temperature conditions.

The nK_a value obtained for drug binding by LDL is expected to be larger than that obtained by HDL due to the fact that LDL has a much larger portion of hydrophobic components (i.e., cholesterol and triacylglycerides) than HDL [7-9,17]. Previous studies that compared drug binding by LDL and HDL have confirmed this trend [16,17]. The nK_a values measured for the non-saturable interaction of *R*- and *S*-propranolol with LDL were approximately five- to nine-fold higher than values of 3.7-4.1 × 10^4 M^{-1} that were measured at pH 7.4 and between 4 °C and 37 °C for the same type of interaction of these enantiomers with immobilized HDL [20]. Despite the fact that LDL and HDL contain different types of apolipoproteins [7], the K_{a1} values measured for the saturable binding of *R*-propranolol with LDL were similar to values of 1.4-1.9 × 10^5 M^{-1} that were estimated for saturable binding of the same solute with HDL [20]. In addition, the range of K_{a1} and nK_a values obtained during this study agreed with the previously reported range of 1-4 × 10^5 M^{-1} in overall affinities obtained with soluble LDL at pH 7.4 and 25 °C to 37 °C for *R*- and *S*-propranolol when using only a non-saturable binding model [16,17].

In this study, the binding of propranolol to LDL was determined to be stereoselective. This is supported by the fact that *R*- and *S*-propranolol consistently followed different binding models at the temperatures employed in this report (i.e. 20 ^{o}C to 37 ^{o}C). This stereoselectivity arises from the observation that only the *R*-enantiomer had significant saturable binding to LDL under the conditions of this study. This stereoselective binding likely occurred with apoB100. Stereoselective interactions were not noted in earlier studies with HDL, where both *R*- and *S*-propranolol were found to undergo two types of interactions, i.e., a saturable interaction that probably involved apolipoproteins and a non-saturable, partition-like interaction [20]. Prior work examining the binding of propranolol with LDL either used a racemic preparation of the drug [16] or did not note significant, stereoselective interactions when using only a non-saturable binding model [17]. Due to the similarity in the binding constants that were determined in this study for the saturable and/or non-saturable interactions of *R*- and *S*-propranolol with LDL, it is not surprising these interactions were not previously noted.

HDL and LDL contain different types of apolipoproteins (see Table 1-1), explaining why stereoselective binding occurred for *R*- and *S*-propranolol with LDL but not in prior work with HDL that also used a mixed-mode model [20]. For instance, LDL contains only one apolipoprotein molecule per particle (i.e., ApoB100) while HDL may contain up to 5-6 apolipoproteins per particle [7]. The apolipoproteins associated with HDL (i.e. ApoA1, ApoA2, ApoE and ApoC) are not associated with LDL [7]. The ability of apoB100 to specifically bind to hormones and drug-like compounds has been previously noted for a number of steroids, including 17-β-estradiol, testosterone, and progesterone [31-33]. However, the results of this study are believed to be the first instance in which stereoselective interactions with apoB100, apolipoproteins, or lipoprotein particles have been observed.

CONCLUSIONS

In this chapter, LDL was immobilized in chromatographic columns and used in drug binding studies. Both enantiomers of propranolol were used individually as solutes for this work. Stability studies demonstrated that an LDL column was suitable for use over at least 60 h of continuous operation without any significant loss of retention for *R*-propranolol. The use of columns containing immobilized LDL in frontal analysis studies indicated that propranolol had two distinct types of interactions with LDL. Each of these drug enantiomers underwent non-saturable interactions with LDL, which was most likely due to interactions with the phospholipids or the non-polar core of LDL. The overall affinities for the non-saturable interactions of *R*- and *S*-propranolol were similar and in the range of $1.9\text{-}3.5 \times 10^5$ M^{-1} at 20 °C to 37 ^{o}C. A second, saturable type of binding was observed only with *R*-propranolol. This saturable interaction had an association equilibrium constant in the range of $4.3\text{-}5.2 \times 10^5$ M^{-1} between 20 °C to 37 ºC. These results were in good agreement with binding constants that have been reported for propranolol when using a similar mixed-mode model for immobilized HDL [20] and with the overall affinities that have been measured for soluble LDL based on a non-saturable model [16,17].

Stereoselectivity of the binding was indicated by the differences between the binding of *R*- and *S*-propranolol to LDL, particularly with regard to the presence or absence of measurable saturable interactions. Chiral selectivity is well known to occur as drugs bind to serum proteins such as HSA and AGP, however, this report is the first known example of chiral selectivity for LDL or any other lipoprotein [3,4,34,35]. This stereoselectivity was due to the binding of *R*-propranolol to apoB100, as suggested by the stoichiometry of the saturable interactions for *R*-propranolol with LDL. To our knowledge, this work is also the first example of chiral interactions that involve the binding of a drug with an apolipoprotein. Similar HPAC columns could be used for zonal elution and competition studies [3,4,25,26] to further examine the interactions of *R*- and *S*-propranolol on LDL.. Future work could also focus on the evaluation *R*-propranolol binding in the presence of other compounds known to bind to apoB100 (e.g., testosterone, 17-β-estradiol, and progesterone) [31-33].

This report illustrated the feasibility of utilizing HPAC as a tool for the characterization of mixed-mode interactions that involve LDL and related binding agents. As was observed in previous work with HDL columns [20], this approach can provide analysis times of only a few minutes per run (e.g., see examples in Figures 3-1). The LDL columns developed in this report were also sufficiently stable for use in hundreds of experiments, which significantly reduces the amount of ligand required currently needed for alternative methods. . For example, the CE/frontal analysis studies in Ref. [17] required150 nmol LDL per analysis. In contrast, one HPAC column used for this work contained 350 nmol LDL and was applied to more than 160 experiments, which averages to less than 2.2 nmol LDL per analysis. The ability to utilize the same LDL column for multiple studies made it possible to minimize run-to-run variability.. Furthermore, the ability to utilize these immobilized lipoprotein columns with standard HPLC detectors yields lower limits of detection during the binding studies [3,4,20]. When combined, these advantages enabled the rapid collection of precise data over a wide range of drug concentrations and the identification of mixed-mode interactions and stereoselective binding between LDL and *R*- or *S*-propranolol. These same features should make future studies examining the binding of other drugs and solutes with LDL or alternative lipoproteins using HPAC columns and methods successful.

ACKNOWLEDGEMENTS

This work was supported by the National Institute of Health under grant R01 GM 044931 and was performed in facilities renovated with support under grant RR015468-01.

References

1. Otagiri, M. *Drug Metab. Pharmacokinet.* **2005**, *20*, 309–323.
2. Bertucci, C.; Domenici, E. *Curr. Med. Chem.* **2002**, *9*, 1463.
3. Patel, S.; Wainer, I.W.; Lough, J.W. In *Handbook of Affinity Chromatography,* 2nd ed; Hage, D.S. Ed.; CRC Press: Boca Raton, **2006**, pp 663-683.
4. Hage, D.S.; Jackson, A.; Sobansky, M.; Schiel, J.E.; Yoo, M.Y.; Joseph, K.S. *J. Sep. Sci.* **2009,** *32*, 835–853.
5. Xuan, H.; Hage, D.S. *Anal. Biochem.* **2005**, *346*, 300–310.
6. Mallik, R.; Xuan, H.; Guiochon, G.; Hage, D.S. *Anal. Biochem.* **2008** *376*, 154–156.
7. Jonas, A. In *Biochemistry of Lipids, Lipoproteins, and Membranes*; Vance, D.E.; Vance, J.E. Eds.; Elsevier: Amsterdam, **2002**, pp 483–504.
8. Barklay, M. In *Blood Lipids and Lipoproteins: Quantitation, Composition, and Metabolism*; Nelson, G.J. Ed.; Wiley: New York, **1972**, pp 587–603.
9. Wasan, K.M.; Cassidy, S.M. *J. Pharm. Sci*. **1998**, *87*, 411–424.
10. Harmony, J.A.K.; Aleson, A.L.; McCarthy, B.M. In *Biochemistry and Biology of Plasma Lipoproteins*; Scanu, A.M.; Spector, A.A. Eds.; Marcel Dekker: New York, **1986**, pp 403-430.
11. Mbewu, A.D.; Durrington, P.N. *Atherosclerosis.* **1990**, *85*, 1–14.
12. Durrington, P.N.; In *Lipoproteins and Lipids*; Durrington, P.N. Ed.; Wright: London, **1989,** pp 255–277.

13. Havel, R.J.; Kane, J.P. In *The Metabolic and Molecular Basis of Inherited Disease*; Scriver, C.R.; Beaudet, A.L.; Sly, W.S.; Valle, D.; Childs, B.; Kinzler, K.W.; Vogelstein, B. Eds.; McGraw-Hill: New York, **1995**, pp 1129–1138.

14. Skipski, V.R.; In *Blood Lipids and Lipoproteins Quantitation, Composition, and Metabolism*; Nelson, G.J. Ed.; John Wiley: New York, **1972**, pp 471–583.

15. Kwong, T.C. *Clin. Chim. Acta* **1985**, *151*, 193–216.

16. Glasson, S.; Zini, R.; D'Athis, P.; Tillement, J.P. ; Boissier, J.R. *Mol. Pharmacol.* **1980**, *17*, 187–191.

17. Ohnishi. T.; Mohamed, N.A.L.; Shibukawa, A.; Kuroda, Y.; Nakagawa, T.; El Gizawy, S.; Askal, H.F.; El Kommos, M.E. *J. Pharm. Biomed. Anal.* **2002**, *27*, 607–614.

18. Mohamed, N.A.L.; Kuroda, Y.; Shibukawa, A.; Nakagawa, T.; El Gizawy, S.; Askal, H.F.; El Kommos, M.E. *J. Chromatogr. A.* **2000**, *875*, 447–453.

19. Mohamed, N.A.L.; Kuroda, Y.; Shibukawa, A.; Nakagawa, T.; El Gizawy, S.; Askal, H.F.; El Kommos, M.E.; *J. Pharm. Biomed. Anal.* **1999**, *21*, 1037–1043.

20. Chen, S.; Sobansky, M.; Hage, D.S. *Anal. Biochem.* **2010,** *397*, 107-114.

21. Kim, H.S.; Wainer, I.W. *J. Chromatogr. B.* **2008**, *870*, 22–26.

22. Hollósy, F.; Valkó, K.; Hersey, A.; Nunhuck, S.; Kéri, G.; Bevan, C. *J. Med. Chem.* **2006**, *49*, 6958-6971.

23. Buchholz, L.; Cai, C.H.; Andress, L.; Cleton, A.; Brodfuehrer, J.; Cohen, L. *Eur. J. Pharm. Sci.* **2002**, *15*, 209–215.

24. Loun, B.; Hage, D.S. *Anal. Chem*. **1994**, *66*, 3814-3822.

25. Hage, D.S.; Chen, J. In *Handbook of Affinity Chromatography*; Hage, D.S. Ed.; CRC Press/Taylor & Francis: New York, **2006**, pp 595–628.

26. Tweed, S.; Loun, B.; Hage, D.S. *Anal. Chem.* **1997**, *69*, 4790- 4798.

27. Mallik, R.; Xuan, H.; Hage, D.S. *J. Chromatogr. A.* **2007**, *1149*, 294–304.

28. Smith, P.K.; Krohn, R.I.; Hermanson, G.T.; Mallia, A.K.; Gartner, F.H.; Provenzano, M.D.; Fujimoto, E.K.; Goeke, N.M.; Olson, B.J.; Klenk, D.C. *Anal. Biochem*. **1985**, *150*, 76–85.

29. Allain, C.C.; Poon, L.S.; Chan, C.S.G.; Richmond, W.; Fu, P.C. *Clin. Chem.* **1974**, *20*, 470–475.

30. Sobansky, M.R.; Hage, D.S. Anal. Bioanal. Chem. **2012**, *403*, 563-571.

31. Brunelli, R.; Greco, G.; Barteri, M.; Krasnowska, E.K.; Mei, G.; Natella, F.; Pala, A.; Rotella, S.; Ursini, F.; Zichella, L.; Parasassi, T. *FASEB J*. **2003**, *17*, 2127-2129.

32. Wang, A.J.; Vainikka, K.; Witos, J.; D'Ulivo, L.; Cilpa, G; Kovanen, P.T.; Oorni, K.; Jauhiainen, M., Riekkola, M.L. *Anal. Biochem*. **2010**, *399*, 93-101.

33. D'Ulivo, L.; Chen, J.; Meinander, K.; Oorni, K.; Kovanen, P.T.; Riekkola, M.L. *Anal. Biochem*. **2008**, *383*, 38-43.

34. Patel, S.; Wainer, I.W.; Lough, J.W. In *Handbook of Affinity Chromatography,* 2nd ed; Hage, D.S. Ed.; CRC Press: Boca Raton, **2006**, pp 663-683.

35. Allenmark, S. In *Chromatographic Enantioseparation: Methods and Applications*, 2nd ed; Ellis Horwood Ltd.: England, **1991**.

CHAPTER FOUR

ANALYSIS OF DRUG INTERACTIONS WITH VERY LOW DENSITY LIPOPROTEIN BY HIGH PERFORMANCE AFFINITY CHROMATOGRAPHY

Portions of this chapter have previously appeared in M.R. Sobansky, and D.S. Hage, "Analysis of drug interactions with very low density lipoprotein by high-performance affinity chromatography", Analytical and Bioanalytical Chemistry, 2014, 406, 6203-6211.

INTRODUCTION

As discussed in **Chapter 1**, the binding of drugs and other analytes with serum proteins and lipoproteins can influence the activity, toxicity, delivery and pharmacokinetics of such agents in the human body [1-8]. Information about the type and strength of these interactions can be useful in determining how drugs are distributed after their administration and is of potential interest for the design of personalized dosage regimens [4,8]. These interactions may be stereoselective due to the inherent chirality of proteins thereby potentially influencing drug safety and efficacy [9-13].

The basic and chiral drug propranolol (see **Chapter 1**) is known to bind several serum proteins and lipoproteins, including very low density lipoprotein (VLDL) [14-17]. The binding of propranolol by VLDL has been examined with methods based on equilibrium dialysis in previous studies, which revealed a non-saturable interaction [14]. The properties of propranolol (see **Chapter 1**) and the results of previous studies between lipoproteins and propranolol (see **Chapters 2 and 3**) lead to the hypothesis that multiple types of interactions are present. These interactions may include specific interactions with fixed binding regions, interactions with surface phospholipids, or partitioning into the non-polar core of a lipoprotein [7,18-25].

In this chapter, the HPAC methods described previously were modified and extended to the study of drug interactions with VLDL. The *R*- and *S*-enantiomers of propranolol served as model drugs for this work because propranolol is known to interact with VLDL and estimates of the binding constants for this system have been reported for soluble VLDL (i.e., based on the use of a non-saturable binding model and racemic propranolol) [14]. These interactions were examined in the research described herein by preparing and employing columns containing VLDL immobilized to silica and utilizing the columns in frontal analysis experiments. These experiments were completed to determine the types and strength of interactions that occur between VLDL and *R*- and *S*-propranolol at various temperatures. The results obtained were compared to data obtained using equilibrium dialysis and soluble samples of VLDL [14]. The binding constants determined were then evaluated against previous results obtained for the same drugs with HDL and LDL [10,14-17,26]. These experiments are expected to provide a more complete description of the binding mechanisms between *R*- and *S*-propranolol with VLDL *in vivo*. In addition, the results of this study should indicate the possible advantages in using HPAC to examine drug binding with lipoproteins.

EXPERIMENTAL

Reagents

The *R*- and *S*-propranolol and human VLDL (catalog number L7527, lot no. 036K1143) were obtained from Sigma (St. Louis, MO, USA). Nucleosil Si-1000 silica (1000 Å pore size) with a 7 µm particle diameter was obtained from Macherey Nagel (Düren, Germany). Bicinchoninic acid (BCA) protein assay reagents were purchased from Pierce (Rockford, IL, USA). All other chemicals were of the highest grades available and all solutions used in chromatographic studies were prepared using water from a Nanopure purification system (Barnstead, Dubuque, IA, USA) filtered using Osmonics 0.22 µm nylon filters from Fisher Scientific (Pittsburgh, PA, USA).

Apparatus

The chromatographic system utilized in these studies consisted of a Vici F60-AL injection valve (Houston, TX, USA), an Eppendorf CH-500 column heater (Hauppauge, NY, USA), two 510 Waters HPLC pumps (Milford, MA, USA), and a Waters 2487 UV/Vis absorbance detector. Chromatograms were collected using Waters Empower software and processed using programs based on Labview 5.1 (National Instruments, Austin, TX, USA). The chromatographic columns were packed into 100 mm × 2.1 mm i.d. stainless steel columns by using a slurry packer from Alltech (Deerfield, IL, USA).

Table 4-1 Comparison of binding parameters for *R*- and *S*-propranolol with various lipoproteins at pH 7.4 and 37 °C

Lipoprotein	**Type of drug**	**Binding model [Ref.][a]**	**m_{L1} (mol)**	**K_{a1} (M^{-1})**	**nK_a (M^{-1})**
High density lipoprotein (HDL)	*R*-Propranolol	Saturable site + non-saturable binding [31]	$2.2 (\pm 0.7) \times 10^{-9}$	$1.9 (\pm 0.8) \times 10^{5}$	$4.1 (\pm 0.3) \times 10^{4}$
	S-Propranolol	Saturable site + non-saturable binding [31]	$4.5 (\pm 0.2) \times 10^{-9}$	$1.1 (\pm 0.1) \times 10^{5}$	$3.7 (\pm 0.2) \times 10^{4}$
	R/S-Propranolol	Non-saturable binding [14]	N/A	N/A	$1.60 (\pm 0.14) \times 10^{4}$
Low density lipoprotein (LDL)	*R*-Propranolol	Saturable site + non-saturable binding [10]	$7.5 (\pm 1.5) \times 10^{-10}$	$5.2 (\pm 2.3) \times 10^{5}$	$1.9 (\pm 0.1) \times 10^{5}$
	S-Propranolol	Non-saturable binding [10]	N/A	N/A	$2.7 (\pm 0.2) \times 10^{5}$
	R/S-Propranolol	Non-saturable binding [14]	N/A	N/A	$1.76 (\pm 0.01) \times 10^{5}$
Very low density lipoprotein (VLDL)	*R/S*-Propranolol	Non-saturable binding [14]	N/A	N/A	$2.87 (\pm 0.28) \times 10^{5}$

[a] Ref. [14] utilized soluble lipoproteins, while Refs. [10] and [26] used immobilized lipoproteins.
This table is adapted with permission from Ref. [28].

Preparation of VLDL silica

The VLDL was immobilized onto HPLC silica using the Schiff base method under conditions similar to those described in **Chapters 2 and 3** for HDL and LDL. The first step in the preparation of immobilized VLDL was to convert the Nucleosil Si-1000 silica to diol-bonded silica, as previously described [27]. Following preparation of this support, a portion of the diol-bonded silica was utilized as a control support. As prescribed in the Schiff base method, the diol-bonded silica was converted into an aldehyde-activated form by placing 0.9 g of this support into 15 mL of a 90:10 (v/v) mixture of acetic acid and water that contained 0.9 g periodic acid. This mixture was sonicated under vacuum for 10 min and subsequently shaken at room temperature in the dark for 1 h. The resulting aldehyde-activated silica was washed five times with water and three times with 0.10 M potassium phosphate buffer, pH 6.0.

Next, a 0.45 g portion of the aldehyde-activated support was placed into 5 mL of, 0.10 M potassium phosphate buffer, pH 6.0. This suspension was sonicated for 5 min under vacuum and a 5 mg portion of sodium cyanoborohydride was added. The sodium cyanoborohydride functioned to reduce Schiff bases that form between the aldehyde support and primary amine groups on a ligand. This reduction step was followed by the addition of 1 mg VLDL. The mixture was shaken gently at 4 ºC while protected from light for 8 days. The resulting VLDL support was washed four times with 0.067 M potassium phosphate buffer, pH 7.4. Next, 2 mL of a 1.5 mg/mL sodium borohydride 0.067 M potassium phosphate buffer, pH 7.4, was added slowly to the VLDL support slurry to reduce any remaining aldehyde groups that were still present on the silica. This mixture was shaken for 90 min at room temperature and was washed six times with 0.067

M potassium phosphate buffer, pH 7.4. The final VLDL immobilized support stored in the same buffer at 4 ºC until use.

The VLDL support protein content was determined using a BCA protein assay and bovine serum albumin as the protein standard; a method previously employed with supports containing HDL and LDL [10,31]. The samples and standards used in this assay were prepared in pH 7.4, 0.067 M potassium phosphate buffer, with the VLDL silica samples were examined in triplicate, using diol-bonded silica as the blank. Sample and standard solutions were filtered through a 0.22 μm nylon filter to remove particulates prior to determining absorbance readings for this assay.

Chromatographic studies

The VLDL silica or control support were downward slurry packed at 3500 psi into separate 100 mm × 2.1 mm i.d. stainless steel columns using 0.067 M potassium phosphate buffer, pH 7.4, as the packing solution. The packed columns were subsequently stored in this pH 7.4 buffer at 4°C when not in use. The VLDL column or control column was equilibrated with the same buffer at the specified temperature before each chromatographic experiment. All mobile phases were filtered through an Osmonics 0.22 µm nylon filter and vacuum degassed immediately prior to use. A wavelength of 225 nm was used to monitor the elution of *R*- and *S*-propranolol.

The stability of the immobilized VLDL columns was examined through zonal elution studies on the VLDL supports. This evaluation was performed by conducting replicate 20 µL injections of a 25 mM solution of *R*-propranolol dissolved in 0.067 M potassium phosphate buffer, pH 7.4, on the columns. A mobile phase of, 0.067 M potassium phosphate buffer, pH 7.4, was applied at 1.0 mL/min and 37°C for 30 hours in these studies. The retention time for each peak was determined using Waters Empower 2 Software (Waters Corporations, Milford Massachusetts).

Frontal analysis studies were conducted using the VLDL control column to examine both *R*- and *S*-propranolol. The frontal analysis studies were carried out at 20 ºC, 27 ºC or 37 ºC and a flow rate of 0.5 mL/min. These conditions were shown in previous studies with HDL and LDL columns to be suitable for drug binding studies and to have no significant impact on the measured binding capacities or equilibrium constants [10,26]. The mobile phase for sample application and elution was 0.067 M potassium phosphate buffer, pH 7.4. Nine solutions containing 0.2-25 µM of *R*- or *S*-propranolol were applied to each column in triplicate. The results were integrated using programs written in Labview 5.1 to determine the moles of drug that were required to reach the mean breakthrough time at a given concentration of the applied drug [3]. The control column breakthrough times were subtracted from those measured at the same drug concentration on a VLDL column to correct for the void time and non-specific binding of propranolol to the support. This process was also described in previous chapters for studies involving HDL and LDL columns. The degree of non-specific binding was typically comprised 7-15% of the total breakthrough time for *R*- and *S*-propranolol on the VLDL column. The frontal analysis results were fit to the binding models described in Table 1-2 using non-linear regression and Origin 9.1 software (OriginLab, Northampton Massachusetts).

RESULTS AND DISCUSSION

General properties of VLDL support

A protein assay was used to determine the quantity of lipoprotein that was immobilized on the VLDL support; this was combined with the column dimensions to ascertain the moles of lipoprotein in the HPAC column. The VLDL support was determined to contain 1.23 (± 0.03) mg apolipoprotein per gram silica. This result equates to 15.4 (± 0.4) mg or 2.05 (± 0.05) nmol of VLDL per gram silica, when using an average molar mass of 7.5×10^6 g/mol for VLDL [14] and a typical apolipoprotein content for VLDL of 8% (*w/w*) [24]. When taking the column dimensions and silica packing density into account, a total of 0.27 nmol of VLDL was estimated to be in each HPAC column. This amount of immobilized VLDL (15.4 mg, or 2.05 nmol, per gram silica) was lower than the 28 mg (12 nmol) LDL per gram silica and 68 mg (380 nmol) HDL per gram silica that were obtained with the other lipoproteins in **Chapters 2 and 3**. However, as will be seen later, this VLDL content was still in a range that was suitable for drug binding studies.

The lower lipoprotein content observed for the VLDL support when compared to prior LDL or HDL supports was the result of several factors. First, VLDL has a larger diameter than either lipoprotein previously examined (typical diameter: VLDL, 30-80 nm; LDL, 18-25 nm; HDL, 5-12 nm) [19]. This larger size mandates that a support with a larger pore size, and a lower surface area, is used to immobilize VLDL. Silica with a pore size of 1000 Å (100 nm) was used to immobilize VLDL A support with a 500 Å pore size was used in LDL studies, while a 300 Å support was used in HDL studies [10,26]. In addition to lipoprotein diameter, the extent of immobilization was impacted by the greater expense and relatively low solubility of VLDL. These factors resulted in a smaller amount of this lipoprotein being combined with the support during the immobilization process (i.e., a ratio of 2.2 mg VLDL per gram silica in the starting mixture, compared with 16.7 mg LDL per gram silica or 100 mg HDL per gram silica).

VLDL column stability was examined using both zonal elution and frontal analysis studies. First, repeated injections of *R*-propranolol were made onto a VLDL column under controlled temperature and flow rate conditions. A reproducible retention time for *R*-propranolol occurred over the course of several weeks using an equivalent of 30 h of operation at a flow rate of 1 mL/min (i.e., at least 2.8 L of mobile phase, or 9.3×10^3 column volumes). During these zonal elution experiments *R*-propranolol had an average retention time of 3.2 (± 0.3) min and an average retention factor of 9.5 (± 0.9). Frontal analysis studies were conducted on a fresh VLDL column and demonstrated similar stability and reproducibility over the course of several months. These studies included more than 160 measurements and involved the application of at least 3.4 L of the mobile phase (i.e., 1.13×10^4 column volumes). The zonal elution and frontal analysis data indicated that the VLDL support had similar stability to that observed for HDL and LDL supports [10,26]. These studies also indicated that the VLDL support was suitable for use in long-term studies involving multiple drug binding measurements. The stability of these columns and the relatively small amount of immobilized lipoprotein within a column meant that the average amount of VLDL per experiment is extremely low. This is exemplified in this study by the use of an HPAC column containing 0.27 nmol VLDL for 160 experiments, which equates to an average of 1.7 pmol VLDL per sample application. This level of lipoprotein is significantly less than required to perform other methods of analysis (e.g. equilibrium dialysis or CE) [14-17].

Examination of binding mechanisms for *R*- and *S*-propranolol with VLDL

Frontal analysis was used to examine the binding of *R*- or *S*-propranolol to the VLDL support. Typical breakthrough curves obtained on a VLDL column are shown in Figure 4-1. The mean position of the breakthrough curves appeared between 2 and 7 minutes of sample application, depending on the concentration of the applied analyte. The precision of these measurements was typically within the range of ± 1 to 2%. These breakthrough times were similar to those obtained with LDL columns of the same size [26], but were roughly twice as long as the times needed with HDL columns that were half this size [10]. The individual run times in these studies were shorter. The analysis time of 16 min previously reported when using CE to examine drug interactions with lipoproteins [15] and was much shorter than the six hours that have been used to perform drug-lipoprotein binding studies by equilibrium dialysis [14].

Figure 4-1. Typical frontal analysis results obtained for the application of various concentrations of *R*-propranolol solutions to a 100 mm × 2.1 mm i.d. VLDL column at 0.5 mL/min and 37ºC in the presence of 0.067 M phosphate buffer, pH 7.4. This Figure is reproduced with permission from Ref. [28].

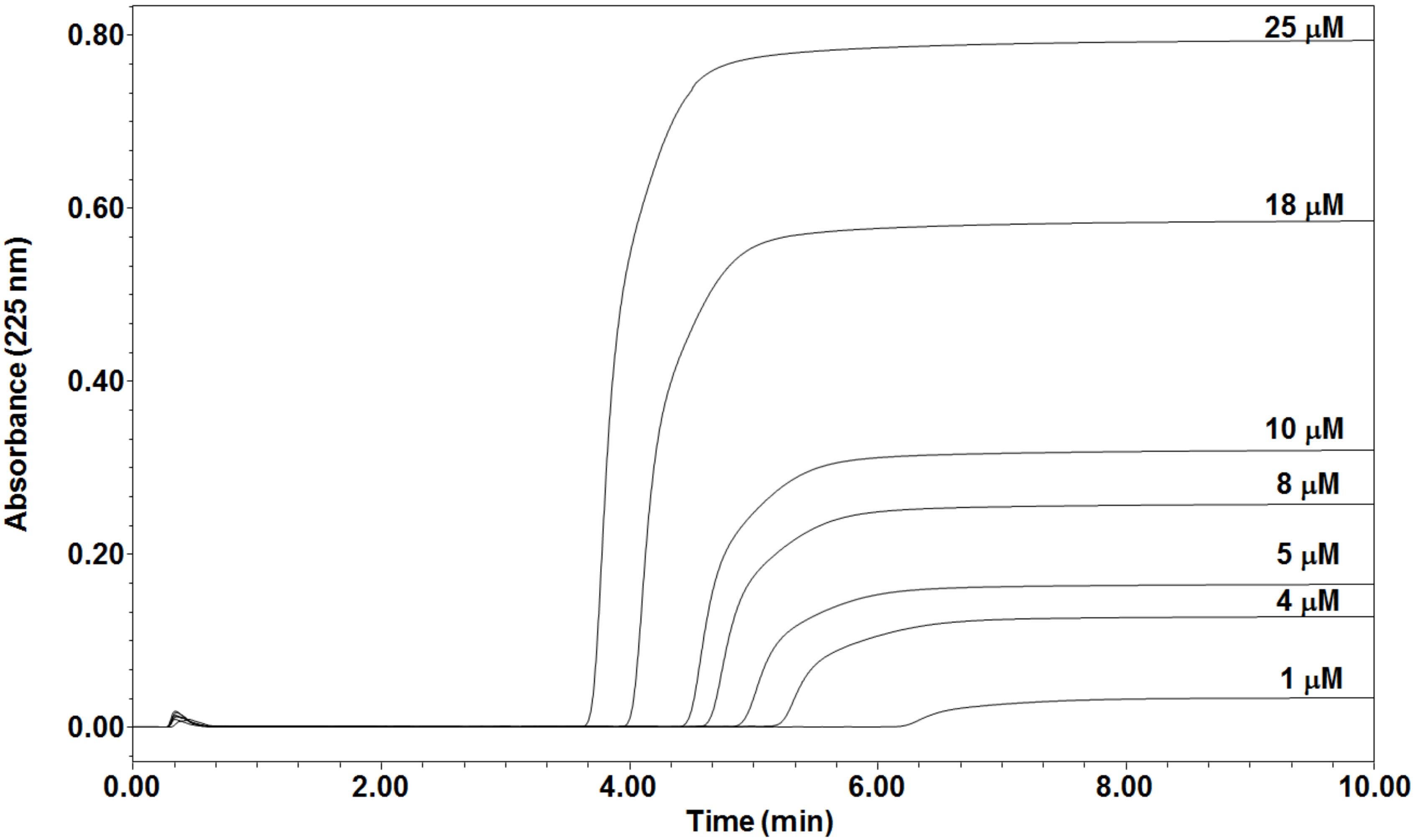

25 μM
18 μM
10 μM
8 μM
5 μM
4 μM
1 μM
0.80
0.60
0.40
0.20
0.00
Absorbance (225 nm)
0.00
2.00
4.00
6.00
8.00
10.00
Time (min)

The moles of drug required to reach the mean position of each breakthrough curve (m_{Lapp}) was determined by integration of the frontal analysis curves. The determined m_{Lapp} values were then used in conjunction with the known concentration of the applied drug ([D]) to generate a double-reciprocal plot of $1/m_{\mathrm{Lapp}}$ versus 1/[D]. Examples of the resulting double-reciprocal plots are shown in Figure 4-2. As described in previous chapters, the presence of only one binding mechanism for the drug on the immobilized ligand is expected to result in a linear relationship for a system with relatively fast association and dissociation kinetics compared to the time scale of the experiment [8]. When multiple binding mechanisms are present, this type of plot should yield deviations from a linear response at large drug concentrations (i.e. low values of 1/[D]) [8]. Each of the double-reciprocal plots produced for *R*- and *S*-propranolol at 20 ºC, 27 ºC and 37 ºC resulted in these negative deviations at high analyte concentrations. Therefore, the double-reciprocal plots are indicative of the presence of multiple binding mechanisms between *R*- or *S*-propranolol and VLDL. This is consistent with what has been previously observed between *R*- or *S*-propranolol with HDL [26], and for *R*-propranolol with LDL [10].

Figure 4-2. Double-reciprocal plots obtained in frontal analysis studies examining the binding of (a) *R*-propranolol and (b) *S*-propranolol to a 100 mm × 2.1 i.d. VLDL column at 37^{o}C and in the presence of pH 7.4, 0.067 M phosphate buffer. The linear fits that are shown were obtained using data points in the upper region of this plot, which are designated by the closed squares (■) and cover *R*- or *S*-propranolol concentrations that range from 0.2 to 4 μM. Data points in the lower regions of these plots (i.e., at higher concentrations of *R*- or *S*-propranolol) showed negative deviations from the linear fit to the upper data points and are represented by open squares (□). Expanded views of the lower regions to the left of these graphs are provided in the insets. This figure is reproduced with permission from Ref. [28].

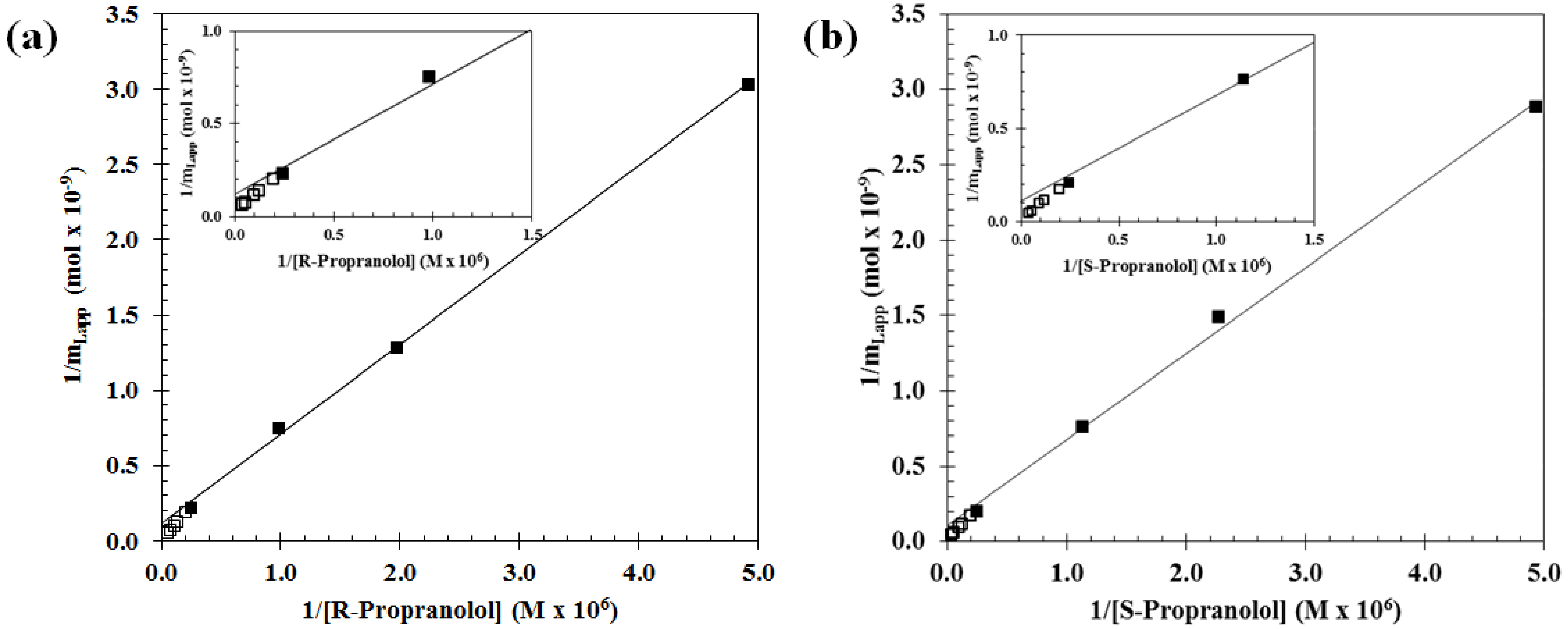
(a)
1/m$_{Lapp}$ (mol x 10^{-9})
1/[R-Propranolol] (M x 10^{6})
0.0
0.5
1.0
1.5
2.0
2.5
3.0
3.5
0.0
1.0
2.0
3.0
4.0
5.0
1/m$_{Lapp}$ (mol x 10^{-9})
1/[R-Propranolol] (M x 10^{6})
0.0
0.5
1.0
1.5
(b)
1/m$_{Lapp}$ (mol x 10^{-9})
1/[S-Propranolol] (M x 10^{6})
0.0
0.5
1.0
1.5
2.0
2.5
3.0
3.5
0.0
1.0
2.0
3.0
4.0
5.0
1/m$_{Lapp}$ (mol x 10^{-9})
1/[S-Propranolol] (M x 10^{6})
0.0
0.5
1.0
1.5

Following the analysis of the frontal analysis data using double-reciprocal plots, the breakthrough curves were examined in more detail using the binding models described in Table 1-2. The first step in these examinations was to prepare non-linear plots of m_{Lapp} versus [D] (see examples in Figure 4-3). Next, the fit of each of the four binding models was tested for use in describing the interactions between *R*- or *S*-propranolol and VLDL. Several previous studies based on equilibrium dialysis or CE have used partitioning to describe the interactions between propranolol and other drugs with lipoproteins [10,14-17,26]. This binding mechanism was also considered in this study using the single non-saturable interaction model. A second type of interaction that may occur is site-specific and saturable binding, as has been noted for *R*- or *S*-propranolol with HDL and for *R*-propranolol with LDL, was considered in describing the interactions with VLDL [10,26]. The double-reciprocal plots indicated that the system under study had the possibility of multiple site-specific binding locations, which was considered by using a model based on two groups of saturable sites [10,26]. Finally, a mixed-mode model was examined in which a single, saturable site and a group of non-saturable interactions were present. The goodness of fit for each model examined was evaluated using the correlation coefficients, residual values, and the distribution of the data about the best-fit line. The corresponding association equilibrium constants, binding capacities, or global affinity constants that were obtained for each model are summarized in the Table 4-2 and Table 4-3.

Figure 4-3. Fit of various binding models to frontal analysis data obtained for *R*-propranolol on a VLDL column at 37 °C and pH 7.4. The models used in this analysis were as follows: (a) non-saturable interactions, (b) a single group of saturable sites, (c) two separate groups of saturable sites, and (d) a group of non-saturable interactions plus a group of saturable sites. The insets show the residual plots for the fit of each model to the experimental data. The correlation coefficients were as follows ($n = 9$): (a) 0.9570, (b) 0.9992, (c) 0.9994, and (d) 0.9998. This figure is reproduced with permission from Ref. [28].

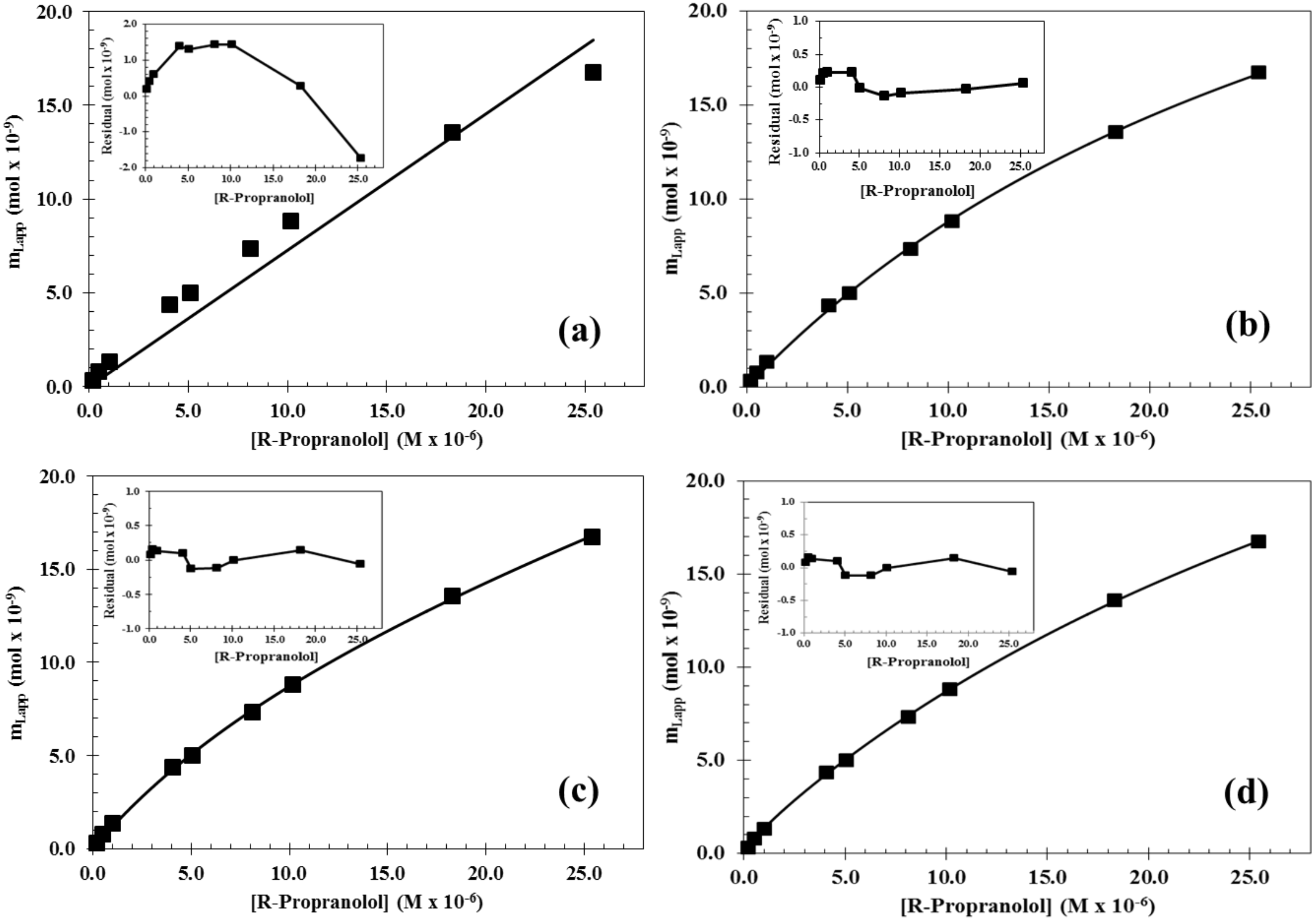
(a)
(b)
(c)
(d)
m_{Lapp} (mol x 10^{-9})
[R-Propranolol] (M x 10^{-6})
0.0
5.0
10.0
15.0
20.0
25.0
Residual (mol x 10^{-9})
[R-Propranolol]
2.0
1.0
0.0
-1.0
-2.0
1.0
0.5
0.0
-0.5
-1.0

The non-saturable interaction model and the model based on a single group of saturable sites (both models that used a single type of interaction) gave reasonably good correlation coefficients (i.e., 0.9570 and 0.9992 respectively) when fit to the frontal analysis data. Despite these reasonable correlation coefficients, the residual plots for the non-saturable model failed to yield a non-random pattern of data points about the best-fit line, as demonstrated by the inset in Figure 4-3(a). Furthermore, both of the single interaction models gave lower correlation coefficients than the two-site or mixed-mode models for the same data. A lower sum of the squares for the residuals (e.g., 0.017-1.59 $\times 10^{-17}$ for the non-saturable or one-site saturable model vs. 0.86-6.01 $\times 10^{-19}$ for the two-site or mixed-mode models) was also obtained for the plots describing multiple interactions. These results support the conclusion drawn from the double-reciprocal plots, i.e., that multiple types of interactions were occurring between *R*- or *S*-propranolol and VLDL.

A more thorough evaluation of the multi-site interaction models in Figure 4-3 (c-d) indicated that similar fits and residual plots were generated when using a two-site saturable model or a mixed-mode model based on one set of saturable sites plus a non-saturable interaction. Despite these similarities, the correlation coefficient obtained for the mixed-mode model was slightly higher than the value for the two-site saturable model (r = 0.9998 vs. 0.9994). Furthermore, the equilibrium constants provided by the mixed-mode model were much more precise than those obtained for the two-site saturable model. The equilibrium binding constants and corresponding precision are listed in Table 4-2 and Table 4-3. All of this information indicated that the mixed-mode model provides the best description of the interactions between *R*- or *S*-propranolol and VLDL.

The same conclusion was reached at all of the temperatures evaluated through the course of this study. These results were consistent with the binding mechanisms that were proposed for the binding by *R*- and *S*-propranolol with HDL and for *R*-propranolol with LDL in **Chapters 2 and 3**.

Determination of equilibrium constants and number of interaction sites

Following determination of the proper model to describe the binding of *R*- and *S*-propranolol with VLDL, the mixed-mode model was used to provide more details on these interactions. This evaluation revealed that neither the temperature nor enantiomer significantly impacts the mixed-mode binding between propranolol and VLDL. One example of this can be seen in the evaluation of the single-site saturable interactions of *R*- and *S*-propranolol with VLDL. The *R*- enantiomer had an association equilibrium constant (K_{a1}) of 7.0 (± 2.3) × 10^4 M^{-1} at 37 ºC while the interaction between *S*-propranolol and VLDL at the same temperature were statistically equivalent (at the 95% confidence level) for K_{a1} of 9.6 (± 2.2) × 10^4 M^{-1}. Furthermore, the K_{a1} value for *R*-propranolol with VLDL varied from only 7.0 to 9.2 × 10^4 M^{-1} between 20 °C and 37 °C while the K_{a1} for *S*-propranolol ranged from 4.6 to 9.6 × 10^4 M^{-1} over this temperature range. For both propranolol enantiomers, no significant variability in K_{a1} occurred at the 95% confidence level over this temperature range for most of these values, with the only exception being a possible decrease in the value obtained for VLDL with *S*-propranolol at 27 °C. A paired Student's *t*-test was used to verify that overall set of values obtained for the two enantiomers were not significant different at the 95% confidence level.

Table 4-2 Binding parameters obtained for *R*-propranolol on a VLDL column at various temperatures[a]

Enantiomer	Binding Model	Temperature	m_{L1} (mol)	K_{a1} (M^{-1})	m_{L1} (mol)	K_{a1} (M^{-1})	nK_a[b] (M^{-1})
R-Propranolol	Non-saturable interaction	20 °C	-	-	-	-	$4.2 (\pm 0.1) \times 10^{6}$
	Single group of saturable sites	20 °C	$9.8 (\pm 0.7) \times 10^{-8}$	$1.5 (\pm 0.1) \times 10^{4}$	-	-	-
	Two groups of saturable sites	20 °C	$4.9^{c} \times 10^{-8}$	$1.5 (\pm 85{,}000) \times 10^{4}$	$4.9^{c} \times 10^{-8}$	$1.5 (\pm 85{,}000) \times 10^{4}$	-
	Two interactions: saturable + non-saturable	**20 °C**	$\mathbf{1.0 (\pm 0.5) \times 10^{-8}}$	$\mathbf{9.2 (\pm 4.8) \times 10^{4}}$	**-**	**-**	$\mathbf{3.0 (\pm 0.3) \times 10^{6}}$
R-Propranolol	Non-saturable interaction	27 °C	-	-	-	-	$4.4 (\pm 0.1) \times 10^{5}$
	Single group of saturable sites	27 °C	$9.7 (\pm 0.7) \times 10^{-8}$	$1.6 (\pm 0.1) \times 10^{4}$	-	-	-
	Two groups of saturable sites	27 °C	$4.9 (\pm 7{,}000{,}000) \times 10^{-8}$	$1.6 (\pm 53{,}000) \times 10^{4}$	$4.9 (\pm 7{,}000{,}000) \times 10^{-8}$	$1.6 (\pm 53{,}000) \times 10^{4}$	-
	Two interactions: saturable + non-saturable	**27 °C**	$\mathbf{1.3 (\pm 0.8) \times 10^{-8}}$	$\mathbf{7.3 (\pm 4.3) \times 10^{4}}$	**-**	**-**	$\mathbf{2.9 (\pm 0.5) \times 10^{6}}$
R-Propranolol	Non-saturable interaction	37 °C	-	-	-	-	$2.7 (\pm 0.1) \times 10^{6}$
	Single group of saturable sites	37 °C	$4.0 (\pm 0.2) \times 10^{-8}$	$2.9 (\pm 0.2) \times 10^{4}$	-	-	-
	Two groups of saturable sites	37 °C	$7.0 (\pm 3.7) \times 10^{-10}$	$1.2 (\pm 1.0) \times 10^{6}$	$4.6 (\pm 0.3) \times 10^{-8}$	$2.1 (\pm 0.3) \times 10^{4}$	-
	Two interactions: saturable + non-saturable	**37 °C**	$\mathbf{1.3 (\pm 0.5) \times 10^{-8}}$	$\mathbf{7.0 (\pm 2.3) \times 10^{4}}$	**-**	**-**	$\mathbf{1.2 (\pm 0.3) \times 10^{6}}$

[a] The numbers in parentheses represent a range of ± 1 S.D. All of these results were measured in pH 7.4, 0.067 M potassium phosphate buffer.

[b] The value for nK_a for a non-saturable interaction was obtained by dividing the best-fit result for $m_L K_a$ by the estimated moles of LDL in the column. This latter value was obtained by using the protein content of the LDL support, using a typical protein content for LDL of 25% (*w/w*), and an average molar mass for LDL of 2.3×10^{6} g/mol.

[c] The fitting program (Origin) was not able to generate an estimate of the standard deviation in these cases.

The best fit model is represented in **bold**.

This table is adapted with permission from Ref. [28].

Table 4-3 **Binding parameters obtained for *S*-propranolol on a VLDL column at various temperatures[a]**

Enantiomer	Binding Model	Temperature	m_{L1} (mol)	K_{a1} (M^{-1})	m_{L1} (mol)	K_{a1} (M^{-1})	nK_a[b] (M^{-1})
S-Propranolol	Non-saturable Interaction	20 °C	-	-	-	-	$4.3 (\pm 0.2) \times 10^{6}$
	Single group of saturable sites	20 °C	$8.1 (\pm 0.5) \times 10^{-8}$	$2.0 (\pm 0.2) \times 10^{4}$	-	-	-
	Two groups of saturable sites	20 °C	$9.5 (\pm 5.7) \times 10^{-10}$	$1.3 (\pm 1.4) \times 10^{6}$	$1.0 (\pm 0.1) \times 10^{-7}$	$1.3 (\pm 0.2) \times 10^{4}$	-
	Two interactions: saturable + non-saturable	**20 °C**	$\mathbf{1.6 (\pm 0.8) \times 10^{-8}}$	$\mathbf{6.9 (\pm 3.4) \times 10^{4}}$	**-**	**-**	$\mathbf{2.5 (\pm 0.5) \times 10^{6}}$
S-Propranolol	Non-saturable Interaction	27 °C	-	-	-	-	$4.1 (\pm 0.2) \times 10^{6}$
	Single group of saturable sites	27 °C	$7.6 (\pm 0.3) \times 10^{-8}$	$2.0 (\pm 0.1) \times 10^{4}$	-	-	-
	Two groups of saturable sites	27 °C	$2.4 (\pm 7.7) \times 10^{-8}$	$4.7 (\pm 7.9) \times 10^{4}$	$9.6 (\pm 660) \times 10^{-7}$	$5.4 (\pm 390) \times 10^{2}$	-
	Two interactions: saturable + non-saturable	**27 °C**	$\mathbf{2.5 (\pm 0.9) \times 10^{-8}}$	$\mathbf{4.6 (\pm 1.3) \times 10^{4}}$	**-**	**-**	$\mathbf{1.8 (\pm 0.4) \times 10^{6}}$
S-Propranolol	Non-saturable Interaction	37 °C	-	-	-	-	$3.5 (\pm 0.1) \times 10^{6}$
	Single group of saturable sites	37 °C	$8.5 (\pm 0.9) \times 10^{-8}$	$1.4 (\pm 0.2) \times 10^{4}$	-	-	-
	Two groups of saturable sites	37 °C	$4.3 (\pm 2{,}700{,}000) \times 10^{-8}$	$1.4^{d} \times 10^{4}$	$4.3 (\pm 2{,}700{,}000) \times 10^{-8}$	$1.4^{d} \times 10^{4}$	$4.3 (\pm 2{,}700{,}000) \times 10^{-8}$
	Two interactions: saturable + non-saturable	**37 °C**	$\mathbf{0.78 (\pm 0.16) \times 10^{-8}}$	$\mathbf{9.6 (\pm 2.2) \times 10^{4}}$	**-**	**-**	$\mathbf{2.4 (\pm 0.6) \times 10^{6}}$

[a] The numbers in parentheses represent a range of ± 1 S.D. All of these results were measured in pH 7.4, 0.067 M potassium phosphate buffer.

[b] The value for nK_a for a non-saturable interaction was obtained by dividing the best-fit result for $m_L K_a$ by the estimated moles of LDL in the column. This latter value was obtained by using the protein content of the LDL support, using a typical protein content for LDL of 25% (*w/w*), and an average molar mass for LDL of 2.3×10^{6} g/mol.

[c] The fitting program (Origin) was not able to generate an estimate of the standard deviation in these cases.

The best fit model is represented in **bold**.

This table is adapted with permission from Ref. [28].

The non-linear regression indicated that the VLDL column had an amount of the saturable binding sites in the range of 7.8 to 25 nmol for *R*- and *S*-propranolol at 20 °C to 37 °C (average: *R*-propranolol = 12 nmol, *S*-propranolol = 16 nmol). This value is 5.4- to 17-fold larger (average, 9.7-fold larger) than the moles of VLDL particles that were estimated to be present in the column using the BCA protein assay. This result is expected based upon work with HDL and LDL that demonstrated saturable binding occurs with apolipoproteins [10,26], which can have many copies present on a large lipoprotein particle such as VLDL [19].

Several apolipoproteins may be present on a single copy of VLDL. The apolipoproteins present on VLDL may include B-100, C-I, C-II, C-III, and/or E [7]. Most of these apolipoproteins are also found in HDL or LDL, with LDL containing apolipoprotein B-100 and HDL comprised of apolipoproteins A-I, A-II, C-I, C-II, C-III, D, and E [7]. The K_{a1} values that are listed in Table 4-2 and Table 4-3 for *R*- and *S*-propranolol with VLDL are similar to or only slightly lower than the values of $1.1\text{-}1.9 \times 10^5$ M^{-1} measured under the same pH and temperature conditions for the saturable binding by propranolol with HDL (e.g., see results in Table 4-1) [31]. This suggests that apolipoproteins responsible for the saturable interactions with propranolol are common between HDL and VLDL (e.g., apolipoproteins C-I, C-II, C-III, and E) [7].

Although apolipoprotein is common between VLDL and LDL, the stereoselectivity that was described in **Chapter 3** for the binding of *R*- and *S*-propranolol to LDL (and proposed to be due to apolipoprotein B-100) was not detected in studies with VLDL. Furthermore, the K_{a1} values that have been measured for *R*-propranolol with LDL are 4.6- to 11.3 times higher than the values for VLDL under the same pH and temperature conditions [10]. The lower binding strength and lack of stereoselectivity with VLDL indicates that apolipoprotein B-100 is probably not a significant source of the saturable binding compared to that for VLDL and propranolol. The presence of a greater amount of apolipoproteins other than B-100 in VLDL may be responsible for this phenomenon. Alternatively, the presence of these other apolipoproteins may impact the accessibility and/or conformation of apolipoprotein B-100 in the region at which the stereoselective binding of propranolol occurs with LDL. The latter possibility is supported by other reports that have shown that the presence of other apolipoproteins (e.g., apolipoproteins C and E) impacts the ability of apolipoprotein B-100 to bind to enzymes and cell surface receptors through protein-protein interactions [29].

Non-saturable binding was the second mechanism that made up the total interaction between *R*- and *S*-propranolol with VLDL. This interaction had an overall affinity (nK_a) at pH 7.4 and 37 ºC of $1.2\ (\pm\ 0.3) \times 10^6\ M^{-1}$ for *R*-propranolol and $2.4\ (\pm\ 0.6) \times 10^6\ M^{-1}$ for *S*-propranolol. The overall affinity values ranged from 1.2 to $3.0 \times 10^6\ M^{-1}$ for *R*-propranolol and 1.8 to $2.5 \times 10^6\ M^{-1}$ for *S*-propranolol at temperatures between 20 ºC and 37 ºC. There was no significant difference in the overall set of values obtained for the two enantiomers, as determined by using a paired Student's *t*-test at the 95% confidence level. This type of interaction has been suggested in previous work in this dissertation to describe the partitioning of *R*- and *S*-propranolol or other drugs into the non-polar core of a lipoprotein, or an interaction with phospholipids on the surface [10,14,15,26]. The overall affinity values for the non-saturable binding of *R*- and *S*-propranolol with VLDL were approximately 30- to 200-times higher than the values of $1.6\text{-}4.1 \times 10^4\ M^{-1}$ that have been measured at pH 7.4 and between 4 °C and 37 °C for the same type of interaction of these enantiomers with HDL [14,15,26]. Furthermore, these values were 3- to 17-times larger than nK_a values that have been obtained for *R*- and *S*-propranolol with LDL [10,14,15]. The difference in nK_a values is consistent with a mechanism based on the partitioning of these drugs into the non-polar core of these lipoproteins, as the order of these nK_a values agrees with the fact that VLDL has a much larger portion of hydrophobic components (i.e., cholesterol and triacylglycerides) than either HDL or LDL [7,15,18,19].

CONCLUSIONS

The studies described in this chapter examined the extension and use of HPAC with immobilized VLDL to examine the binding of drugs such as *R*- and *S*-propranolol to this lipoprotein. The use of HPAC methodologies revealed that *R*- and *S*-propranolol had a combination of two distinct types of interactions with VLDL. One of the interactions was non-saturable in nature and probably involved the partitioning of propranolol into the non-polar core of VLDL. This interaction is described by an overall affinity constant ranging from $1.4\text{-}3.6 \times 10^6$ M^{-1} between 20 °C and 37 ^{o}C. The second interaction identified during the HPAC studies was the result of site-specific, saturable binding. This interaction is believed to occur between these drugs and apolipoproteins on the surface of VLDL. The association equilibrium constants for these site-specific, saturable interactions were in the range of $4.6\text{-}9.2 \times 10^4$ M^{-1} between 20 °C and 37 ºC.

The binding parameters determined in these studies with VLDL were in the general range of those reported for propranolol when using a similar mixed-mode model for immobilized HDL and LDL [10,26]. Previous studies utilizing soluble VLDL have reported binding constants for racemic propranolol reported results based upon a non-saturable model, when the HPAC data presented in this chapter was examined using a non-saturable model (see Table 4-2 and Table 4-3). The resulting overall affinities of 10^5-10^6 M^{-1} were consistently within the range that has been reported with soluble VLDL [14]. The studies reported in this chapter also demonstrated that, despite the possible presence of apolipoprotein B-100, VLDL does not exhibit stereoselectivity in propranolol binding as was observed with LDL [10]. This difference is potentially due to the difference in apolipoprotein content between VLDL and LDL. The lack of stereoselectivity may also be related to changes in the accessibility and/or conformation of apolipoprotein B-100 in the presence of other apolipoproteins in VLDL [29].

The suitability of HPAC as a technique to characterize mixed-mode binding mechanisms between lipoproteins, such as VLDL, and drugs was again demonstrated in these studies. As noted in work presented in **Chapters 2 and 3**, HPAC methodologies provide a significant improvement over CE and equilibrium dialysis in terms of analysis times [14,15]. In addition to the relatively short analysis times, HPAC columns containing VLDL were sufficiently stable to be used for a large number of experiments. In combination, these features enable the ability to achieve a significant reduction in the amount of ligand needed for a large number of experiments when using HPAC methodologies in lieu of equilibrium dialysis or CE studies.

The ability to use the same VLDL column for multiple studies eliminated or minimized variations due to batch-to-batch changes in the binding agent preparations. In addition, the use of the VLDL columns with standard HPLC equipment and detectors provided good limits of detection and relatively high precision in the chromatographic results [3,4,10,26]. These advantages make the reliable acquisition of data over a variety of drug concentrations possible. In turn, these features make it possible to compare several binding mechanisms and enabled the identification of mixed-mode interactions between VLDL and *R*- or *S*-propranolol. These features make similar HPAC columns and methods a viable tool in future studies aimed at examining the binding of additional drugs and solutes with VLDL or with other complex binding agents.

ACKNOWLEDGEMENTS

This work was supported by the National Institute of Health under grant R01 GM 044931 and was performed in facilities renovated with support under grant RR015468-01.

References

1. Otagiri, M. *Drug Metab. Pharmacokinet.* **2005**, *20*, 309–323.
2. Bertucci, C.; Domenici, E. *Curr. Med. Chem.* **2002**, *9*, 1463.
3. Patel, S.; Wainer, I.W.; Lough, J.W. In *Handbook of Affinity Chromatography,* 2nd ed; Hage, D.S. Ed.; CRC Press: Boca Raton, **2006**, pp 663-683.
4. Hage, D.S.; Jackson, A.; Sobansky, M.; Schiel, J.E.; Yoo, M.Y.; Joseph, K.S. *J. Sep. Sci.* **2009,** *32*, 835–853.
5. Xuan, H.; Hage, D.S. *Anal. Biochem.* **2005**, *346*, 300–310.
6. Mallik, R.; Xuan, H.; Guiochon, G.; Hage, D.S. *Anal. Biochem.* **2008** *376*, 154–156.
7. Jonas, A. In *Biochemistry of Lipids, Lipoproteins, and Membranes*; Vance, D.E.; Vance, J.E. Eds.; Elsevier: Amsterdam, **2002**, pp 483–504.
8. Hage, D.S. *J. Chromatogr. B.* **2002,** *768*, 3-30.
9. Kuroda, Y.; Cao, B.; Shibukawa, A.; Nakagawa, T. *Electrophoresis* **2001,** *22*, 3401-3407.
10. Sobansky, M.R.; Hage, D.S. Anal. Bioanal. Chem. **2012**, *403*, 563-571.
11. Shen, Q.; Wang, L.; Zhou, H.; Jiang, H.; Yu, L.; Zeng, S. *Acta Pharmacol. Sin.* **2013**, *34*, 998-1006.
12. Noctor, T.A.G. In *Drug Stereochemistry: Analytical Methods and Pharmacology*; Wainer, I.W. Ed.; CRC Press/Marcel Dekker: New York, **1993,** pp 337-364.
13. Dong, H.; Guo, X.; Li, Z. In *Chiral Drugs: Chemistry and Biological Action*; Lin, G.; You, Q.; Cheng, J. Ed.; Wiley: Hoboken, **2011**, pp 347-380.

14. Glasson, S.; Zini, R.; D'Athis, P.; Tillement, J.P. ; Boissier, J.R. *Mol. Pharmacol.* **1980**, *17*, 187–191.

15. Ohnishi. T.; Mohamed, N.A.L.; Shibukawa, A.; Kuroda, Y.; Nakagawa, T.; El Gizawy, S.; Askal, H.F.; El Kommos, M.E. *J. Pharm. Biomed. Anal.* **2002**, *27*, 607–614.

16. Mohamed, N.A.L.; Kuroda, Y.; Shibukawa, A.; Nakagawa, T.; El Gizawy, S.; Askal, H.F.; El Kommos, M.E. *J. Chromatogr. A.* **2000**, *875*, 447–453.

17. Mohamed, N.A.L.; Kuroda, Y.; Shibukawa, A.; Nakagawa, T.; El Gizawy, S.; Askal, H.F.; El Kommos, M.E.; *J. Pharm. Biomed. Anal.* **1999**, *21*, 1037–1043.

18. Barklay, M. In *Blood Lipids and Lipoproteins: Quantitation, Composition, and Metabolism*; Nelson, G.J. Ed.; Wiley: New York, **1972**, pp 587–603.

19. Wasan, K.M.; Cassidy, S.M. *J. Pharm. Sci*. **1998**, *87*, 411–424.

20. Harmony, J.A.K.; Aleson, A.L.; McCarthy, B.M. In *Biochemistry and Biology of Plasma Lipoproteins*; Scanu, A.M.; Spector, A.A. Eds.; Marcel Dekker: New York, **1986**, pp 403-430.

21. Mbewu, A.D.; Durrington, P.N. *Atherosclerosis* **1990**, *85*, 1–14.

22. Durrington, P.N.; In *Lipoproteins and Lipids*; Durrington, P.N. Ed.; Wright: London, **1989,** pp 255–277.

23. Havel, R.J.; Kane, J.P. In *The Metabolic and Molecular Basis of Inherited Disease*; Scriver, C.R.; Beaudet, A.L.; Sly, W.S.; Valle, D.; Childs, B.; Kinzler, K.W.; Vogelstein, B. Eds.; McGraw-Hill: New York, **1995**, pp 1129–1138.

24. Skipski, V.R.; In *Blood Lipids and Lipoproteins Quantitation, Composition, and Metabolism*; Nelson, G.J. Ed.; John Wiley: New York, **1972**, pp 471–583.

25. Kwong, T.C. *Clin. Chim. Acta* **1985**, *151*, 193–216.

26. Chen, S.; Sobansky, M.; Hage, D.S. *Anal. Biochem.* **2010,** *397*, 107-114.

27. Tweed, S.; Loun, B.; Hage, D.S. *Anal. Chem.* **1997**, *69*, 4790- 4798.

28. Sobansky, M.R.; Hage, D.S. *Anal. Bioanal. Chem*. **2014**, *406*, 6203-6211.

29. Yang, C.Y.; Gu, Z.W.; Valentinova, N.; Pownall, H.J.; Lee, B.; Yang, M.; Xie, Y.H.; Guyton, J.R.; Vlasik, T.N.; Fruchart, J.C.; Gotto, A.M. *J. Lipid Res.* **1993**, *34*, 1311-1321.

CHAPTER FIVE

EVALUATION OF MIXED-MODE INTERACTIONS BETWEEN DRUGS AND LIPOPROTEINS BY HIGH-PERFORMANCE AFFINITY CHROMATOGRAPHY

INTRODUCTION

Frontal analysis high performance affinity chromatography (HPAC) was used throughout this dissertation to evaluate the properties of lipoprotein columns, as described in **Chapter 1**. These methods have been used to evaluate many binding agents that contain a single type of interaction for an analyte [1-3] and to identify mixed-mode interactions between several model drugs and HDL, LDL, or VLDL as cited previously. These mixed-mode interactions are the result of the complex structure of lipoproteins, which can give rise to both high-affinity binding at saturable sites and non-saturable interactions with the lipoprotein core.

The goal of this study was to examine methods for detecting mixed-mode binding of biological interactions and when using frontal analysis and HPAC. An emphasis was placed on the evaluation of double-reciprocal plots for data analysis, though the use of traditional binding isotherms was also evaluated. The binding of *R*-propranolol by LDL served as a model system to illustrate such an analysis. This same model system was examined in **Chapter 3** and was shown to undergo mixed-mode interactions that involved binding by *R*-propranolol by a group of high-affinity, saturable sites and a non-saturable interaction. The ability of double-reciprocal plots to detect mixed-mode binding was examined by using chromatographic theory. The expected result of these studies was that an improved method for the identification and study of mixed-mode binding by frontal analysis HPAC would be determined. This method is expected to be applicable to other systems that may involve in mixed-mode interactions.

THEORY

Frontal analysis data for a system containing a single group of saturable sites may be analyzed by using the adsorption isotherm that is shown in Eq. (1) Alternatively, these data can be analyzed by using the double-reciprocal form of the same isotherm, as shown in Eq. (2) [3-4].

$$m_{Lapp} = \frac{m_{Ltot}K_{a1}[\mathrm{D}]}{(1+K_{a1}[\mathrm{D}])} \tag{1}$$

$$\frac{1}{m_{Lapp}} = \frac{1}{(K_{a1}m_{Ltot}[\mathrm{D}])} + \frac{1}{m_{Ltot}} \tag{2}$$

Likewise, frontal analysis data for a system containing only a non-saturable interaction may be analyzed by using the isotherm shown in Eq. (3) below, or via the double-reciprocal -form that is displayed in Eq. (4) [5-7].

$$m_{Lapp} = m_{L1}K_{a1}[\mathrm{D}] \tag{3}$$

$$\frac{1}{m_{Lapp}} = \frac{1}{(m_{L1}K_{a1}[\mathrm{D}])} \tag{4}$$

In these equations, m_{Lapp} is the apparent moles of analyte that are required to reach the mean breakthrough point in a frontal analysis isotherm at a drug concentration of [D].

The term m_{Ltot} is the total binding capacity (in moles) of the column for the applied drug or target. The association equilibrium constant for the drug's interactions with the immobilized binding agent is represented by the term K_{a1}. Plotting the frontal analysis data according to the expressions that are presented in Eqs. (1) and (3) is expected to yield a linear response when non-saturable interactions are present and a non-linear response if a single saturable group of binding sites is present. The difference in response between these models makes distinguishing them relatively easy when evaluating the binding isotherms.

A double-reciprocal plot of either the non-saturable model or a model for a single group of saturable sites, as represented by Eqs. (2) and (4), is expected to yield a linear response, although for non-saturable model an intercept of zero is obtained while a non-zero intercept appears in a saturable binding model. If deviations from linearity occur at high analyte concentrations (i.e., at low values of 1/[D]), more than one type of interaction must be present for the drug or target analyte [4,8].

Equations similar to these have been previously reported to describe the results in frontal analysis experiments for systems that have two saturable groups of binding sites [4,8]. The mathematical description of this latter binding model is shown in Eq. (5). The double-reciprocal plot for this type of system is described by Eq. (6) [4,8].

$$m_{Lapp} = \frac{m_{L1}K_{a1}[\mathrm{D}]}{(1+K_{a1}[\mathrm{D}])} + \frac{m_{L2}K_{a2}[\mathrm{D}]}{(1+K_{a2}[\mathrm{D}])} \tag{5}$$

$$\frac{1}{m_{Lapp}} = \frac{1+K_{a1}[\mathrm{D}]+\beta_2 K_{a1}[\mathrm{D}]+\beta_2 K_{a1}^2[\mathrm{D}]^2}{m_{Ltot}\{(\alpha_1+\beta_2-\alpha_1\beta_2)K_{a1}[\mathrm{D}]+\beta_2 K_{a1}^2[\mathrm{D}]^2\}} \tag{6}$$

In these equations, K_{a1} is the association equilibrium constant for the drug or target analyte at the binding site with the highest affinity (L_1), and K_{a2} is the association equilibrium constant for the drug or target analyte at its binding site with the lower affinity (L_2). The values of m_{L1} and m_{L2} (or $m_{L1,tot}$ and $m_{L2,tot}$) are the moles of these saturable affinity binding sites. The term β is a dimensionless parameter that is defined as the ratio of the association equilibrium constant for a specific site versus the highest affinity site in the population (e.g., $\beta_2 = K_{a2}/K_{a1}$, where $0 < K_{a2} < K_{a1}$; and $\beta_1 = K_{a1}/K_{a1} = 1.00$). The term α is also a dimensionless parameter and corresponds to the mole fraction of all the binding regions that make up a given group of sites (e.g., for a two-site saturable system, $\alpha_1 = m_{L1}/m_{Ltot}$ and $\alpha_2 = m_{L2}/m_{L,tot}$, where $1 = \alpha_1 + \alpha_2$) [4,8].

Interactions between drugs and lipoproteins have been shown in the previous chapters of this dissertation to follow mixed-mode binding in many situations. The equation describing this binding model is shown in Eq. (7). This equation can be rewritten in terms of K_{a1} by using the parameter β_2, where β_2 is now equal to the term n_2K_{a2}/K_{a1}, and n_2K_{a2} represents the overall affinity for the non-saturable interaction. This modified version of Eq. (7) is given in Eq. (8). The double-reciprocal form for this equation is provided in Eq. (9).

$$m_{Lapp} = \frac{m_{L1}K_{a1}[\mathrm{D}]}{1+ K_{a1}[\mathrm{D}]} + m_{L2}K_{a2}[\mathrm{D}] \tag{7}$$

$$m_{Lapp} = \frac{m_{L1}K_{a1}[\mathrm{D}]}{1+ K_{a1}[\mathrm{D}]} + \beta_2 K_{a1}[\mathrm{D}] \tag{8}$$

$$\frac{1}{m_{Lapp}} = \frac{1+ K_{a1}[\mathrm{D}]}{m_{Ltot}\left(K_{a1}[D]+ \beta_2 K_{a1}[\mathrm{D}]+ \beta_2 K_{a1}^2[\mathrm{D}]^2\right)} \tag{9}$$

A double-reciprocal plot of $1/m_{Lapp}$ versus 1/[D], as made according to Eq. (6) or (9), is expected to be non-linear across a broad range of analyte concentrations. However, previous reports have demonstrated that these plots approach linear behavior at low analyte concentrations for a two-site system [4,8]. This phenomenon also holds true for a mixed-mode system, as shown by Eq. (10).

$$\lim_{[\mathrm{D}]\to 0} \frac{1}{m_{Lapp}} = \frac{1}{m_{Ltot}(K_{a1}[\mathrm{D}]+\beta_2 K_{a1}[\mathrm{D}])} + \frac{1}{m_{Ltot}(1+\beta_2)} \qquad (10)$$

In this study Eqs. (9) and (10) were modified to the forms given in Eqs. (11) and (12) and used in the examination of the effects of mixed-mode binding in frontal analysis.

$$\frac{m_{Ltot}}{m_{Lapp}} = \frac{1+K_{a1}[\mathrm{D}]}{(K_{a1}[\mathrm{D}]+\beta_2 K_{a1}[\mathrm{D}]+\beta_2 K_{a1}^2[\mathrm{D}]^2)} \qquad (11)$$

$$\lim_{[\mathrm{D}]\to 0} \frac{m_{Ltot}}{m_{Lapp}} = \frac{1}{(K_{a1}[\mathrm{D}]+\beta_2 K_{a1}[\mathrm{D}])} + \frac{1}{(1+\beta_2)} \qquad (12)$$

All terms in Eqs. (11) and (12) are now expressed through the use of dimensionless parameters. These parameters include the term β_2, which was discussed previously, and also include the combined term $1/(K_{a1}[\mathrm{D}])$ (i.e., the independent variable in a dimensionless double-reciprocal plot) and the ratio m_{Ltot}/m_{Lapp} (i.e., the dependent variable in a dimensionless double-reciprocal plot). These terms and equations were used in this chapter to create universal plots to describe the effects of mixed-mode interactions across a broad range of experimental conditions. A summary of the equations used to describe double-reciprocal plots of each binding model considered are shown in Table 5-1.

EXPERIMENTAL

Reagents

Individual enantiomers of *R*- and *S*-propranolol and the human LDL (catalog number L7914, lot no. 036K1143), were purchased from Sigma (St. Louis, MO, USA). Nucleosil Si-500 silica (7 µm particle diameter, 500 Å pore size) was procured from Macherey Nagel (Düren, Germany). All other chemicals and reagents were of the highest grades available. Reagents for the bicinchoninic acid (BCA) protein assay were from Pierce (Rockford, IL, USA). Water dispensed from a Nanopure purification system (Barnstead, Dubuque, IA, USA) and filtered using Osmonics 0.22 µm nylon filters from Fisher Scientific (Pittsburgh, PA, USA) was used to prepare all solutions.

Apparatus

Frontal analysis studies were performed using a high performance liquid chromatographic system comprised of two 510 HPLC pumps (Waters, Milford, MA, USA), an F60-AL injection valve (Vici, Houston, TX, USA), a CH-500 column heater (Eppendorf, Hauppauge, NY, USA) and a Waters 2487 UV/Vis variable wavelength absorbance detector. Chromatograms were collected using Waters Empower software and processed by programs based on Labview 5.1 (National Instruments, Austin, TX, USA). Supports were placed into HPLC columns by using a slurry packer from Alltech (Deerfield, IL, USA).

Table 5-1. **Summary of double-reciprocal expressions for binding models used with frontal analysis data for drugs on lipoprotein columns**

Binding model	**Predicted response**[a]	
Non-saturable interaction	$1/m_{\mathrm{Lapp}} = 1/(m_{\mathrm{Ltot}}K_{\mathrm{a1}}[\mathrm{D}])$	(7)
Single group of saturable sites	$1/m_{\mathrm{Lapp}} = 1/(\mathrm{m}_{\mathrm{Ltot}}K_{\mathrm{a1}}[\mathrm{D}]) + (1/m_{\mathrm{Ltot}})$	(8)
Saturable sites + non-saturable interaction	$1/m_{\mathrm{Lapp}} = (1+K_{\mathrm{a1}}[\mathrm{D}])/(m_{\mathrm{Ltot}}(K_{\mathrm{a1}}[\mathrm{D}] + \beta_2 K_{\mathrm{a1}}[\mathrm{D}]+\beta_2 K_{\mathrm{a1}}{}^2[\mathrm{D}]^2))$	(9)
Two groups of saturable sites	$1/m_{\mathrm{Lapp}} = (1+K_{\mathrm{a1}}[\mathrm{D}]+\beta_2 K_{\mathrm{a1}}[\mathrm{D}]+\beta_2 K_{\mathrm{a1}}{}^2[\mathrm{D}]^2)/(\mathrm{m}_{\mathrm{Ltot}}\ (\alpha_1+\beta_2 - \alpha_1\beta_2)\ K_{\mathrm{a1}}[\mathrm{D}]+ \beta_2 K_{\mathrm{a1}}{}^2[\mathrm{D}]^2)$ where: $\alpha_1 = m_{\mathrm{L1}}/\mathrm{m}_{\mathrm{Ltot}}$ $\beta_2 = K_{\mathrm{a2}}/K_{\mathrm{a1}}$	(10)

[a] Symbols: m_{Lapp}, moles of applied analyte required to reach the mean position of the breakthrough curve; m_{L1}, total moles of active binding site 1; K_{a1}, association equilibrium constant for binding of the analyte to the ligand at site 1; [D], concentration of the applied drug; m_{L2}, total moles of active binding site 2; K_{a2}, association equilibrium constant for binding of the analyte to the ligand at site 2.

Adapted from Refs. [7].

Chromatographic studies

The LDL support was prepared as described in **Chapter 3** and using the Schiff base immobilization technique with Nucleosil Si-500 silica. A BCA protein assay was conducted to determine the protein content of the support; this experiment revealed that the LDL support contained 6.9 (± 0.4) mg protein per gram silica. The protein content was used to determine the LDL content based on an average molar mass of 2.3×10^6 g/mol for LDL and a typical apolipoprotein content of 25% for LDL particles [6]. This conversion indicated that 27.7 (± 1.6) mg or 12 (± 1) nmol of LDL per gram silica was present (see **Chapter 3**). Diol silica was used as a control support in this study. The LDL columns had previously been shown to be stable over the amount of time required to collect the data required in this study, with no significant changes in the binding properties of the column during these experiments (see **Chapter 3**).

Chromatographic data were collected using the HPAC system described earlier. The LDL and control columns were stored in pH 7.4, 0.067 M phosphate buffer at 4°C and equilibrated to 37 ºC prior to use. All mobile phases were filtered through Osmonics 0.22 µm nylon filters and degassed under vacuum prior to use. A wavelength of 225 nm was utilized to monitor the elution of *R*- or *S*-propranolol in the frontal analysis studies. These studies were performed in triplicate using 100 mm × 2.1 mm i.d. columns packed with the LDL support or control support and using a mobile phase of pH 7.4, 0.067 M potassium phosphate buffer that was applied at a flow rate of 1.0 mL/min at 37 ºC.

Nine solutions containing *R*- or *S*-propranolol, with concentrations ranging from 0.2-25 µM in the pH 7.4, 0.067 M potassium phosphate buffer, were applied to the LDL and control columns during the frontal analysis studies. This range was selected as 0.2

µM was approximately equivalent to the lowest concentration at which breakthrough times for *R*- and *S*-propranolol could be reliably determined, and 25 µM provided a response within the linear range of the detector and overlapped with drug concentrations that have been used in prior CE/frontal analysis studies [9]. Following the frontal analysis measurements, the retained drug was eluted by passing pH 7.4, 0.067 M potassium phosphate buffer through the column prior to the next experiment.

At the conclusion of frontal analysis experiments, the moles of applied drug needed to reach the mean point of each breakthrough curve was determined by integration of this curve by using a program based on Labview software [10]**.** Corrections were made for the void time and non-specific binding of the drug to the LDL support by subtracting the breakthrough time obtained using the control support from the time measured for the same drug on the LDL support at each concentration of drug that was examined.

Linear regression was performed with Excel 2010 (Microsoft, Redmond, WA, USA). Nonlinear regression was executed using Origin 9.1 software (OriginLab, Northampton, MS, USA). Surface plots and contour plots were prepared using Origin 9.1.

RESULTS AND DISCUSSION

Evaluation of binding isotherms and double-reciprocal plots

Evaluation of drug-lipoprotein binding throughout this dissertation has usually fit a model with two types of interactions.. The interactions between these drugs and lipoproteins are described by a model in which high affinity, saturable interactions occur between the drug and apolipoproteins, and a second non-saturable interaction occurs between the drug and the non-polar core of the lipoprotein. This was confirmed by evaluating *R*-propranolol interactions with LDL. As reported in **Chapter 3**, this system had a single saturable, high affinity site with a K_{a1} of 5.2 (± 2.3) × 10^5 and a non-saturable interaction with an overall affinity of 1.9 (± 0.1) × 10^5 at 37 ºC. The interactions of propranolol with LDL were stereoselective, and the interactions between *S*-propranolol and LDL followed a non-saturable interaction model between the drug and non-polar core of LDL.. The overall affinity of this interaction was determined to be 2.7 (± 0.2) × 10^5 at 37 ºC.

The effect that these mixed-mode interactions have on the use of traditional binding isotherms is demonstrated by Figure 5-1. As shown by this figure (and in **Chapter 3**), the binding of *R*-propranolol to LDL gives reasonable agreement with the non-saturable, one-site saturable, and mixed-mode models across the concentration range that was evaluated. The goodness of fit exhibited for each of these binding models may make it difficult to distinguish between these models, particularly if a narrower concentration range were used during the experiments. This demonstrates that determining association equilibrium binding constants and number of binding sites through this method requires a suitable number of data points that span a broad range of concentrations to accurately assess the number and type of interactions that may be present.

An alternate approach utilizing double-reciprocal plots for the initial detection of multiple types of interactions has been proposed in previous work with other systems [11-13] and was utilized in previous chapters of this dissertation. Based upon the equations given in Table 5-1, the double-reciprocal plot of a non-saturable or one-site saturable binding model should yield a linear response. The two-site saturable and mixed-mode models should approach a linear relationship at low analyte concentrations (or high values of 1/[D]). At high analyte concentrations (or low values of 1/[D]), these second two models predict that deviations from a linear response will occur. The presence of these types of deviations can be used to assess whether a system exhibits single or multiple types of interactions [4,11-13]. An example of a double-reciprocal plot is shown in Figure 5-2; this plot was prepared using the same data for *R*-propranolol/LDL interactions as were used in Figure 5-1. This plot shows that at low concentrations of *R*-propranolol (i.e., high concentrations of 1/[D]), a linear range is present as predicted. In addition, lower values of 1/[D] show negative deviations from the linear range, indicating that multiple types of interactions were present between *R*-propranolol and LDL. Additional examples of double-reciprocal plots are shown in **Chapters 2, 3, and 4**.

Further evaluation of Figures 5-1 and 5-2 reveals the primary advantage of using double-reciprocal plots to examine frontal analysis data for multiple types of interactions. This advantage lies in the fact that significantly less data are required to detect multiple interactions, which occurred for interactions between *R*- or *S*-propranolol and HDL, LDL, or VLDL, as well as between *R/S*-verapamil and HDL. For example, the studies with *R*-propranolol and LDL presented in Figure 5-1 required nine measurements in the drug concentration range of 0.2 to 25 μM to differentiate between the four binding models presented in Table 5-1 (i.e., the non-saturable interaction, single group of saturable sites, mixed-mode with single group of saturable sites and non-saturable interactions, and two groups of saturable sites). When analyzing the double-reciprocal plot, the three highest values of 1/[D] agreed with the best fit line within ± 4%, however, the next four highest values of 1/[D] deviated from this line by 30.8%, 35.1%, 46.9%, and 53.2%, respectively. These deviations are significantly larger than the typical experimental precision of ± 4-5% that reported in **Chapter 3** for the LDL studies.. Given these levels of deviation, data from as few as five concentrations spanning the concentration range of 1 to 10 μM could have been used to detect mixed-mode interactions when using a double-reciprocal plot. This observation supports the prior results in Ref. [4] that the use of a double-reciprocal plot instead of a normal binding isotherm requires fewer experiments and a significantly smaller amount of drug for the detection of binding site heterogeneity in systems with multiple types of saturable interactions.

Figure 5-1. Frontal analysis data for the binding of *R*-propranolol to LDL, as examined according to binding isotherms described by the non-saturable (red dashed line), one-site saturable (blue dashed line), and mixed-mode binding models (solid line).

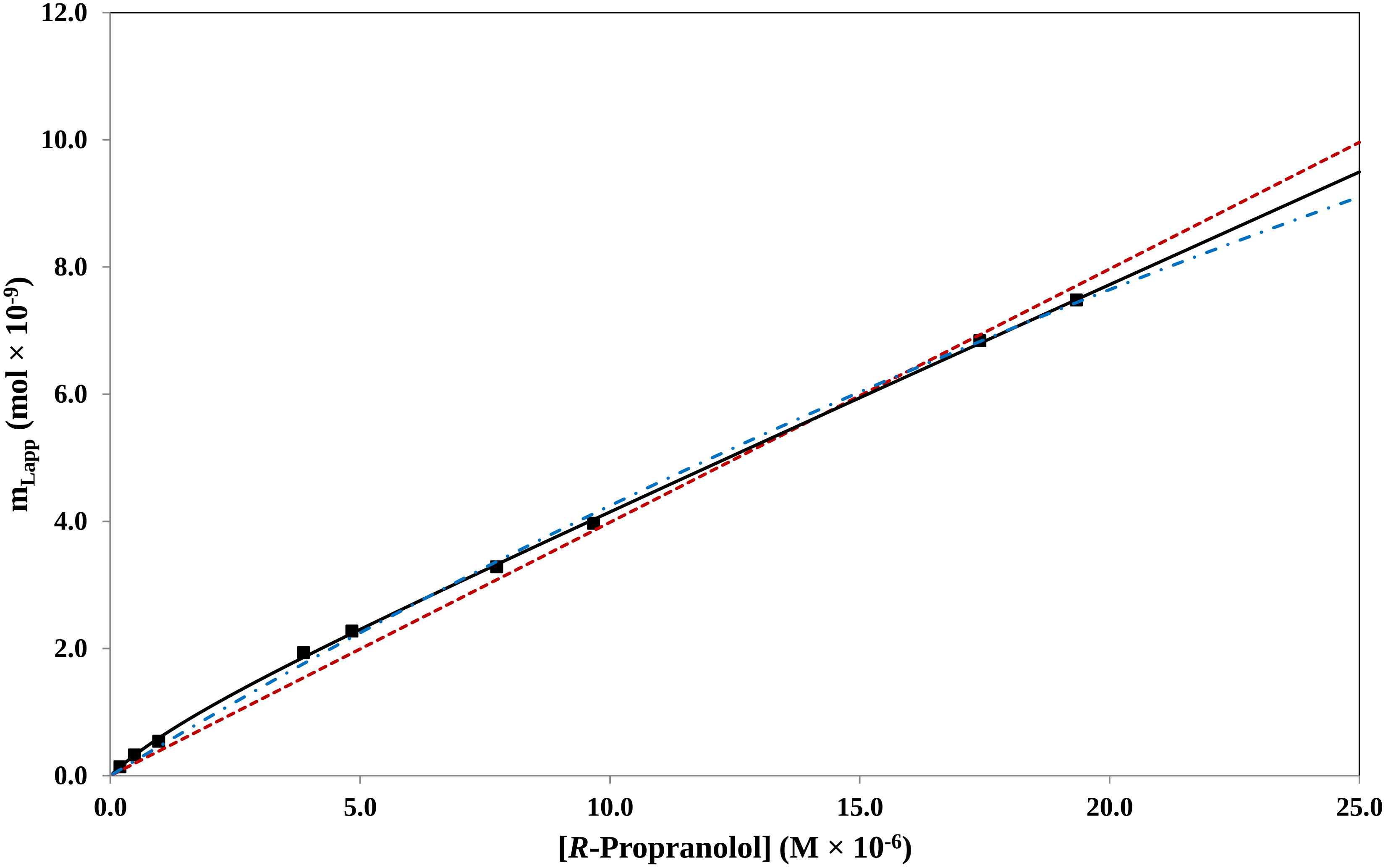
12.0
10.0
8.0
6.0
4.0
2.0
0.0
0.0
5.0
10.0
15.0
20.0
25.0
m_{Lapp} (mol × 10^{-9})
[*R*-Propranolol] (M × 10^{-6})

Figure 5-2. Frontal analysis data for the binding of *R*-propranolol to LDL, as examined using a double-reciprocal plot. The best fit line was obtained using data points in the upper region of this plot, which are designated by the closed squares (■). Data points in the lower region of this plot (i.e., at higher concentrations propranolol) showed negative deviations from the linear fit for *R*-propranolol and are represented by open squares (□).

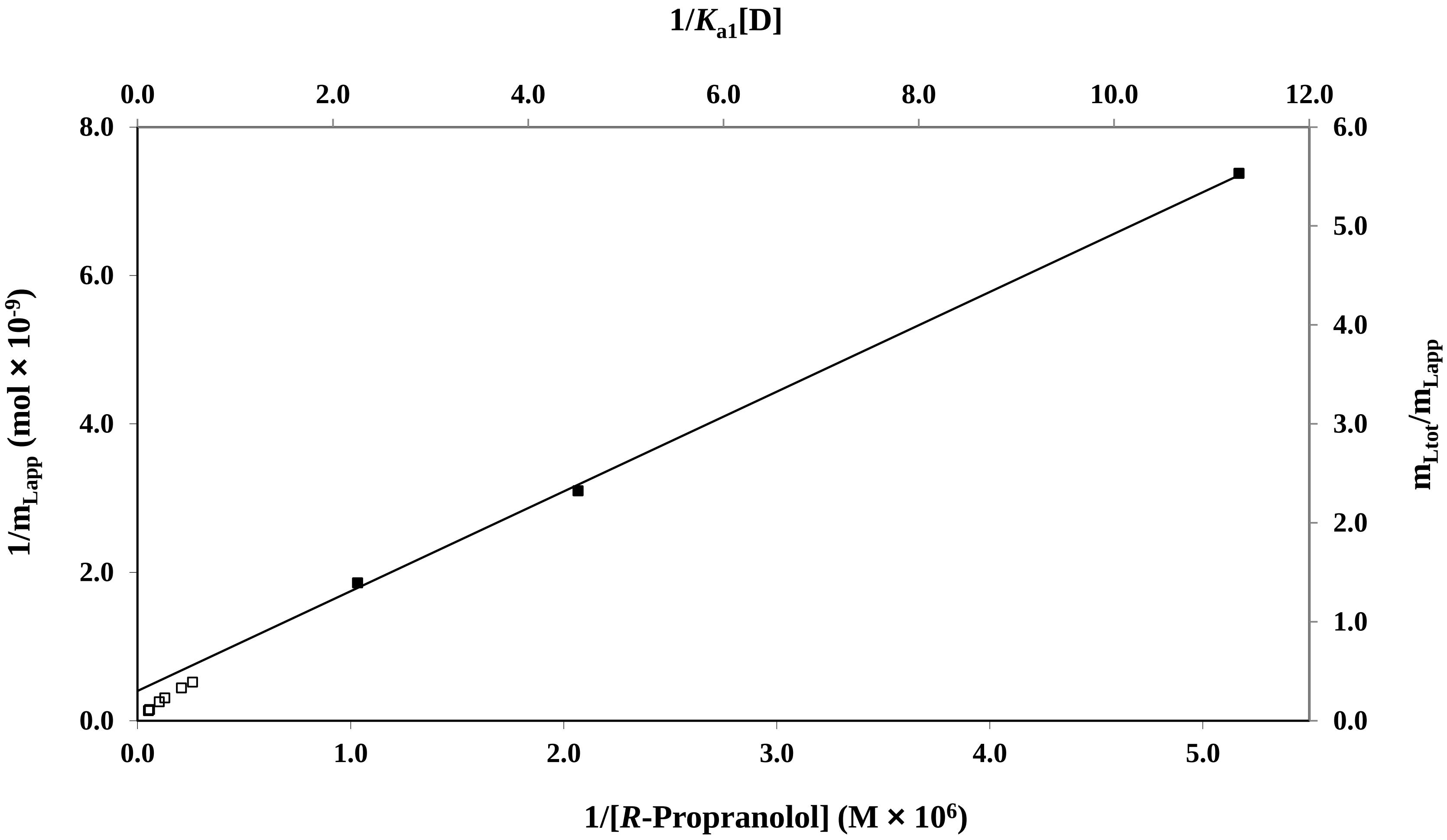
1/K_{a1}[D]
0.0
2.0
4.0
6.0
8.0
10.0
12.0
1/m_{Lapp} (mol × 10^{-9})
8.0
6.0
4.0
2.0
0.0
m_{Ltot}/m_{Lapp}
6.0
5.0
4.0
3.0
2.0
1.0
0.0
0.0
1.0
2.0
3.0
4.0
5.0
1/[*R*-Propranolol] (M × 10^6)

Conditions leading to deviations from linearity in mixed-mode plots

The ability of double-reciprocal plots to detect binding heterogeneity in a two-site system has been previously examined, but no work to date has extended this approach to the evaluation of a mixed-mode system containing a saturable group of binding sites and a non-saturable group of sites [4]. The work presented here examined the degree of deviations from linearity in double-reciprocal plots that are obtained for systems with varying degrees of impact from the two interaction modes. Examination of Eq. (12) reveals that two system constants can be varied to evaluate the impact and magnitude of a deviation from linearity in this type of system (β_2 and K_{a1}). The impact of varying these parameters was evaluated by determining the relative deviation from linearity, as described in Eq. (13).

$$\%\ \text{Deviation} = \frac{\text{Eq. (12)-Eq. (11)}}{\text{Eq. (12)}} \times 100\% \qquad (13)$$

This equation was used to determine the difference between the actual response of a double-reciprocal plot (as predicted by Eq. 11) and the response of the linear region (as predicted by Eq. 12); the difference in this response was subsequently converted to a percentage by dividing by the linear response and multiplying by 100%. The use of Eq. (13) in this approach produced a mechanism by which the relative deviation from linearity could be predicted when varying the values of β_2 and $1/(Ka_1[\text{D}])$ for any mixed-mode system.

The first evaluation performed by this method was to determine the relative deviation from a linear response when the value of $1/(K_{a1}[\text{D}])$ was varied between 0.05

and 0.50. Figure 5-3 shows that the greatest deviations from a linear response occurred when small values of $1/(K_{a1}[\mathrm{D}])$ were present. The impact of the relative deviations increased as the value of β_2 increased. These results are aligned with the data presented in Figure 5-2, where the deviations from linearity increased as the value of $1/(K_{a1}[\mathrm{D}])$ decreased. The relative deviation from a linear response when the value of β_2 was varied was also determined between 0.2 and 10.0. Figure 5-4 confirmed that the largest deviations from a linear response occurred when β_2 was large and $1/(K_{a1}[\mathrm{D}])$ was small.

Figure 5-3. Percent deviation from a linear response in the value of m_{Ltot}/m_{Lapp} for a double-reciprocal frontal analysis plot for a mixed-mode system in which $1/(K_{a1}[D]) = 0.05$, 0.10, 0.20, or 0.50 as a function of the ratio of the total affinity of non-saturable sites versus the affinity of saturable sites.

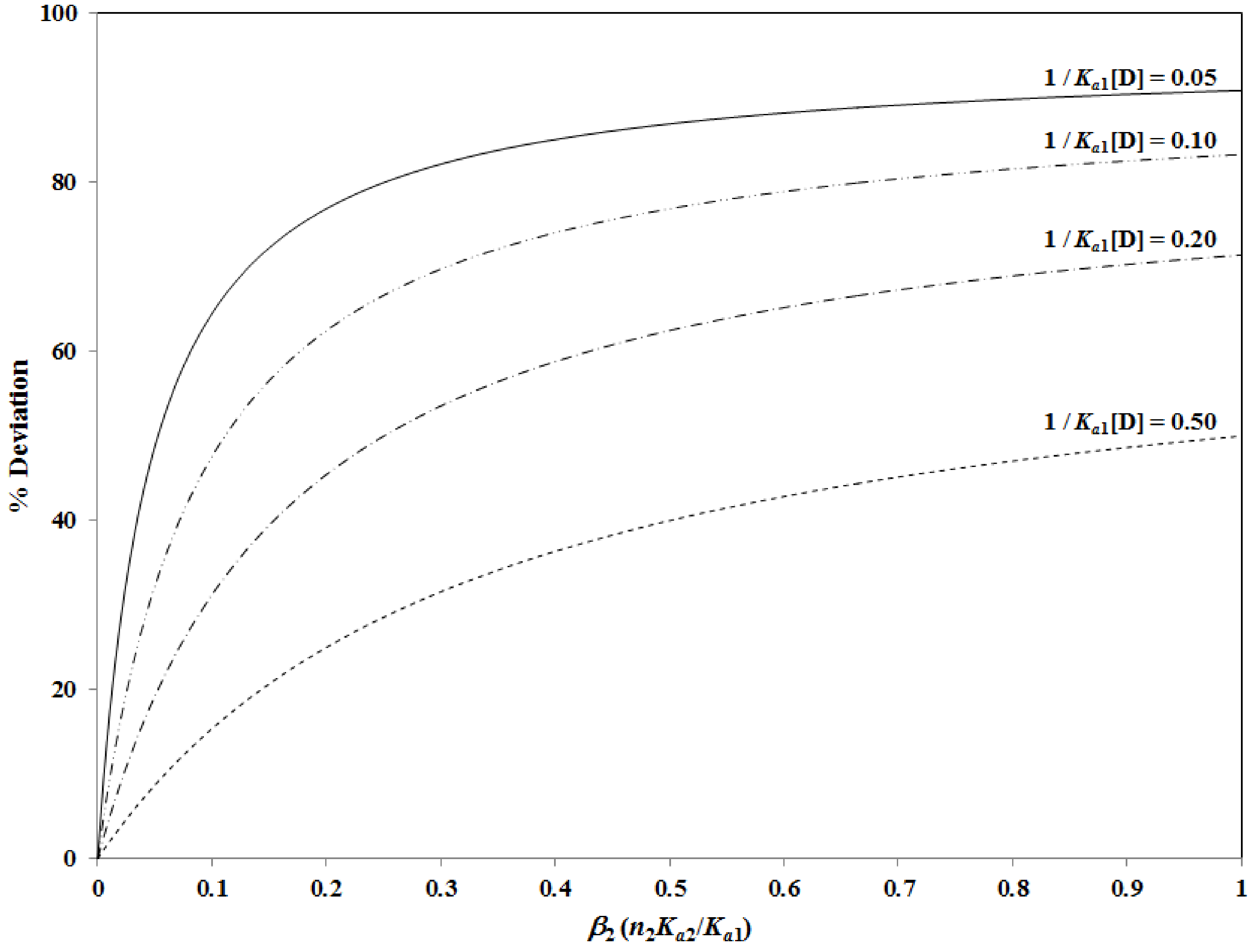
100
80
60
40
20
0
% Deviation
0
0.1
0.2
0.3
0.4
0.5
0.6
0.7
0.8
0.9
1
β_2 (n_2K_{a2}/K_{a1})
$1 / K_{a1}$[D] = 0.05
$1 / K_{a1}$[D] = 0.10
$1 / K_{a1}$[D] = 0.20
$1 / K_{a1}$[D] = 0.50

Figure 5-4. Percent deviation from a linear response in the value of m_{Ltot}/m_{Lapp} for a double-reciprocal frontal analysis plot for a mixed-mode system in which β_2 = 0.20, 0.365, 1.0 and 10.0 as a function of the value of $1/K_{a1}$. The β_2 value was selected as the approximate value obtained for nK_a/K_{a1} in frontal analysis studies between R-propranolol and LDL at 37 ºC (refer to **Chapter 3**).

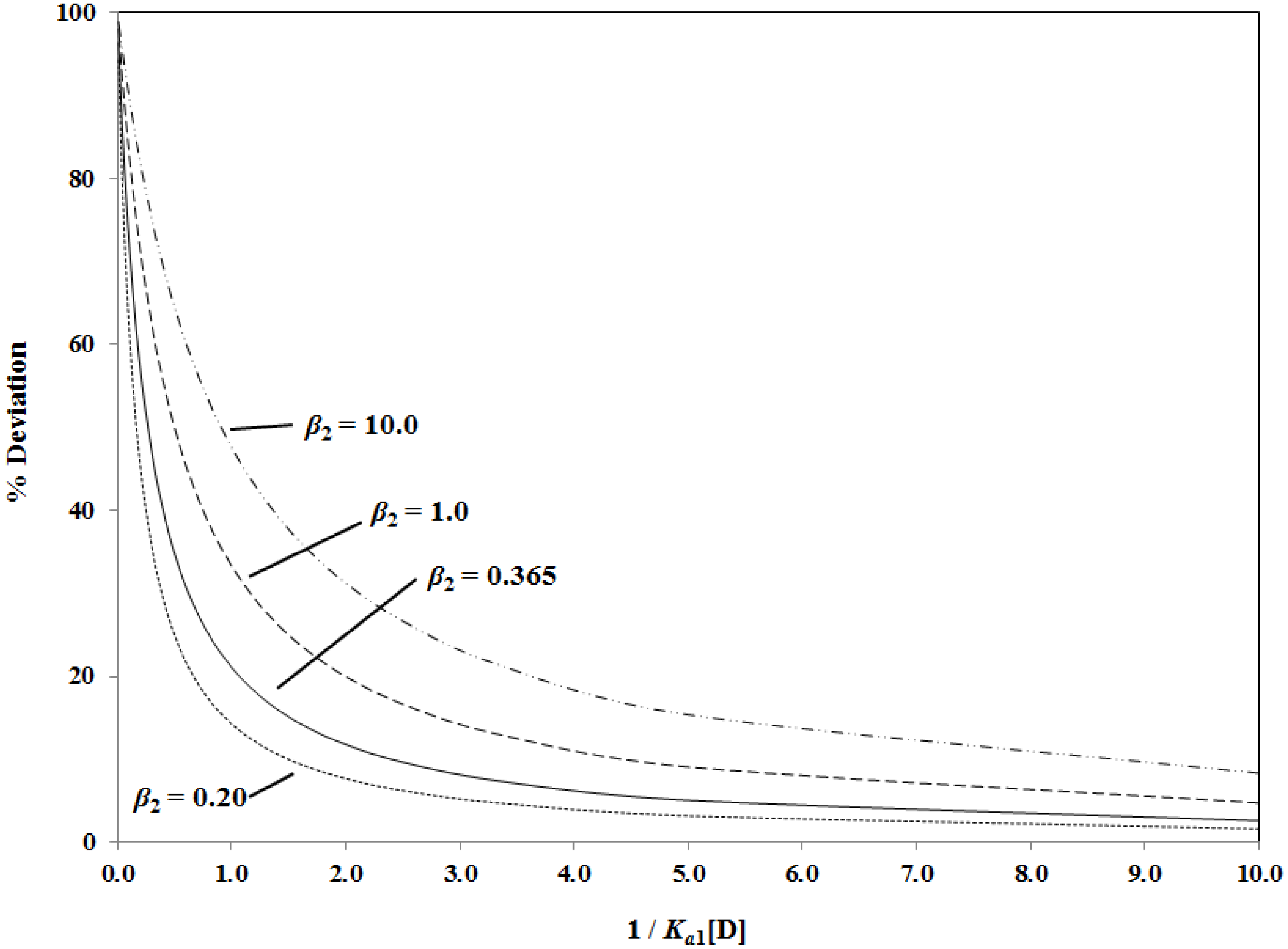

100
80
60
40
20
0
% Deviation
$\beta_2 = 10.0$
$\beta_2 = 1.0$
$\beta_2 = 0.365$
$\beta_2 = 0.20$
0.0
1.0
2.0
3.0
4.0
5.0
6.0
7.0
8.0
9.0
10.0
$1 / K_{a1}[D]$

The impact that simultaneous variations in the values of β_2 and $1/(K_{a1}[\mathrm{D}])$ have on the relative deviation from linearity was evaluated using surface and contour plots. These plots are shown in Figures 5-5 and 5-6. The plot trends agree with those noted in Figures 5-3 and 5-4, in which the relative deviations from a linear response increased as the value of β_2 increased or $1/(K_{a1}[\mathrm{D}])$ decreased. This also fits the experimental data presented in Figure 5-2.

These results are logical when considered in conjunction with the models presented above. A decreasing value of β_2 represents a decrease in the value of n_2K_{a2}/K_{a1}. This is indicative of a diminished portion of non-saturable binding relative to site-specific, saturable binding. As the value of n_2K_{a2}/K_{a1} begins to approach zero, the mixed-mode model begins to reflect the one-site saturable model, which has a linear double-reciprocal plot. Similarly, an increase in the value $1/(K_{a1}[\mathrm{D}])$ reflects a decrease in the association equilibrium constant K_{a1} or the value of [D]. As the value of K_{a1} or [D] approaches zero, the mixed-mode binding model begins to reflect the non-saturable model. The double-reciprocal plot for non-saturable binding is depicted by a linear relationship.

Figure 5-5. Surface plot showing the relative deviation from a linear response in the value of m_{Ltot}/m_{Lapp} for a double-reciprocal frontal analysis plot for a mixed-mode system.

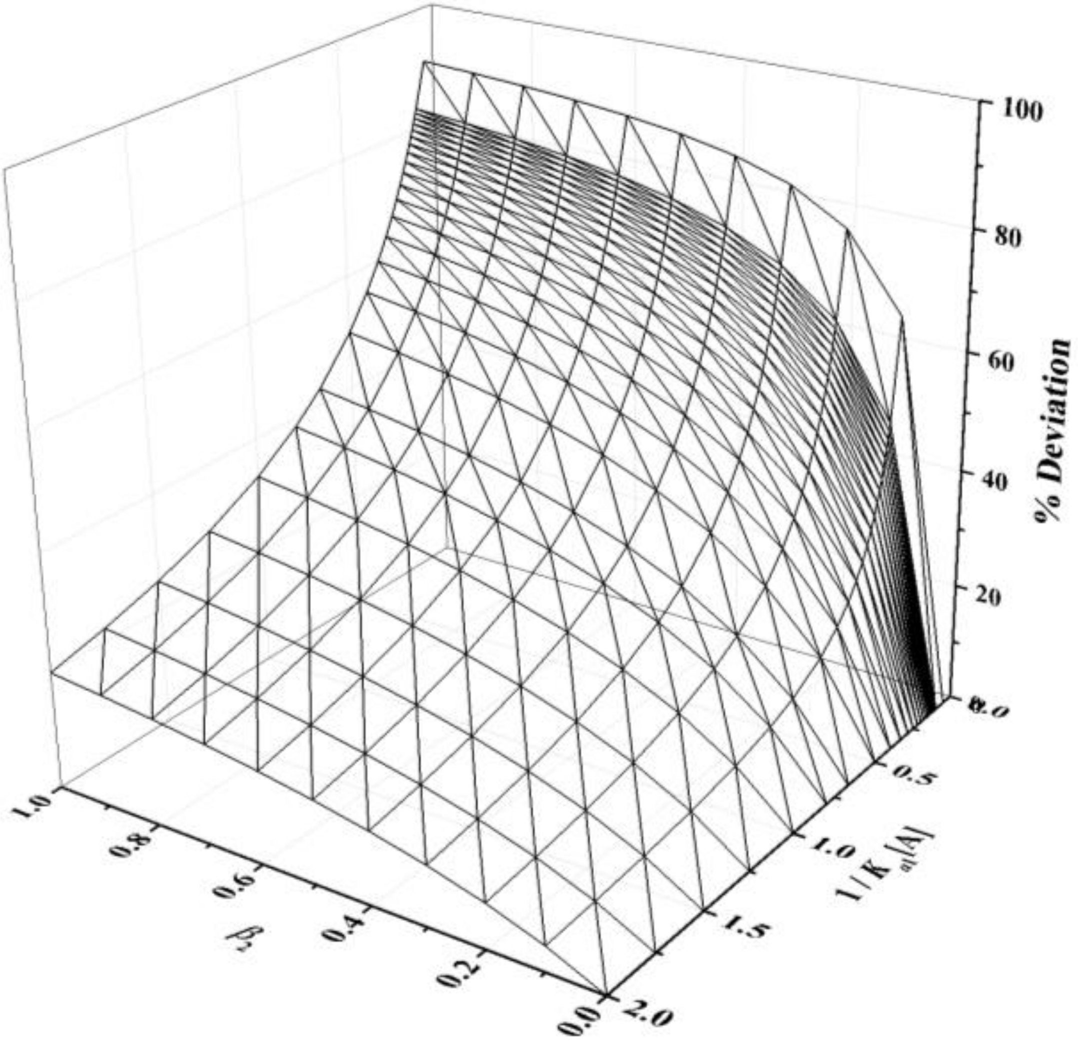
% Deviation
100
80
60
40
20
0
0.0
0.5
1.0
1.5
2.0
$1 / K_{a1}[A]$
1.0
0.8
0.6
0.4
0.2
0.0
β_2

Figure 5-6. Contour plot showing the relative deviation from a linear response in the value of m_{Ltot}/m_{Lapp} for a double-reciprocal frontal analysis plot for a mixed-mode system.

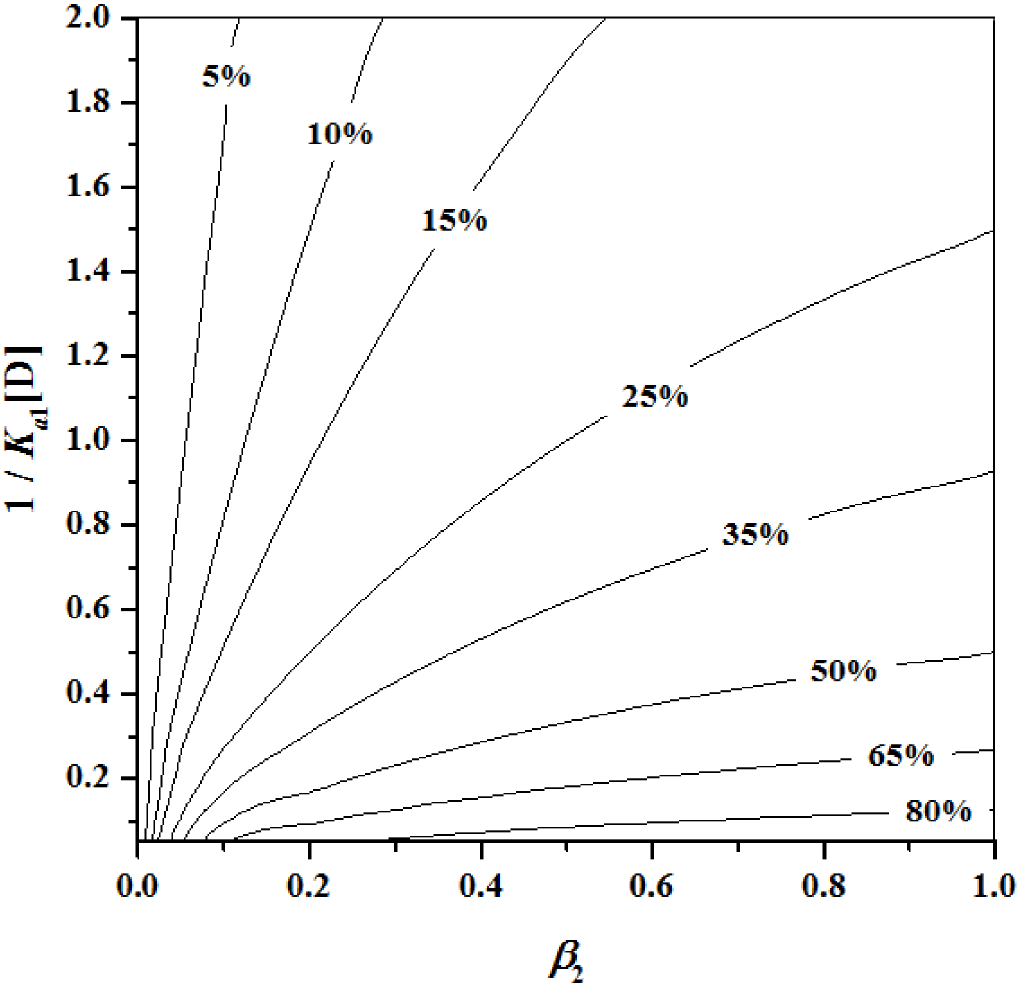
5%
10%
15%
25%
35%
50%
65%
80%
1 / K_{d1}[D]
2.0
1.8
1.6
1.4
1.2
1.0
0.8
0.6
0.4
0.2
0.0
0.2
0.4
0.6
0.8
1.0
β_2

CONCLUSIONS

The work in this chapter evaluated the use of data collected from HPAC-frontal analysis studies to detect mixed-mode binding of analytes in biological systems such as drug-lipoprotein interactions. The use of double-reciprocal plots in the detection of mixed-mode binding was emphasized. Theoretical evaluations were conducted to determine the effects mixed-mode binding would have on double-reciprocal plots and to predict the extent of deviations from linearity that would be expected in these plots for various mixed-mode systems. Frontal analysis experiments analyzing the interactions between *R*-propranolol and LDL were used to provide double-reciprocal plots and to access if such plots could simplify the detection of mixed-mode binding when compared to traditional binding isotherms. Examination of this system also demonstrated that double-reciprocal plots can be used to identify mixed-mode binding with fewer measurements, and therefore less target analyte, than would be required when utilizing traditional binding isotherms. Therefore, double-reciprocal plots are an attractive alternative for screening systems for mixed-mode interactions.

This report also demonstrated that the relative deviations that result from mixed-mode interactions are predictable. The deviations from linearity observed in a double-reciprocal plot for a mixed-mode interaction are a function of the applied drug's concentration, the relative affinity of the saturable binding site, and the overall affinity of the non-saturable interaction. The results of this study showed that as the relative affinity of the saturable binding (as represented by K_{a1}) or the applied drug's concentration decreased, so did the deviations from a linear response. This is due to the fact that as the value of K_{a1} or [D] approaches zero, the mixed-mode binding model begins to reflect the non-saturable model. This study also demonstrated that as the overall affinity of the non-saturable interaction (as represented by β_2) decreased the mixed-mode model began to reflect the one-site saturable model and deviations from linearity were reduced. These findings should be applicable to any mixed-mode binding system and are not limited to the evaluation of drug interactions with lipoproteins.

ACKNOWLEDGEMENTS

This work was supported by the National Institute of Health under grant R01 GM044931 and was performed in facilities renovated with support under grant RR015468-01.

References

1. Schiel, J.E.; Joseph, K.S., Hage, D.S. In *Advances in Chromatography,* 48; Grushka, E.; Grinberg, N. Eds.; CRC Press, Boca Raton, FL, **2010**.
2. Schriemer, D.S. *Anal. Chem*. **2004**, *76*, 440-448.
3. Hage, D.S.; Chen, J. In *Handbook of Affinity Chromatography*; Hage, D.S. Ed.; CRC Press/Taylor & Francis: New York, **2006**, pp 595–628.
4. Tong, Z.; Joseph, K.S.; Hage, D.S. *J. Chromatogr. A* 2011, 1218, 8915-8924.
5. Chen, S.; Sobansky, M.; Hage, D.S. *Anal. Biochem.* **2010,** *397*, 107-114.
6. Sobansky, M.R.; Hage, D.S. *Anal. Bioanal. Chem*. **2012**, *403*, 563-571.
7. Sobansky, M.R.; Hage, D.S. *Anal. Bioanal. Chem*. **2014**, *406*, 6203-6211.
8. Tweed, S.; Loun, B.; Hage, D.S. *Anal. Chem.* **1997**, *69*, 4790- 4798.
9. Mohamed, N.A.L.; Kuroda, Y.; Shibukawa, A.; Nakagawa, T.; El Gizawy, S.; Askal, H.F.; El Kommos, M.E.; *J. Pharm. Biomed. Anal.* **1999**, *21*, 1037–1043.
10. Patel, S.; Wainer, I.W.; Lough, J.W. In *Handbook of Affinity Chromatography,* 2nd ed; Hage, D.S. Ed.; CRC Press: Boca Raton, **2006**, pp 663-683.
11. Joseph, K.S.; Anguizola, J.; Hage, D.S. *J. Pharm. Biomed. Anal.* **2011**, *54*, 426-432.
12. Joseph, K.S.; Hage, D.S. *J. Chromatogr. B* **2010**, *878*, 1590-1598.
13. Joseph, K.S.; Anguizola, J.; Jackson, A.J.; Hage, D.S. *J. Chromatogr. B* **2010**, *878*, 2775-2781.

CHAPTER SIX

SUMMARY AND FUTURE WORK

SUMMARY OF WORK

The work in this dissertation examined the interactions of drug with lipoproteins, where lipoproteins are soluble macromolecular complexes of proteins and lipids that are present in the serum to transport hydrophobic compounds, such as cholesterols and triglycerides [1-3]. As was shown in the previous chapters, these complexes are able to bind several basic and neutral hydrophobic drugs, including propranolol and verapamil [4]. The reversible nature of the interactions between these drugs and lipoproteins influences the activity, pharmacokinetics and toxicity of drugs in the human body and impacts the distribution, delivery, metabolism, and excretion of these drugs [5-10]. This dissertation evaluated the binding of propranolol and verapamil, to various lipoproteins. These studies focused on the use of high-performance affinity chromatography (HPAC) to evaluate the interactions between such drugs or solutes and lipoproteins.

The application of HPAC was first implemented in the **Chapter 2** in studies conducted with high density lipoprotein (HDL). Chromatographic columns containing immobilized HDL were used in HPAC studies to examine interactions between HDL and propranolol or verapamil. These columns were prepared by immobilizing HDL to HPLC-grade silica by using the Schiff base method and placing the resulting support into a column. The stability of these columns was confirmed for up to 120 h of continuous operation in the presence of pH 7.4, 0.067 M potassium phosphate buffer and when they were used in zonal elution studies. Following the establishment of this column stability, frontal analysis experiments were conducted to determine the type and strength of interactions that occurred between the given drugs and HDL. It was determined that two types of interactions occurred between HDL and propranolol or verapamil. The first type of interaction had a relatively high affinity and was probably related to an interaction between the drugs and apolipoproteins on the surface of HDL. The second type of interaction fit a non-saturable binding model, as would be expected to occur in interactions of these drugs with phospholipids or the non-polar core of HDL. The high affinity sites had association constants of $1.1\text{-}1.9 \times 10^5$ M^{-1} for *R*- or *S*-propranolol and 6.0×10^4 M^{-1} for *R/S*-verapamil at 37 ºC. The overall affinity (nK_a) for the weaker interactions at 37 ^oC was estimated to be $3.7\text{-}4.1 \times 10^4$ M^{-1} for *R*- or *S*-propranolol and 2.5×10^4 M^{-1} for *R/S*-verapamil at 37 ^oC. The non-saturable interaction constants that were obtained for each drug were in close agreement with the results of previous solution-phase studies [11-13].

The use of HPAC in the analysis of lipoprotein-drug interactions was extended to low density lipoprotein (LDL) in **Chapter 3**. HPAC columns containing immobilized LDL were again prepared via the Schiff base reaction. These columns were used to analyze the nature and strength of *R*- and *S*-Propranolol interactions with LDL. Frontal analysis experiments indicated that two types of interactions occurred between *R*-propranolol and LDL, while only a single type of interaction resulted between *S*-propranolol and LDL. The interactions for both enantiomers involved non-saturable binding; this interaction had an overall affinity (nK_a) of $1.9\ (\pm 0.1) \times 10^5$ M^{-1} for *R*-propranolol and $2.7\ (\pm 0.2) \times 10^5$ M^{-1} for *S*-propranolol at 37 ºC. The second type of interaction was targeted only *R*-propranolol and involved saturable binding that had an association equilibrium constant (K_a) of 5.2 ($\pm$ 2.3) × 10^5 M^{-1} at 37 ºC. Differences in binding behavior were similar for the two enantiomers at 20 ºC and 27 ºC. These results were approximately the same as the overall affinities that have been measured for the same drugs with soluble LDL and based on a non-saturable model [10,14]. These results also represented the first known report and example of stereoselective binding by drugs to LDL or other lipoproteins.

Chapter 4 described the use of HPAC to examine the binding of very low density lipoprotein (VLDL) with drugs, using *R*- and *S*-propranolol as model solutes. These studies identified the existence of two binding mechanisms between *R*- and *S*-propranolol and VLDL. The first mechanism involved non-saturable partitioning of these drugs with VLDL. This partition-type interaction was described by overall affinity constants of 1.2 (± 0.3) × 10^6 M^{-1} for *R*-propranolol and 2.4 (± 0.6) × 10^6 M^{-1} for *S*-propranolol at pH 7.4 and 37 ºC. The second mechanism occurred through saturable binding by these drugs at fixed sites, such as apolipoproteins on the surface of VLDL. The association equilibrium constants for this saturable binding at 37 ºC were 7.0 (± 2.3) × 10^4 M^{-1} for *R*-propranolol and 9.6 (± 2.2) × 10^4 M^{-1} for *S*-propranolol. Comparable results were obtained at 20 ºC and 27 ºC for the propranolol enantiomers. No stereoselectivity was observed in the binding of *R*- or *S*-propranolol with VLDL.

The results obtained in **Chapters 2, 3, and 4** also demonstrate the suitability of using immobilized lipoproteins and HPAC to study the interactions that occur between lipoprotein and drugs or other analytes. When compared with equilibrium dialysis (i.e., the method used in Ref. [11] and a common reference method for drug binding studies), HPAC has several benefits, including analysis times of only a few minutes per run and use of the same lipoprotein ligand for many experiments. An alternative method based on capillary electrophoresis (CE) has been applied to drug binding studies with lipoproteins [12-14]. This CE method requires less protein than HPAC for a single analysis; however, the ability to reuse HPAC columns that contain immobilized lipoproteins results in a method that needs a similar or smaller amount of ligand than CE when dealing with a large number of samples or studies. Furthermore, the ability to use the same lipoprotein preparation for multiple studies helped reduce the effects of batch-to-batch variability in the ligand in the HPAC method. The ability to utilize HPLC detectors with such columns allowed the examination of a relatively wide range of low and high drug concentrations possible in the HPAC approach and enabled the identification of high affinity interactions located on HDL, LDL, and VLDL. The same interactions were not observed in previous studies using CE or equilibrium dialysis [11-14].

The work performed in **Chapter 5** examined the theory and experimental conditions needed for the detection of multiple binding mechanisms in HPAC columns when using frontal analysis. This work focused on evaluating binding models that incorporated both a saturable type of binding and a non-saturable interaction. These evaluations made it possible to determine the experimental conditions that would be required for detection of this type of multi-mode interaction.

FUTURE WORK

Analysis of oxidized lipoproteins

The results presented throughout this dissertation have demonstrated that the HPAC is an effective method for examining interactions between solutes and various lipoproteins (i.e. HDL, LDL, and VLDL). This method has the ability to identify multiple types of binding or interactions that are not typically observed in studies based upon equilibrium dialysis or CE. HPAC also enabled the identification of stereoselective interactions between lipoproteins and solutes. Based upon this ability of HPAC to obtain additional information regarding interactions with lipoproteins, further studies involving the application of HPAC in the examination of lipoprotein binding is logical. The examination of the effects of lipoprotein oxidation on drug binding is one area that merits further research.

Plasma LDL has been shown to undergo *in vivo* chemical modification, such as oxidation and acetylation by endothelial cells, arterial smooth muscle cells, macrophages, and lymphocytes [15]. These modifications impact both the protein and lipid components of LDL and are often associated with atherosclerosis [16]. Furthermore, previous studies have shown that this process can impact the uptake of LDL and the binding affinity of drugs to this lipoprotein [13-15]. The impact of LDL oxidation on binding by the drugs verapamil and nilvadipine has been studied via methods based upon CE [13-15]. These studies showed that the total affinity of each drug increased upon LDL oxidation. The degree to which each drug is impacted varied, with the basic drug verapamil being impacted more than the neutral drug nilvadipine [13-15].

Despite the reported results, it is logical that the use of CE would suffer from the same drawbacks as reported in **Chapters 2, 3, and 4**. The use of HPAC methods in studying the interactions of oxidized LDL with drugs would be expected to yield additional information regarding the nature and strength of these interactions. The realization of such additional information is expected to arise from the use of the binding models presented in Table 1-2 that consider multiple interactions. Furthermore, the ability to use utilize HPLC detectors in these studies should allow for the examination of a wider range of low and high drug concentrations that was used in the studies with CE, thus enabling the identification and assessment of the impact of oxidation on more types of interactions.

The execution of drug binding studies using oxidized LDL (or other lipoproteins) via HPAC would employ similar methods to those described in **Chapters 2, 3, and 4**. The first step in this evaluation would be the oxidation of the lipoprotein. Previous methods have described a process by which Cu^{2+} can induce the oxidation of LDL [17]. This oxidation would be carried out by placing a preparation of this lipoprotein in pH 7.4, 0.067 M phosphate buffer containing 5 μM $CuSO_4$, with this mixture then being incubated at 37 ºC for 0.5 to 12 h to obtain various levels of oxidation. The reaction could be terminated using ultrafiltration to remove the $CuSO_4$. The oxidation state of LDL could be monitored by using three separate methods, as reported previously [15]. The simplest method would be to monitor the UV absorption at 234 nm. Oxidation of LDL results in conjugated diene structures in unsaturated acyl chains, and the formation of these structures results in an increase in UV absorption. Alternatively, the oxidation state of LDL may be monitored via fluorescence or the electrophoretic mobility of LDL versus oxidized LDL [15].

Following the oxidation of LDL, this lipoprotein could be immobilized and placed in a chromatographic column for use in HPAC studies. This immobilization to HPLC grade silica would be accomplished using the Schiff base reactions described in **Chapters 2, 3, and 4**. Oxidation of LDL does have the potential to diminish or alter the immobilization efficiency due to the formation of Schiff bases between the ε-amino groups of lysine residues on the apolipoproteins and aldehyde group formed by degradation of the unsaturated acyl chains in the lipids of LDL [15]. In the event that the immobilization efficiency is diminished to the point that the Schiff base method is not viable, alternative immobilization techniques may be used. Entrapment would be an alternative immobilization technique that is likely to be successful. Entrapment of LDL would occur by placing the lipoprotein within the pores of dihydrazide-activated silica and then capping the pores with oxidized glycogen, as has recently been used for the immobilization of some serum proteins [18]. The support containing oxidized LDL would then be packed within chromatographic columns and employed in HPAC studies using zonal elution or frontal analysis.

The stability of the oxidized LDL supports would be assessed using zonal elution, as described in previous lipoprotein studies (see **Chapters 2, 3, and 4**). Following determination of the column’s usable lifetime, frontal analysis would be initiated. Analysis of the breakthrough times obtained from frontal analysis, and using double-reciprocal plots or non-linear regression, will be carried out according to binding models based upon non-saturable interactions, one group of saturable sites, two groups of saturable sites, and the mixed mode model (i.e., one group of saturable sites plus a non-saturable interaction), as described in Table 1-2. Analysis using these binding models should provide information regarding the impact oxidation has on the ability of apolipoprotein B-100 to selectively bind *R*-propranolol. The impact that the oxidation of lipids has on the partitioning of propranolol into the non-polar core of LDL should also be revealed through these experiments.

Analysis of glycated lipoproteins

In vivo oxidation has been long studied as an atherogenic modification of lipoproteins that impacts the function of these agents [16,17,19]. Recently, there has also been an increasing interest in the role that glycation plays in the impairment of lipoprotein function [19]. This interest has arisen from a failure of antioxidant therapy to reduce the occurrence of atherogenic cardiovascular diseases in high-risk individuals [19]. Glycation is a non-enzymatic reaction that proceeds via formation of a Schiff base; the product of this reaction may undergo an Amadori rearrangement and form a stable ketoamine link with exposed lysine residues of the apolipoprotein to produce an early glycation product [19]. Glycation may be induced by reactive sugars (e.g., glucose) and may impact each class of lipoproteins [19]. Glycated lipoproteins are present in the circulation under physiological conditions and are present at high concentrations in individuals with diabetes or other conditions [19]. The prominence of glycated lipoproteins *in vivo* and the impact that disease states such as diabetes have on their formation makes the study of interactions between glycated lipoproteins and drugs or other solutes of interest.

The glycated lipoprotein that has been the most studies is LDL [19]. Therefore, this glycated lipoprotein will be the first analyzed in drug binding studies by HPAC. These studies will involve a further adaptation of the methodologies that were described previously in this dissertation. As with drug binding studies involving oxidized LDL, the success of this method will depend on the ability to produce and immobilize glycated LDL. A number of *in vitro* methods for the generation of glycated LDL (and other lipoproteins) have been reported previously, these can be seen in Table 6-1. Commercially available LDL will be glycated according to one of these methods. Following glycation, the modified LDL will be immobilized and placed in a chromatographic column for use in HPAC. This immobilization to HPLC grade silica could be accomplished by using the Schiff base method, described in **Chapters 2, 3, and 4** of this dissertation. As with oxidized LDL, the immobilization efficiency of glycated LDL may be diminished to the point that the Schiff base method is not viable. If this occurs, entrapment may be an effective alternative immobilization technique. Entrapment of LDL would occur by placing the lipoprotein within the pores of dihydrazide-activated silica and then capping the pores with oxidized glycogen [18]. HPAC studies using zonal elution and frontal analysis would then be employed to evaluate the column stability and interactions between drugs (e.g., propranolol) and the glycated LDL.

Table 6-1 ***In vitro* conditions that have been used to synthesize glycated LDL [19]**

Glycating agent[a]	**Glycating agent**	**LDL (mg/mL)**	**Duration**	**Temperature**	**Other Factors**
Glucose	80 mM	2.4 - 2.7	5 days	37 ºC	$NaCNBH_3$ (200 mM); gas not specified
Glucose	25 mM	3	6 days	37 ºC	NaN_3; EDTA; 5% (v/v) CO_2, 95% (v/v) O_2
Glucose	500 mM	0.25	28 days	37 ºC	Under air; EDTA; dark
GA, MG, or glucose	100 mM	0.35 – 30.45	14 days	37 ºC	5% (v/v) CO_2; 95% (v/v) O_2
Glucose	100 mM	0.5	6 days	37 ºC	N_2 0.5 mM; EDTA
GA, MG, or glucose	100 mM	1	7 days	37 ºC	5% (v/v) CO_2; 95% (v/v) O_2
GA or MG	10 mM	1	7 days	37 ºC	5% (v/v) CO_2; 95% (v/v) O_2
Glucose	30-80 mM	1	7 days	37 ºC	N_2; NaN_3

[a] Abbreviations: GA, glycoaldehyde; MG, methylglyoxyl.

Zonal elution studies

The analysis of drug interactions with lipoproteins by HPAC in this dissertation has revealed that HDL, LDL, and VLDL are all capable of multiple interactions with drugs (see **Chapters 2, 3, and 4**). In addition to the non-saturable, partition type interactions that have been identified through prior work [11-14], these current studies have revealed that apolipoproteins on the surface of HDL, LDL, and VLDL are capable of high affinity, site-specific interactions. These high-affinity, site-specific interactions have not been identified previously when using equilibrium dialysis or CE methods and, as a result, have not been the subject of further study. The study of these saturable binding sites is a potential area for future study. The use of zonal elution and HPAC could provide an effective mechanism for the study of these sites.

Zonal elution studies in HPAC were described in **Chapter 1** and used in conducting column stability studies throughout this dissertation. In this technique, a narrow plug of the analyte is injected onto the affinity column under isocratic conditions as a detector is used to monitor the elution time of the injected compound [20]. When the kinetics of association and dissociation are fast relative to the time scale of the experiment, the retention time of the analyte is directly related to its strength of binding to the immobilized agent and the amount of binding agent that is present in the column [18,20]. The conditions utilized in these experiments (e.g., pH, ionic strength, temperature, type of target, type of affinity ligand, and presence of competing agents in the mobile phase) may be altered to yield changes in the analyte retention [18,20]. Monitoring these changes as the conditions are varied can provide detailed data regarding the nature of interactions between the analyte and immobilized binding agent [18,20].

The frontal analysis experiments described in **Chapter 2** revealed that both verapamil and propranolol are capable of site-specific interactions with HDL. These experiments allowed for the identification of this type of binding between the drugs and HDL, but did not give specific information regarding the location of these binding sites on HDL's apolipoprotein. Execution of zonal elution experiments in which one of the drugs is dissolved in the mobile phase as a competing agent at varying concentrations would aid in determining if these compounds are competing for the same apolipoprotein binding sites. A decrease in the retention of the injected analyte as the drug in the mobile phase (i.e., pH 7.4, 0.067 M phosphate buffer) is increased would indicate whether direct competition, no competition or allosteric effects are occurring between the two compounds on HDL. In the event that the binding of propranolol and verapamil occur independently (e.g., at different sites on the apolipoproteins), no change in the retention of the injected analyte would be observed as the concentration of the drug in the mobile phase is increased. Similar studies could be conducted with LDL and VLDL columns or with additional drugs that have been found to undergo site-specific interactions with these lipoproteins.

The frontal analysis experiments conducted in **Chapter 3** revealed the presence of stereoselective binding of *R*- and *S*-propranolol by LDL; this phenomena may also be the subject of further study through zonal elution. The stereoselective nature of this interaction may be evaluated by using multiple types of studies on columns prepared as described in **Chapter 3**. One mechanism to confirm the stereoselectivity of this binding would be to conduct a competition study, as described in the previous paragraph. In such a study, *S*-propranolol could be dissolved in the mobile phase (i.e., pH 7.4, 0.067 M phosphate buffer) while *R*-propranolol is injected and monitored for its elution. As the concentration of *S*-propranolol in the mobile phase is increased, the retention of *R*-propranolol would be expected to remain constant. A constant retention time for *R*-propranolol would indicate a lack of competition for saturable binding sites on the apolipoprotein and confirm the stereoselective nature of this interaction. The stereoselectivity of *R*- and *S*-propranolol binding by LDL could also be evaluated by performing a chiral separation of the two compounds. In these studies, the two enantiomers would be injected as racemic mixture in the zonal elution mode. A chiral separation would be expected to yield a distinct peak for each enantiomer; this separation would not be expected in a system that did not exhibit stereoselective binding. Experimental conditions such as temperature, pH, ionic strength, and polarity may be modified to increase the resolution between these enantiomers or to increase the speed of this separation [20].

References

1. Otagiri, M. *Drug Metab. Pharmacokinet.* **2005**, *20*, 309–323.

2. Bertucci, C.; Domenici, E. *Curr. Med. Chem.* **2002**, *9*, 1463.

3. Hage, D.S. *J. Chromatogr. B* **2002**, *768*, 3-30.

4. Lindup, W.E. In *Progress in Drug Metabolism, Vol. 10*; Bridges, J.W.; Chasseaud, L.F.; Gibson G.G. Eds.; Tylor & Francis: New York, **1987**, Ch. 4.

5. Kwong, T.C. *Clin. Chim. Acta* **1985**, *151*, 193–216.

6. Svensson, C.K.; Woodruff, M.N.; Baxter, J.G.; Lalka, D. *Clin. Pharmacokinet.* **1986**, *11*, 450-469.

7. Wainer, I.W. *Trends Anal. Chem.* **1993**, *12*, 153-158.

8. Hage, D.S.; Tweed, S.A. *J. Chromatogr. B* **1997**, *699*, 499-525.

9. Hage, D.S.; Chen, J. In *Handbook of Affinity Chromatography*; Hage, D.S. Ed.; CRC Press/Taylor & Francis: New York, **2006**, pp 595–628.

10. Hage, D.S.; Jackson, A.; Sobansky, M.; Schiel, J.E.; Yoo, M.Y.; Joseph, K.S. *J. Sep. Sci.* **2009,** *32*, 835–853.

11. Glasson, S.; Zini, R.; D’Athis, P.; Tillement, J.P. ; Boissier, J.R. *Mol. Pharmacol.* **1980**, *17*, 187–191.

12. Ohnishi. T.; Mohamed, N.A.L.; Shibukawa, A.; Kuroda, Y.; Nakagawa, T.; El Gizawy, S.; Askal, H.F.; El Kommos, M.E. *J. Pharm. Biomed. Anal.* **2002**, *27*, 607–614.

13. Mohamed, N.A.L.; Kuroda, Y.; Shibukawa, A.; Nakagawa, T.; El Gizawy, S.; Askal, H.F.; El Kommos, M.E. *J. Chromatogr. A* **2000**, *875*, 447–453.

14. Mohamed, N.A.L.; Kuroda, Y.; Shibukawa, A.; Nakagawa, T.; El Gizawy, S.; Askal, H.F.; El Kommos, M.E.; *J. Pharm. Biomed. Anal.* **1999**, *21*, 1037–1043.

15. Kuroda, Y.; Cao, B.; Shibukawa, A.; Nakagawa, T. *Electrophoresis* **2001**, *22*, 3401-3407.

16. Parthasarathy, S.; Raghavamenon, A.; Garelnabi, M.O.; Santanam, N. *Methods Mol. Biol.* **2010**, *610*, 403-417.

17. Auerbach, B.J.; Bisgaier, C.L.; Wolle, J.; Saxena, U. *J. Biol. Chem.* **1996**, *271*, 1329-1335.

18. Hage, D.S.; Anguizola, J.; Barnaby, O.; Jackson, A.; Yoo, M.J.; Papastavros, E.; Pfaunmiller, E.; Sobansky, M.; Tong, Z. *Curr. Drug Metab*. **2011**, *12*, 313-328.

19. Younis, N.N.; Soran, H.; Sharma, R.; Chrlton-Menys, V.; Durrington, P.N. *Clin. Lipidol*. **2009**, *4*, 781-790.

20. Zheng, X.; Li, Z.; Beeram, S.; Podariu, M.; Matsuda, R.; Pfaunmiller, E.L.; White II, C. J.; Carter, N.; Hage, D.S. *J. Chromatogr. B.* **2014**, *968*, 49-63.